8-2015

Understanding the Molecular Mechanism underlying the Great Thermal Stability of Thermophilic Enzymes using Aminoglycoside Nucleotidyltransferase 4' as a Model

Xiaomin Jing
University of Tennessee - Knoxville, xjing@vols.utk.edu

To the Graduate Council:

I am submitting herewith a dissertation written by Xiaomin Jing entitled "Understanding the Molecular Mechanism underlying the Great Thermal Stability of Thermophilic Enzymes using Aminoglycoside Nucleotidyltransferase 4' as a Model." I have examined the final electronic copy of this dissertation for form and content and recommend that it be accepted in partial fulfillment of the requirements for the degree of Doctor of Philosophy, with a major in Biochemistry and Cellular and Molecular Biology.

Engin H. Serpersu, Major Professor

We have read this dissertation and recommend its acceptance:

Cynthia Peterson, Dan Roberts, Gladys Alexandre, Jaan Mannik

Accepted for the Council:
Dixie L. Thompson

Vice Provost and Dean of the Graduate School

(Original signatures are on file with official student records.)

Understanding the Molecular Mechanism underlying the Great Thermal Stability of Thermophilic Enzymes using Aminoglycoside Nucleotidyltransferase 4' as a Model

A Dissertation Presented for the

Doctor of Philosophy

Degree

The University of Tennessee, Knoxville

Xiaomin Jing

August 2015

ACKNOWLEDGMENTS

I would like to express my deepest gratitude to my PhD advisor Dr. Engin Serpersu who has been always supporting and guiding me over the past five years in the pursuit of completing my PhD degree. It is very generous of him to take so much patience in leading me into the world of protein biochemistry, instilling me the sense of critical thinking, improving my writing and presentation skills, explaining every single question of mine. I sincerely thank Dr. Serpersu for inspiring and indulging my intellectual freedom to explore the molecular mechanism of thermophilicity. There is nothing more gratifying to me than to receive his consistent and illuminating instruction through all the stages of my graduate study as well as the road ahead. All the encouragement from him will embolden me to strive for the beauty of science in my future career.

I would like to extend my appreciation to all my committee members: Dr. Cynthia Peterson, Dr. Gladys Alexandre, Dr. Dan Roberts and Dr. Jaan Mannik for their invaluable advice and critical insights towards my research. Their endeavors to improve my critical thinking, scientific communication, academic professionalism and scientific expertise have benefited me significantly.

My sincere appreciation is extended to Dr. Edward Wright and Dr. Adrianne Serpersu for their technical assistance and advice in the laboratory experiments. I appreciate the help and collaboration from Wilfredo Evangelista and Dr. Jerome Baudry in the computational studies. I am grateful to all the faculty, staff, friends and colleagues in department of Biochemistry, Cellular and Molecular Biology who have being supporting me through many times of stress, excitement, frustration and celebration in the past five and half years. It has been an enjoyable journey to be a part of the team.

Finally, I would like to extend my gratitude to my beloved parents. Without their persistent courage and emotional support, I would not have a chance to pursue my dream in a foreign country.

ABSTRACT

The aminoglycoside nucleotidyltransferase 4' (ANT) is a homodimeric enzyme that detoxifies antibiotics by nucleotidylating at the C4'-OH site. Two thermostable variants T130K and D80Y generated by direct evolution in laboratory differ by only a single residue replacement compared to the wild type mesophilic enzyme. Both variants display enhanced melting temperatures and execute catalysis at temperatures the wild type would be inactive. However, T130K variant still keeps molecular properties of mesophilic enzyme. T130→K130 does not trigger significant change in enzyme's local flexibility or thermodynamics of ligand binding while D80Y variant has distinct properties in ligand recognition and dynamics. We hypothesize that T130K and D80Y variants adopt different strategies to achieve thermal stability. In this respect, T130K is a heat stable mesophilic enzyme with simply higher melting temperature due to more stabilizing intramolecular interactions and may not be a true "thermophilic" enzyme. Thermophilic variant D80Y, on the other hand, displays higher atomic fluctuations than mesophilic enzyme thus increasing the entropic change associated with enzyme denaturation. Here we attempt to draw a line separating heat resistant enzymes like T130K from true thermophilic enzyme like D80Y.

Numerous studies compared the differences in various structural features of thermophilic/thermostable-mesophilic enzymes in order to reach unifying and general mechanisms of greater thermostability/thermophilicity for such enzymes. To date, not a single molecular feature emerged as the parameter defining "thermophilic" properties. We believe that this is because these comparisons included all heat stable enzymes, some of which may simply be heat stable versions of mesophilic enzymes, such as those with added stabilizing interactions (disulfide bonds or salt bridges) based on structural analyses. In this work, we demonstrated that thermodynamic properties of protein-ligand interactions may yield molecular properties of true thermophilic enzymes by using two heat stable variants of ANT to demonstrate that one of them, T130K is simply a heat stable enzyme with proper ties of the wild type while the other, D80Y, shows properties that are significantly different and alters the dynamics of the enzyme.

TABLE OF CONTENTS

LIST OF TABLES

LIST OF FIGURES

CHAPTER I

BACKGROUND

1.1 Thermophilic enzymes

Thermophilic and hyperthermophilic microorganisms thrive at higher temperature intervals, 50-80 and 80-110 ℃ respectively, compared with mesophiles which optimally grow between 20-40 ℃ (1). Enzymes synthesized by thermophiles are capable of executing catalysis at high temperatures that usually render mesophilic enzymes inactive. Such enzymes are therefore termed “thermophilic enzymes”. Thermophilic enzymes are exclusively originated from Archaea and Bacteria inhabiting hot natural environments including volcanic pools, hallow marine and hot spring sediments(2). Enzymes from thermophiles and hyperthermophiles have drawn much attention to biotechnology and industry in recent decades. Their high stability and optimal activity at high temperatures makes them more suitable for harsh industrial processing environment compared to their mesophilic counterparts.

1.2 Literature review: how do thermophilic enzymes deal with heat?

Compared with mesophilic enzymes, thermophilic enzymes do not adopt completely new machineries to achieve thermal resistance. Pairwise comparisons have suggested that many thermophilic and mesophilic homologs have high sequential identities (40%-80%)(3, 4), superimposable crystal structures (5-9) and also share same catalytic mechanisms and catalytic efficiencies under respective physiological conditions (4, 10, 11). To date, studies on the molecular mechanisms of heat resistance of thermophilic enzymes can be divided into two categories. The first one is computer-assisted systematic comparisons of structural and sequential features between groups of thermophilic and mesophilic enzymes in order to reach general conclusions. The second category is focused on the differences of single pair of thermophilic/mesophilic homologs using various experimental and simulation approaches. Both types of studies, especially the first one, have suggested that many structural factors distinct for mesophilic and thermophilic enzymes are responsible for the greater stability of

thermophilic enzymes. Those features include salt bridges(12-15), side chain-side chain hydrogen bonds(16, 17), internal hydrophobic packing(18, 19), oligomeric state(20), preferred or avoided residues(19, 21) et al. However, these factors observed in the individual families do not always show consistent trends in other families. Not a single structural feature is common for all tested data sets to define thermophilic properties and there are always exceptions to every set of rules that were proposed to be the unifying one.

For example, the role of salt bridges toward protein stability has been controversial. Numerous studies suggest that salt bridges stabilize thermophilic proteins. One example of this is the comparison of crystal structures of thermophilic and mesophilic Glyceraldhyde-3-phosphate dehydrogenases that indicates a strong correlation between salt bridges and melting temperatures(22). Such correlations have been also observed for enzymes in additional families determined by site-directed mutagenesis(23, 24). A statistical examination of structures from 18 different families of thermophilic and mesophilic proteins indicated that salt bridge content increases in most thermophilic proteins(25). However, many studies questioned the stabilizing effect of salt bridges and provided evidence that salt bridges not always stabilize mesophilic enzymes. A greater ionic interaction network in *T. maritima* Glutamate Dehydrogenase resulted in a decrease in thermal denaturation resistance. The stability was restored with residue mutations that destabilized the network of salt bridges(26).

To date, it is still difficult to draw a general conclusion to underlie the mechanisms of all thermophilic proteins. It is a widely accepted common view that thermophilic proteins adopt various structural strategies to achieve thermal adaptation.

It is worth noting that, first, the sample sizes in previous systematic studies were relatively small due to the limitation of the available crystal structures of both thermophilic and mesophilic homologs from the same family. The largest data set in such comparison only contains 29 thermophilic and 64 mesophilic protein structures from 25 protein families in 2000(27). Second, not all the structural differences observed in mesophilic and thermophilic enzymes necessarily account for thermal stability differences as some thermophiles are also subject to other selective pressures such as acidity and high pressure. Moreover, each crystal structure simply presents a single

static snapshot among a Boltzmann ensemble of conformers of protein. A protein in its native state is suggested to have a certain population of sub-stable conformations besides its predominating conformation(s) which locates at the basin in free energy landscape. Dynamics (the alternation between different conformations) is one of the most important properties of protein. For some time, the relation between dynamics and thermophilicity has been overlooked.

In 1990s, a few labs investigated the correlation between protein rigidity/flexibility and thermostabilty. A hydrogen /deuterium (H/D) exchange study on a pair of mesophilic-thermophilic enzyme show that the thermophilic enzyme presents significantly larger rigidity than its mesophilic counterpart at room temperature. However, two enzymes have similar flexibilities at each optimal temperatures(28). Heat resistance of thermophilic proteins was suggested to be correlated with structural rigidity of protein as a result of stabilizing interactions such as salt bridges and hydrophobic interactions(28, 29) and proteins having greater stability tend to have fewer local fluctuations/flexibilities(30). It is worth noting that measurements of accessibility of buried residues such H/D exchange studies rely on global unfolding of protein and does not reveal the local fluctuations that occur in the native folded state of protein. Also, protein dynamics consist of a hierarchical network of motions occurring at different time scale, spanning from femtosecond to second. The motions detected in H/D exchange are exclusively in timescale from millisecond to second.

In recent years, extensive nuclear magnetic resonance studies and neutron scattering studies (31-33) on atomic fluctuations from pairs of thermophilic-mesophilic counterparts have re-examined the relation between flexibility and stability of thermophilic proteins. Molecular Dynamic simulation of the hyperthermophilic elongation factor G-domain during microsecond time scale suggests that (hyper-) thermophilic proteins are characterized by a larger number of conformation ensembles than mesophilic counterparts result in enhancement in entropy at native state which further contributing to the enhanced stability of (hyper-) thermophilic proteins(27)(Figure 1). Also, an NMR relaxation study estimated the contribution of native state conformational entropy to the stability of protein and suggested that enhanced internal protein motions may increase thermostability by raising the entropy of native state. This somewhat

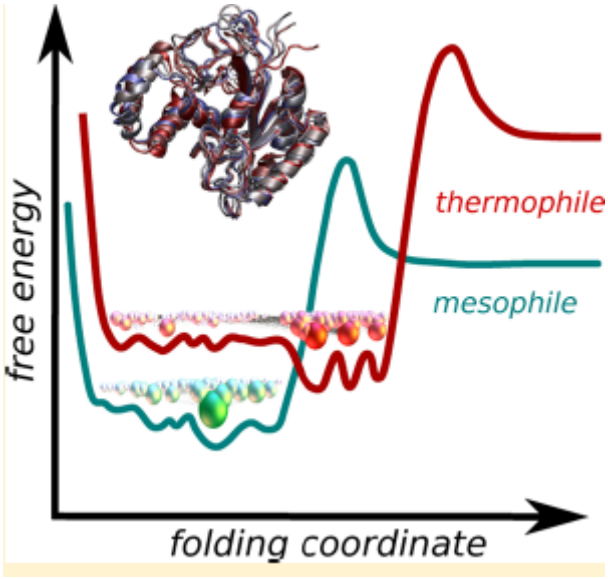

Figure 1- Free energy landscape of mesophilic and thermophilic proteins. Adapted from Kalimeri et al.(34)

counter-intuitive idea that thermophilic proteins have larger internal fluctuations at fast time scale (picosecond-microsecond) than mesophilic proteins at ambient temperatures has been reinforced by various studies.

1.3 Protein thermal stability as seen by solvent effects

Water molecules influence the conformations of protein by acting as a polarizable dielectric medium. Native structure of a protein is the consequence of a dynamical balance of various inter- and intra- molecular interactions. The dynamic balance is easily influenced by solvent- protein interactions. Solvent molecules are capable of stabilizing charged and polar side chains on the surface as well as competing with intramolecular interactions. Therefore, solvent-protein interactions have been suggested to play an important role in protein folding and stability for decades(35).

The enhanced conformational fluctuations of thermophilic enzymes compared to mesophilic homologs discussed earlier are further suggested to be induced by solvent. Amide exchange experiments monitoring the kinetics of conformational opening suggest that conformational fluctuations of thermophiles take place in the time scale of protein-solvent hydrogen bond lifetime(36). Water-exposed surface of protein is observed to positively correlate with the degree of thermophilicity(1). Molecular Dynamic simulation study on mesophilic, thermophilic and hyperthermophilic homologues of EF-Tu (elongation factor thermos unstable) showed that the superficial and volume hydrogen bond densities decreased as temperature increases for all three species and the hyperthermophilic protein presents the highest density of hydrogen bonds followed by thermophilic enzyme(1). Taken together, the hydration shell is suggested to serve as a protection layer by connecting to protein surface and it protects protein from penetration by bulk solvent molecules as temperature raises. Solvent-induced local fluctuations of thermophilic proteins protect proteins against thermal stress by increasing conformational entropy.

Solvent-protein interactions are at distinct intensity levels for thermophilic, mesophilic and psychrophilic enzymes. As discussed above, extensive protein-water

interplay is suggested to be a “morphological indicator” of protein thermostability compared to mesophilic counterparts(37). Contrary to that, psychrophilic enzymes, the cold-adaptive enzymes, display a smaller solvent accessible region and higher portion of exposed nonpolar side chains. Most characterized psychrophilic enzymes share heat-labile activity as a common feature besides its great cryostability. Less intense interaction between solvent and protein surface is suggested to serve as an entropy-driven destabilizing factor(38). The extreme example of less solvent-protein interactions comes from antifreeze proteins which naturally exist in Antarctic fish and other organisms. Antifreeze proteins have the unique solvent recognition pattern in a way such that they selectively bind to ice (instead of liquid solvents) to prevent the growth of ice nuclei. X-ray crystallography(39, 40) and MD simulation(41) studies suggest that ice –binding face is relatively hydrophobic and water molecules keep ordered structure and low dynamics around ice-binding face. In summary, comparison of solvent-protein interactions for many thermophilic, mesophilic and psychrophilic enzymes suggests a continuum of adjustment of solvents effects accompany to thermostability adjustment.

1.4 Correlation between activity and thermal stability of thermophilic enzymes

A trade-off between activity and thermal stability was observed for many mesophilic/thermophilic enzymes. It has been detected that (hyper-) thermophilic and mesophilic enzymes have approximately the same activities and catalytic efficiencies under their physiological conditions. However, they displayed weaker activity at ambient temperature. To date, it is widely accepted that there is a critical balance between stability and activity. Alternatively, reduced activity is a consequence of thermostability.

However, a few studies questioned the trade-off between activity and thermal stability. Van den Burg(42) *et al* engineered a moderate thermophilic thermolysin-like protease (TLP) into a hyperthermophilic TLP with optimal temperature improved by 21℃, however, it still presented wild type-like proteolytic activity at 37 ℃. Therefore it can be concluded that the greater thermal stability of thermophilic enzymes does not

necessarily cause compensation in enzymatic activity. It is possible to engineer thermophilic enzymes that retain full activity at ambient temperature.

Nearly all the reported natural thermophilic enzymes have been shown to have lower catalytic efficiencies at ambient temperatures than their mesophilic counterparts. It is likely to be a consequence of random drift as efficient catalysis at ambient temperature is simply not required by organisms that live in hot environments so that such catalysis has reduced over time. If temperature adaptation happens in an opposite direction from hot to ambient temperatures, then thermostability would be no longer required over time. But enzymes do not necessarily sacrifice one property (thermostability or activity) in order to achieve another.

The relation between activity and thermal stability of thermophilic enzymes can be explained in the view of enzyme dynamics. The greater thermal stability of thermophilic enzymes is likely caused by enhanced solvent-induced fluctuations compared with mesophilic counterparts but not necessarily indicates that dynamics of active sites is also enhanced. For a thermophilic alcohol dehydrogenase, hydrogen-deuterium exchange studies demonstrated that a rigidification of the protein below 30 ℃ occurs primarily within the substrate binding domain instead of the whole protein(43). It is possible that regional (i.e. active site), instead of global thermal fluctuation are linked to enzyme catalysis; while thermal stability is related to thermal fluctuations caused by solvent effects.

1.5 Challenges in design of thermostable/thermophilic enzymes

The very first thermophilic enzyme that has been discovered is *Taq* polymerase known for its wide application in PCR techniques. It was isolated from *Thermus aquaticus* by Tomas Brock in 1969(44). Henceforth numerous protein engineering studies have been performed in order to discover, design and engineer thermophilic enzymes. However, isolation of pure thermophile cultures from their native environments and growth of pure cultures in laboratory still remains a challenge for thermophile discovery(2).

In rational protein design, the stabilization mechanism inferred from thermophilic protein studies has been employed with the aim of formation of new salt bridges and hydrophobic interactions in the core region. However, outcome is not always as predicted. For example, more salt bridge networks have been shown to destabilize some mesophilic enzymes(26). To date, the bottleneck for rational design is the limited understanding of the relation among protein sequence-structure-thermal stability.

Direct evolution enriches the beneficial mutations by selection of random mutations. It has been proved to be a more powerful approach to design enzymes with increased thermostability compared with rational protein design. Enzymes with improved thermostability by directed evolution have already been commercialized(45). However, few studies have been done to investigate the mechanisms of enhanced thermostabilty as a result of a few amino acids alteration. In this work, we use a set of previously identified thermostable variants of Aminoglycoside nucleotidyltransferase 4' (ANT4) by directed evolution as model enzymes to dissect how amino acid alterations structurally contribute to enhanced enzymatic thermostability.

1.6 Protein model - thermostable variants of aminoglycoside nucleotidyltransferase 4'

1.6.1 Aminoglycoside modifying enzymes (AGMEs)

Aminoglycosides are a group of broad-spectrum antibiotics and have been widely used to treat bacterial infections. Almost all aminoglycosides are composed of a central deoxystreptamine ring and amino sugars connected to the ring by glycosidic bonds (Figure 2). Aminoglycosides bind to the 16s ribosome RNA of prokaryotes and interfere with protein translation by causing mistranslations and premature stops. However, some bacteria evolved to be antibiotic resistant by encoding enzymes that covalently modify and detoxify aminoglycosides. Aminoglycoside modifying enzymes (AGMEs) can be classified into three families: *O*-phosphotransferases, *N*-acetyltransferases and *O*-

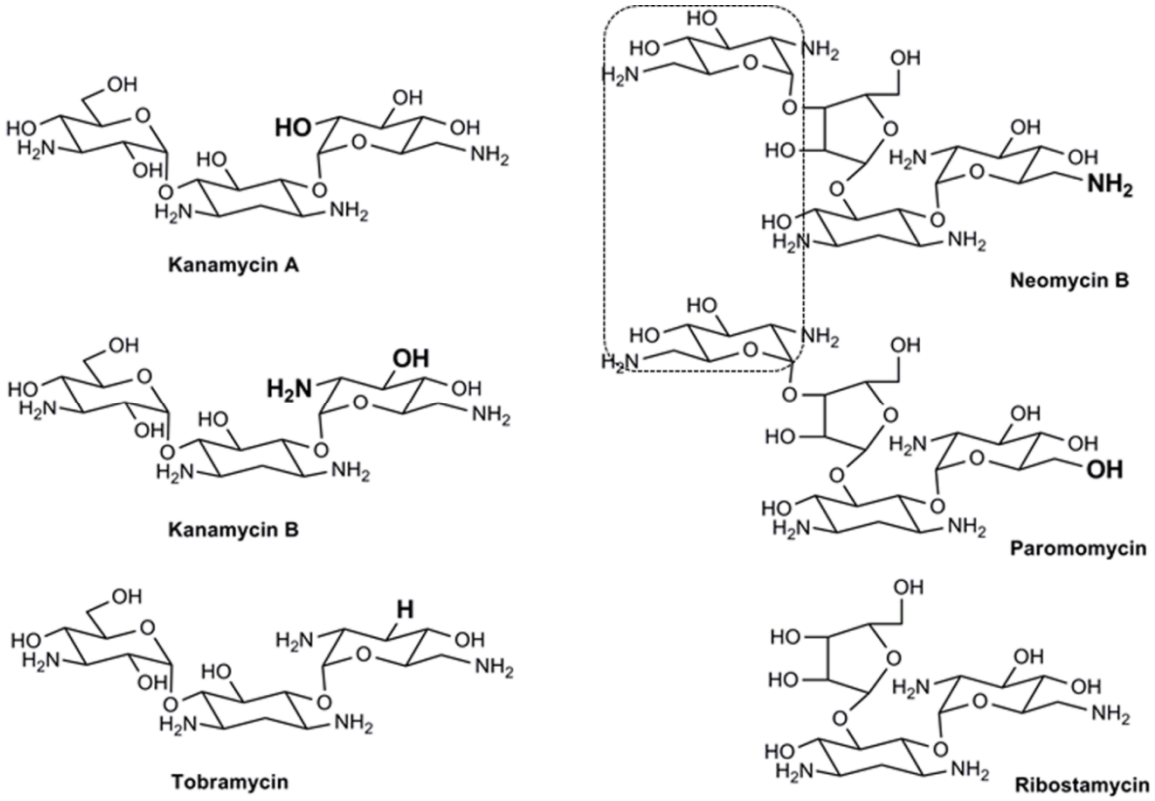

Figure 2-Chemical structures of aminoglycoside antibiotics. Ring D of neomycin class is shown within the dotted rectangle. Kanamycin A, kanamycin B and Tobramycin are aminoglycosides with 4, 6- disubstituted and neomycin B, paromomycin and ribostamycin are with 4, 5- disubstituted central 2-deoxystreptamine ring respectively.

nucleotidyltransferases based on the enzymatic modifications.

Aminoglycoside nucleotidyltransferases represent the smallest family of AGMEs. There are only 10 nucleotidyltransferases identified to date(46). These enzymes transfer the AMP group from MgATP to a hydroxyl group of aminoglycosides to form the O-adenylyated aminoglycoside and leaving group-magnesium chelate of inorganic pyrophosphate. To date, the aminoglycoside nucleotidyltransferase 4' (ANT4) is the only nucleotidyltransferase with an available crystal structure.

1.6.2 Aminoglycoside nucleotidyltransferase 4' (ANT4)

Wild type (WT) ANT is encoded by a bacterial plasmid pUB110 that was isolated from a mesophile *Staphylococcus aureus*(47). Several thermostable variants were previously obtained by introducing ANT gene coding plasmid from the mesophilic organism into a thermophile (*Bacillus stearothermophilus*) and selection of spontaneous mutants for kanamycin resistance at elevated growth temperatures(48, 49). Compared to WT, these variants only differed by a single or double amino acid changes in their primary amino acid sequences but displayed enhanced thermostability as well as increased resistance to proteinase, urea and detergent(50) in the order of T130K (with a Thr130→ Lys80 substitution), D80Y (with an Asp80→ Tyr80 substitution) and double variant D80Y/T130K (with both substitutions) (Table 1).

A crystal structure is available for an ANT variant, D80Y/T130K, which was determined at 3.0Å resolution in the absence of substrates (51). Additionally, the D80Y variant structure was solved at 2.5Å resolution with kanamycin and MgAMPCPP (52). Both the apo- and substrate-bound structures are homodimers with high similarity and a 0.75 Å root-mean-square deviation of superimposed alpha carbon positions. Each monomer is shown to bind both, the antibiotic and the metal-nucleotide (Figure 3). The binding sites for both substrates are solvent-exposed and contain charged residues contributed by both subunits, establishing an active site between the two protein monomers. The orientation of substrates facilitates transfer of the nucleotidyl group between the substrates bound to different monomers

Table 1. Previous characterization of ANT thermostable variants. Specific activities of variants were presented as per cent of wild type enzyme at 37℃. Specific activities at each optimum temperature are nearly identical for all enzymes.

Table 1. Previous characterization of ANT thermostable variants*

Enzyme	Selection temperature (℃)	Residue at 80	Residue at 130	Half-life at 60℃ (min)	Specific activity (%)	Optimum temperature (℃)
Wild type	<55	Asp	Thr	<0.3	100	52
T130K	61	Asp	Lys	1	95	57
D80Y	63	Tyr	Thr	16.5	85	60
D80Y/T130K	70	Tyr	Lys	>60	80	62

*Adapted from Liao et al.**(50)** and Matsumura el al**(53)**

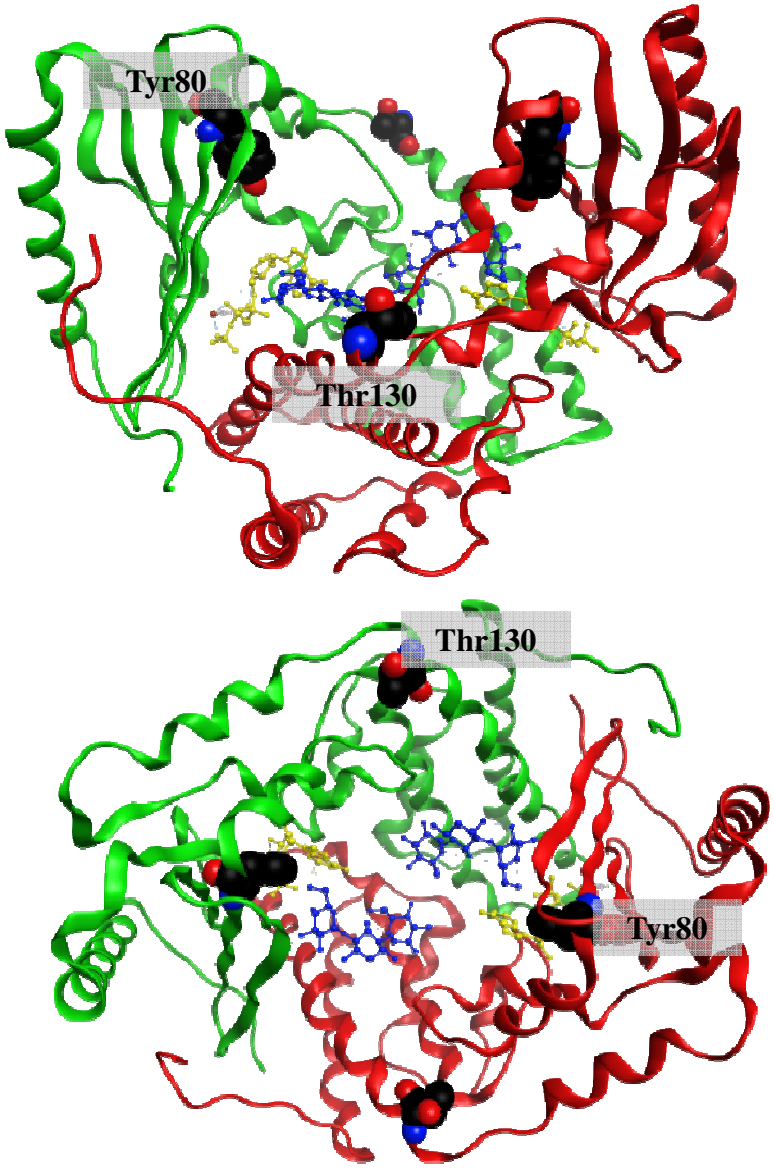

Figure 3. Crystal structure of ANT D80Y variant. Two monomer subunits are shown in red and green ribbons respectively. Bound kanamycin A molecules are colored blue and Mg-AMPCPP molecules are colored yellow. (PDB ID: 1KNY) Thr130 and Tyr80 residues are highlighted in sphere representation.

.

Engineering protein for thermostability enhancement is a critical subject for industrial processes as process at high temperature could enhance enzymatic activity, substrate specificity and reduce contaminations. Direct evolution has been proven to be a powerful tool to improve thermostability of proteins by accumulating multiple mutations. In this work, we use a set of previously identified thermostable variants of Aminoglycoside nucleotidyltransferase 4' (ANT4) by direct evolution as model enzymes to dissect how amino acid alterations contribute to enhanced enzymatic thermostability. We believe that our current research on ANT thermostable variants will open up a deeper perspective about structure-stability relationships and shed light on the evolution of thermophilic organisms and rational protein design.

CHAPTER II

THERMOPHILIC AND HEAT STABLE MESOPHILIC ENZYMES: CAN WE DRAW A SEPARATING LINE?

2.1 Abstract

The aminoglycoside nucleotidyltransferase 4' (ANT) is a homodimeric enzyme that detoxifies antibiotics by nucleotidylating at the C4'-OH site. There are several thermostable variants for this enzyme (T130K, D80Y and D80Y/T130K) that show a single and double amino acid changes in their primary amino acid sequences. It is not clear how the residue replacements, which are distant from active site and monomer-monomer interface, result in various degrees of changes on enzymatic thermostability. In this work, we characterized contribution of each residue replacement towards the changes in dynamic property, ligand recognition and thermal denaturation of each variant. The melting temperatures systematically increased in the order of wild type, T130K, D80Y and D80Y/T130K variants, however, studies on local flexibility and ligand binding properties clearly showed that T130K variant resembles mesophilic enzyme in both tested properties whereas D80Y variant present distinct features. Our data suggest that T130→K130 and D80→Y80 substitutions adopt different strategies to achieve different levels of thermostability: T130K variant display higher melting temperature simply as a result of specific stabilizing interaction from residue mutagenesis but it still keeps many features of mesophilic enzymes such as local flexibility and ligand binding. However, D80Y variant may stabilize previously sub-stable conformers in mesophilic enzyme and display more stable basins that native protein can visit, thus increasing the entropic change associated with enzyme denaturation. We hypothesize that T130K and D80Y variants represent two different categories of heat resistant enzymes- simply a heat stable mesophilic versus true thermophilic enzymes respectively. Heat stable mesophilic enzymes have simply improved melting temperatures due to the existence of more specific stabilizing local interactions without altering molecular features such as atomic fluctuations, compared with mesophilic counterparts.

2.2 Introduction

Pairwise comparison of mesophilic/thermophilic enzymes have suggested that many thermophilic and mesophilic homologs have superimposable crystal structures and they share high identify in sequence alignment (40%-80%). Numerous studies attempted to reveal the molecular mechanism(s) responsible for the difference in thermal stability, such as salt bridges(12-15), side chain-side chain hydrogen bonds(16, 17), internal hydrophobic packing(18, 19), oligomeric state, preferred or avoided residues etc. However, these properties that are observed in the individual families do not always show consistent trends in other families. To date, not a single unifying molecular feature has emerged.

In this work, we use a set of previously identified thermostable variants of Aminoglycoside nucleotidyltransferase 4' (ANT4) by direct evolution as model enzymes to dissect how amino acid alterations contribute to enhanced enzymatic thermostability. We determined the contribution of each residue replacement towards the changes in enzyme dynamics, thermostability and ligand recognition. Previously solved crystal structures of enzymes and our circular dichroism analysis suggest all thermostable variants adopt similar three dimensional folds with the mesophilic enzyme. Sedimentation velocity study showed that all the tested enzymes exist as mixtures of monomers and dimers in solution, however, the dissociation constant of dimers steadily increased in the order of D80Y/T130K variant → D80Y variant → T130K variant → WT (mesophilic). To our knowledge, this is the first report of single residue alteration distal from monomer-monomer interface affecting monomer-dimer equilibrium without changing the three dimensional structure of the enzyme. Furthermore, antibiotic binding tests were performed in order to probe the differences in ligand recognition between thermostable variants and mesophilic ANT. Surprisingly, antibiotic recognition yielded the first clues on the separation of heat stable mesophilic enzymes from true thermophilic enzyme such that WT enzyme and the T130K variant have similar binding parameters with both tested aminoglycosides – neomycin and tobramycin; while D80Y variant resembles double variant in association of both ligands. Additionally, molecular

dynamics simulations reveals similar local fluctuations for WT and T130K variant in most residues, however, D80Y displays slightly higher flexibility in specific regions compared to WT and T130K variant. These observations indicated the different structural strategies of improving thermostability for T130K variant and D80Y variant. T130K variant- simply a mesophilic variant with enhanced thermostability still resembles WT enzyme in ligand binding and enzyme dynamical properties; D80Y variant - a true thermophilic variant displays weaker binding affinities to tested ligands and altered dynamics at room temperature. We hypothesized that T130K and D80Y variants represented two different categories of heat resistance – heat stable mesophilic versus true thermophilic enzymes respectively. Heat stable mesophilic enzymes are mesophilic enzymes with simply improved melting temperatures due to the existence of more specific stabilizing local interactions without essential differences in molecular features such as atomic fluctuations, compared with mesophilic counterparts.

Investigation on these two similar yet different types of enzymes would open a different perspective on the molecular mechanisms for protein stability and potentially shed light on future rational protein design and engineering.

2.3 Experimental Procedures

Reagents

All materials were of the highest purity commercially available and were purchased from Sigma-Aldrich Co. (St. Louis, Mo) unless otherwise noted. All the primers for polymerase chain reactions (PCR) were synthesized by IDT (Coralville, IA). All the mutagenesis was performed using the Quikchange Lightning site-directed mutagenesis kit from Stratagene (La Jolla, CA). Plasmid preparation was done by using QIAprep Spin Miniprep Kit from Qiagen (Germany). Ni^{2+} Sepharose High Performance resin was purchased from GE Healthcare (Piscataway, NJ). *E.coli* BL21 (DE3) Gold and BL21(DE3) PlysS competent cells were purchased from Invitrogen (Waltham, MA). Marco-Prep High Q Support strong anion exchange column was purchased from Bio-

Rad Laboratories (Hercules, CA). Thrombin, prepared from thrombostat by cation exchange chromatography as described previously (54), was graciously provided by Dr. Elias Fernandez (The University of Tennessee, Knoxville).

Analytical ultracentrifugation (AUC)

Sedimentation velocity experiments were performed in a Beckman XL-I analytical ultracentrifuge using an An-50Ti rotor. Sample volumes of 400 µL were loaded into double-sector cells and allowed to equilibrate for an hour at 25°C prior to the run. Different detection strategies were required to maximize sensitivity and ensure that measurements were within the linear region over this concentration range. At lower concentrations (1.0-3.0 µM) absorbance at 230 nm was used to monitor sedimentation. Absorbance data at 280 nm were acquired for ANT at 5-20 µM. For enzyme at concentration higher than 40 µM, the interference optical system was used for detection. All the scans were collected at a rotor speed of 50,000 rpm at 25°C. Sedimentation data were fit to a continuous (c(s)) distribution model using SEDFIT (version 12.44) (55). Protein partial specific volume, buffer density and buffer viscosity were calculated using SEDNTERP (56).

Prior to all experiments, the enzyme was dialyzed extensively against the buffer contained 50 mM PIPES, pH 7.5, and variable concentrations of NaCl – zero or 100mM. For data analysis, the weight-average sedimentation coefficients (s_w(S)) were determined at each concentration by integrating the peaks from the c(s) distributions using SEDFIT (55). Isotherm analysis of s_w(S) as a function of protein concentration with the monomer-dimer self-association model in SEDPHAT was employed to determine the dissociation constant (57). The values from isotherm analysis were used as the initial guesses in global analysis to determine the kinetics of the interaction (57, 58).

Site-directed mutagenesis

T130K gene-containing plasmid was provided by Dr. Barry Bruce (University of Tennessee, Knoxville). The target gene was inserted into a pET15b vector with an N-

terminal 6xHis tag and transformed into an *Escherichia coli* BL21 (DE3) pLysS cell line. The pET15b vector harboring the gene of T130K variant was used as the template in polymerase chain reaction (PCR) amplification to create wild type and double variant clones. For D80Y variant, wild type clone was used as the template in PCR reaction. The primers used are listed in Table2. The mutated codons are underlined. PCR products were transformed into competent XL10 cells. pET15b plasmids with wild type/each variant were isolated by Miniprep kit and confirmed by sequencing check (University of Tennessee sequencing facility). Positive clone was transformed into *E.coli* BL21 (DE3) Gold competent cells.

Overexpression and purification

For T130K variant, bacteria containing plasmid were selected on LB plates with 50 µg/ml ampicillin and 34 µg/ml chloramphenicol. Cells were grown at 37℃, induced by 1 mM IPTG and harvested after four hours of induction. Cells were re-suspended in 50 mM Tris-HCl, pH 7.5, 100 mM NaCl, and 1 mM EDTA and lysed by three freeze-thaw cycles. The lysate was treated with DNase for 1h and centrifuged at 14,000 rpm for 30 min. ANT, carrying a Histag made up of 6 histidines, was isolated by Ni^{2+} affinity chromatography. The 6xHis tag was removed by thrombin cleavage for 1 h at room temperature. Following cleavage, the protease was removed by chromatography over a strong anion exchange resin. Fractions containing ANT were pooled and dialyzed against 50 mM PIPES buffer pH 7.5, concentrated by ultrafiltration, and stored at 4℃. Under these conditions, the enzyme remained active for several weeks.

Overexpression and purification of wild type enzyme, D80Y and double variants are performed similarly with T130K variant except cell lysing was performed by three cycles of French press. Enzymes remained active for at least a month at -20℃. Protein concentration were determined by absorbance at 280nm using extinction coefficient of 49390 $M^{-1}cm^{-1}$ for wild type enzyme and 50880 $M^{-1}cm^{-1}$ for all variants. Protein concentrations are reported as monomer concentrations unless otherwise indicated.

Table 2. PCR primers used in site-directed mutagenesis. The mutated nucleotides are underlined

	Template	Forward primer	Reverse primer	Mutated codon
Wild type	T130K	5'-CAAAAGCGTGGAAGCCCAAACCTTTCACGATGCCATTTGCG-3'	5'-CGCAAATGGCATCGTGAAAGGTTTGGGCTTCCACGCTTTTA-3'	AAA(Lys) → ACC(Thr)
D80Y T130K	T130K	5'-GGAAAGTGGAAGTGAACTTTTATAGCGAAGAAATTCTGCTGG-3'	5'-CCAGCAGAATTTCTTCGCTATAAAAGTTCACTTCCACTTTCC-3'	GAT(Asp) → TAT(Tyr)
D80Y	Wild type	5'-GGAAAGTGGAAGTGAACTTTTATAGCGAAGAAATTCTGCTGG-3'	5'-CCAGCAGAATTTCTTCGCTATAAAAGTTCACTTCCACTTTCC-3'	GAT(Asp) → TAT(Tyr)

Isothermal titration calorimetry (ITC)

ITC experiments were performed at 25℃ using a VP_ITC mircocalorimeter from Microcal, Inc. (Northampton, MA). The concentrations of aminoglycoside antibiotics were determined by enzymatic assay with aminoglycoside acetyltransferase(3)-IIIb as described previously (59). Both enzyme and ligand solutions were degassed under vacuum for 10 min at 20℃. Titrations consisted of 27 injections of 10 μL and were separated by 240 s. Cell stirring speed of 300 rpm was used. The observed heat change (Δ*H*) evolving from binary complex formation and the binding affinity were directly determined from titration. Free energy (Δ*G*) and entropy (Δ*S*) changes associated with binding were determined from equations (1) and (2). All data were fit to a single-site binding model using Origin 5.0 software from Microcal, Inc.

$$\Delta G = -RTlnK_a \qquad (1)$$

$$\Delta G = \Delta H - T\Delta S \qquad (2)$$

Determination of the intrinsic enthalpy of binding was done as described earlier (60). Briefly, the following equation was used to evaluate and subtract the contribution, if any, by pK_a shifts of titratable sites:

$$\Delta H_{obs} = \Delta H_{int} + \Delta H_{ion}\Delta n \qquad (3)$$

Here, ΔH_{obs} is the observed enthalpy change, ΔH_{int} is the intrinsic enthalpy change, ΔH_{ion} is the heat of ionization of the buffer and Δn is the net transfer of protons by the buffer upon complex formation. ΔH_{int} and Δn are determined from the intercept and slope respectively. Under these experimental conditions, a net proton uptake by the enzyme-ligand complex yields a positive Δ*n*.

Circular Dichroism (CD)

CD spectroscopy was performed on a Jasco J-815 spectrometer using a cuvette with a path length of 2 mm. Spectra were recorded with an acquisition time of

50nm/min and single scan for thermal denaturation. Protein concentration was 18uM (monomer) for all the runs.

Molecular Dynamic (MD) simulations

Systems were constructed based on the crystal structure of D80Y variant (Protein Data Bank ID: 1KNY). By using Molecular Operating Environment (MOE) ligands and cofactor were removed from the system such that the apo form of the wild type, and T130K variant were built. Molecular Dynamics simulations were carried out by using Gromacs 4.6.1 and force field AMBER-f99sb on each system. Each structure was explicitly solvated by using TIP3P water molecules in a cubic simulation box of 8 nm x 8 nm x 8 nm. Next, 18000 steps of energy minimization was carried out using the steepest decent algorithm.

Equilibration for 50 nanoseconds was performed under conditions of constant particle number, pressure, and temperature (NPT thermodynamic ensemble) at 300K and 1 bar pressure by using the Nosé-Hoover and Berendsen weak coupling algorithms to control temperature and pressure respectively. Finally, 100 nanoseconds of production time were run but replacing the Berendsen algorithm by the Panirello-Rahman algorithm. A two femtosecond integration time step was used for both stages: equilibration and production. The trajectory was formed by saving the atomic coordinates every 5 ps.

The trajectories obtained from the production time were analyzed by using Gromacs tools, root mean standard deviation (RMSD) of the backbone respect to its initial structure, and root mean square fluctuations (RMSF) of the backbone Cα respect to the average structure were obtained to study the stability of the molecule and the flexibility of residues in the different domains of the enzyme.

2.4 Results

Site-directed mutagenesis and protein purification

Positive clones were confirmed by sequencing. Purity of wild type enzyme and variants (>95%) were visualized by 10% SDS-PAGE and further validated by analytical ultracentrifugation tests.

Melting temperature of dimeric apo-enzymes is improved by amino acid replacements

Thermal denaturation Circular Dichroism (CD) spectra of wild type as well as thermostable variants were recorded at 222nm. The melting temperatures (T_m) are shown to systematically increase in the order of wild type (40.9±0.5℃), T130K variant (49.1±0.6℃), D80Y variant (56.2±0.2℃) and double variant (62.6±0.1℃) (Figure 4). The thermal denaturation follows a two-state transition process.

Compared with wild type enzyme, T_m of three variants has been improved by about 8.2℃ for T130K, 15.3℃ for D80Y and 21.7℃ for double variants respectively. This suggests that D80→Y80 replacement confers higher thermostability on ANT enzyme more than T130→K130 replacement. The effect of T130→K130 and D80→Y80 substitutions in improving T_m of apo-enzyme appears to be cumulative as evidenced by T_m of the double mutant.

Thermal denaturation of all four enzymes was irreversible and aggregation was observed post denaturation. However, similar denaturation profiles were obtained for the same sample at different heating rates, which indicates that thermal denaturation of enzymes were not perturbed by kinetics of aggregation(61). Differential scanning calorimetry tests were also performed in order to characterize heat capacity change of enzyme unfolding. However, no significant change in heat capacity transition was observed as in the temperature range of 20 to 95℃ for D80Y and T130/D80Y variants.

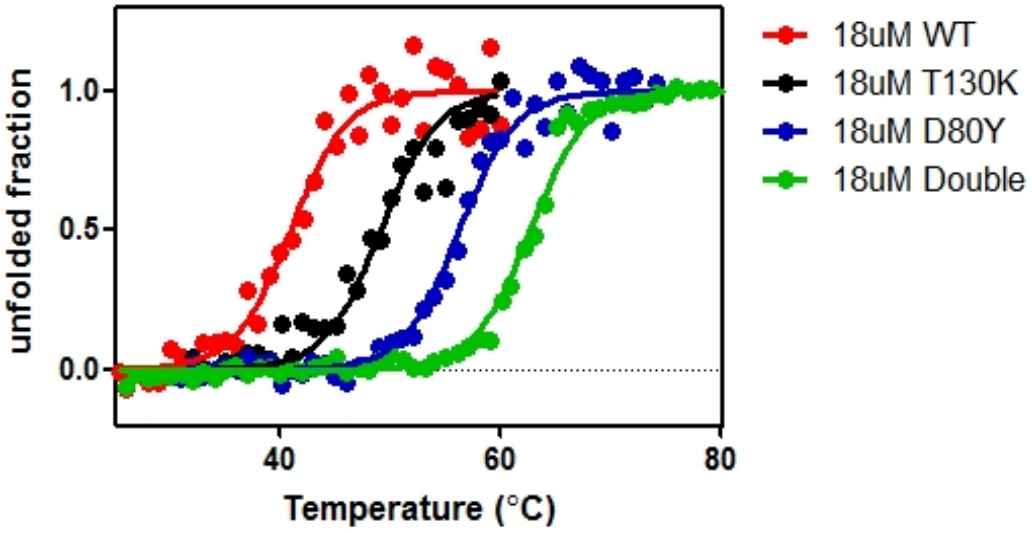

Figure 4. Thermal denaturation of WT and thermostable variants of ANT.

Large-domain dynamics of enzyme is affected by amino acid replacements.

Initial sedimentation velocity data with T130K variant at 5 µM in the absence of substrates showed a broad peak with a sedimentation coefficient (S) of 3.7 and a frictional coefficient (f/f_0) of 1.17. These values result in a molecular weight of 43.2 kDa which is intermediate between the monomeric (28.9 kDa) and dimeric species of this protein. Subsequent experiments showed a concentration-dependent increase in S. These observations suggested that the apo-enzyme is in equilibrium between monomer and dimer species with fast association/dissociation kinetics relative to the timescale of the sedimentation experiment. Therefore the observed peak positions reflect the weight-averaged S of monomeric and dimeric species. It is suggested that T130K variant is in equilibrium between monomeric and dimeric forms. Analogous to T130K variant, all tested three enzymes displayed that increasing concentration of apo-enzymes favored the formation of dimers. (Figure 5)

In order to reveal the quantitative information about monomer-dimer equilibrium, we determined dissociation constants of dimer (K_d) for all enzymes. We plotted weight average sedimentation coefficients as a function of protein concentration for all four enzymes. The isotherms shown were fitted to the monomer-dimer self-association model in SEDPHAT (57). The curves shown in Figure 6 represent the best fit to the data points for all the tested enzymes. Additionally, individual sedimentation velocity runs were used to further validate all above dissociation constants estimated from global fitting. An example is shown in Figure 7.The range of K_d values for dimers for wild type, T130K and D80Y and D80Y/T130K variants were estimated to be (28.2 - 31.6uM), (1.58 - 1.78uM), (0.78 - 0.93uM), (0.40 - 0.46uM) respectively. K_d of dimers steadily increased from the most thermophilic to mesophilic variant by ~70-fold.

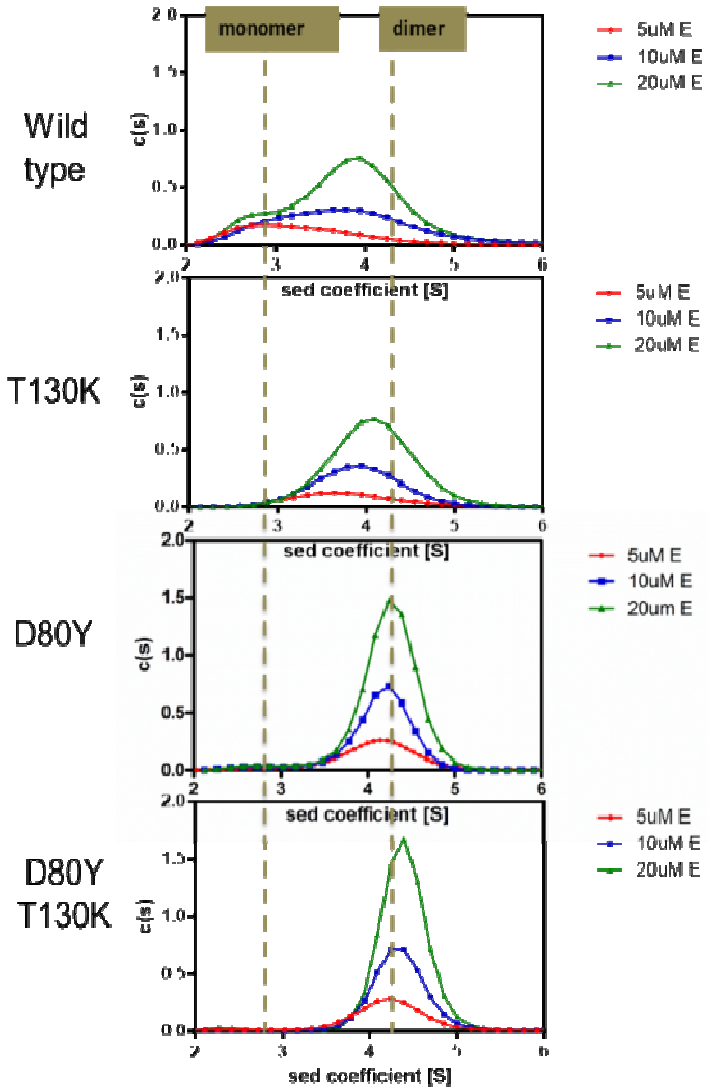

Figure 5. Size distribution of apo enzyme at different concentrations. Red, blue and green lines represent data for 5, 10 and 20uM respectively. All the runs were performed in 50mM PIPES (pH7.5) and 100mM NaCl condition.

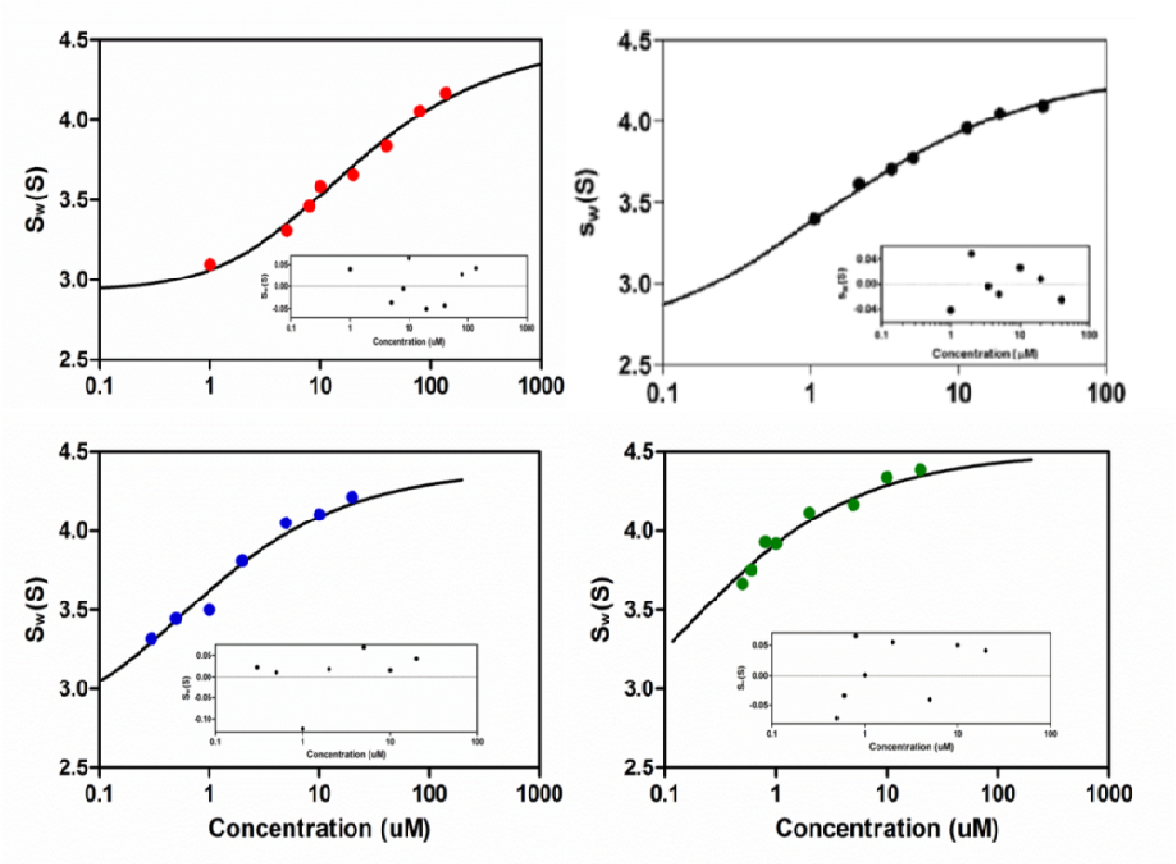

Figure 6. Isotherm of the weight-average sedimentation coefficient as a function of monomer concentration for all tested enzymes - wild type (red dots), T130K (black dots), D80Y (blue dots) and double variant (green dots). The fitted curve is shown with the original data points. The monomer-monomer self-association model was utilized to characterize the dissociation constants of dimer. The insets show the residuals. Sedimentation velocity experiments were done in 50mM PIPES pH7.5 buffer with 100mM NaCl.

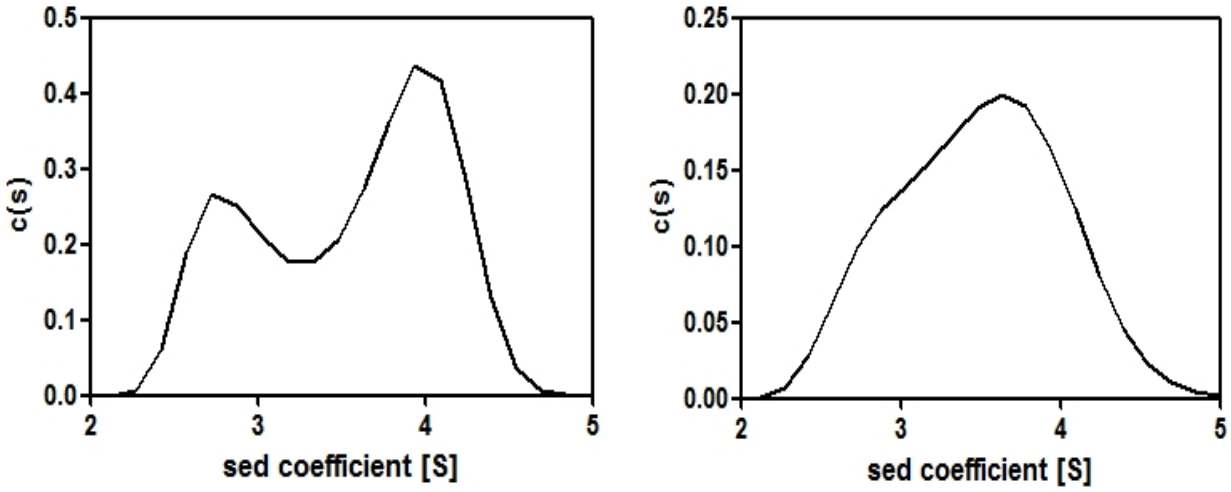

Figure 7. K_d validation. Left panel shows size distribution of 10uM D80Y variant at zero salt condition with Sw=3.55. (K_d from global fit is around 10.8 uM) Right panel shows data for 1uM D80Y at 100mM NaCl condition with Sw=3.50. (K_d from global fit is around 0.85uM.) Sw is expected to be around 3.55 when enzyme concentration reaches K_d of dimer.

Salt effect on monomer-dimer equilibria

Similar sedimentation velocity experiments were performed for wild type, T130K, D80Y and D80Y/T130K variants at zero salt buffer condition (50mM PIPES pH7.5). K_d ranges of dimers for wild type, T130K and D80Y and D80Y/T130K variants were estimated to be (174 - 209uM), (33.11 - 38.02uM), (9.55 - 12.30uM), (3.57 - 4.17uM) respectively (Figure 8). Comparison of K_d values in the presence of zero and 100mM NaCl suggests that increasing salt concentration favored the formation of dimer for all tested enzymes. This strongly suggested that hydrophobic interactions are the major cause of dimerization. Monomer-dimer equilibria of enzymes showed various degrees of sensitivity to salt and not correlated to their thermal stability. The extent of K_d improvement in no salt condition for all enzymes are around 6 fold for WT, 21 fold for T130K variant, 13 fold for D80Y and 9 fold for D80Y/T130K.

D80→Y80 substitution affects thermostability and large-domain motion more significantly than T130→K130 replacement

Replacement of Asp with Tyr at position 80 increases T_m by 14℃ and converts the mesophilic enzyme into a thermostable variant. Besides, this alteration has significantly affected the large domain motion and inter-subunit interface of enzyme. Overall, D80→Y80 replacement confers higher thermostability on ANT enzyme more than T130→K130 replacement. The effects of single replacement of D80→Y80 and T130→K130 on thermostability are independent and cumulative.

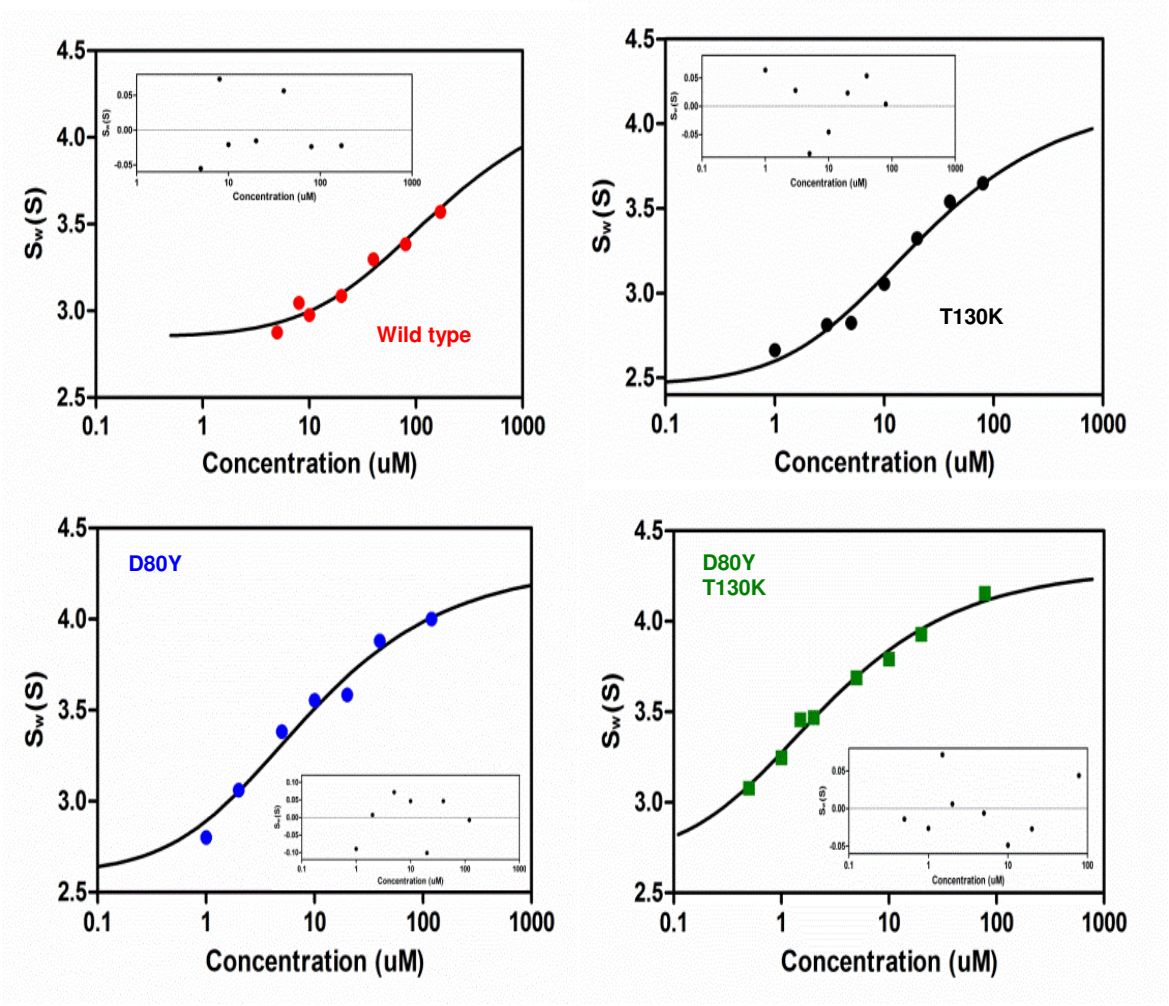

Figure 8. Isotherm of the weight-average sedimentation coefficient as a function of monomer concentration for all tested enzymes - wild type (red dots), T130K (black dots), D80Y (blue dots) and double variant (green dots). The fitted curve is shown with the original data points. The monomer-monomer self-association model was utilized to characterize the dissociation constants of dimer. The insets show the residuals. Sedimentation velocity experiments were done in 50mM PIPES pH7.5 buffer.

Comparison of aminoglycoside recognition by wild type and thermostable variants

Aminoglycoside binding sites are composed of several negatively charged residues that are contributed from both subunits(52). We tested effects of these replacements on aminoglycoside recognition. We chose the three-ring antibiotic-tobramycin, which is a member from kanamycin class, and the four-ring antibiotic- neomycin, a member from neomycin class, as substrates to perform titration binding studies. Binding of aminoglycosides to AGMEs are typically accompanied by changes in the net protonation due to shifts in pK_as of functional groups in both the enzyme and the ligand (59, 60, 62). Therefore, we determined binding enthalpies in three different buffers with different heats of ionization to evaluate the intrinsic binding enthalpies (ΔH_{int}) and the change in net protonation (Δn) for wild type and thermostable variants of ANT (Figure 9 and Figure 10).

Binding of tobramycin was characterized with similar binding affinities for all tested enzymes, with K_d in low micro molar range. However, the binding affinity of neomycin was enzyme-dependent. Wild type and T130K variant have K_d in nano molar range; D80Y and double mutant were characterized with much weaker binding affinities with K_d in micro molar range (Table 3).

Overall, WT enzyme and T130K variant have similar binding parameters to both ligands while the thermodynamic parameters of ligand binding to D80Y and the double mutant were similar to each other but were significantly different than those observed with WT and T130K.

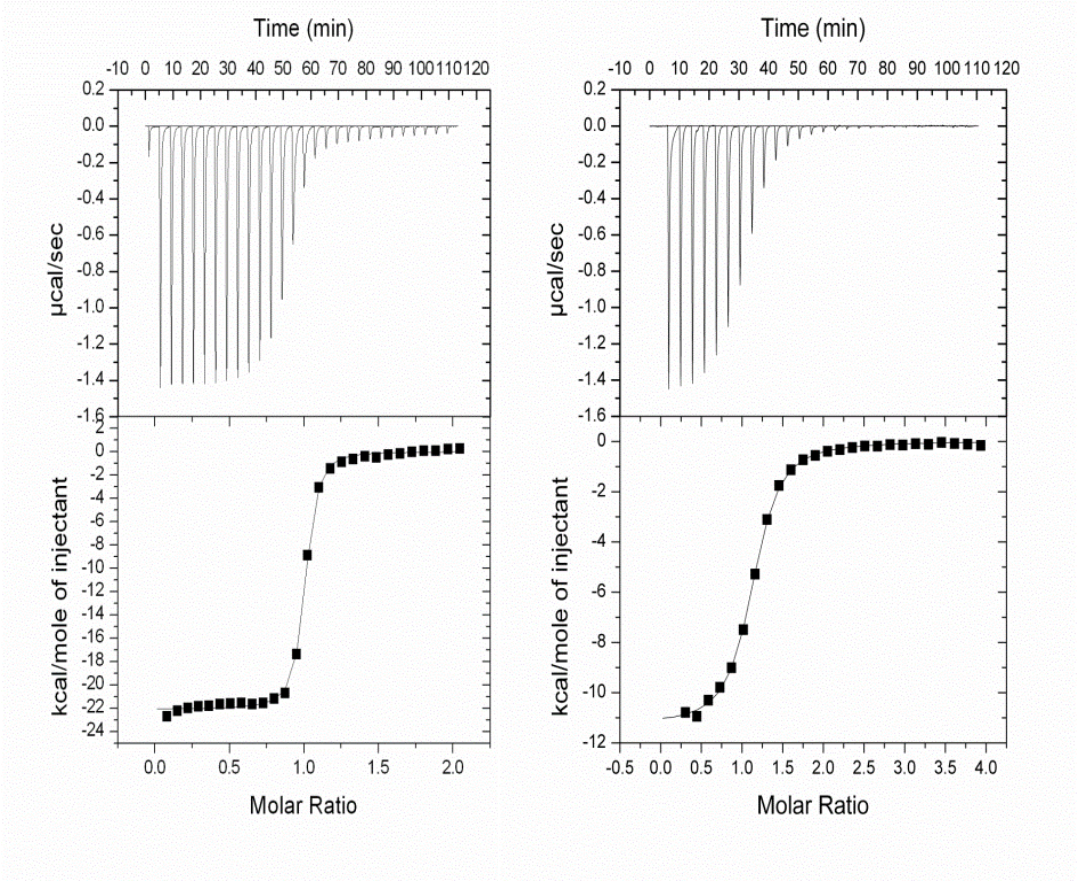

Figure 9. The thermograms and isotherms obtained from the titration of neomycin into WT (left) and double variant (right). Solutions contained 50 mM HEPES pH 7.5, 100 mM NaCl at 25℃.

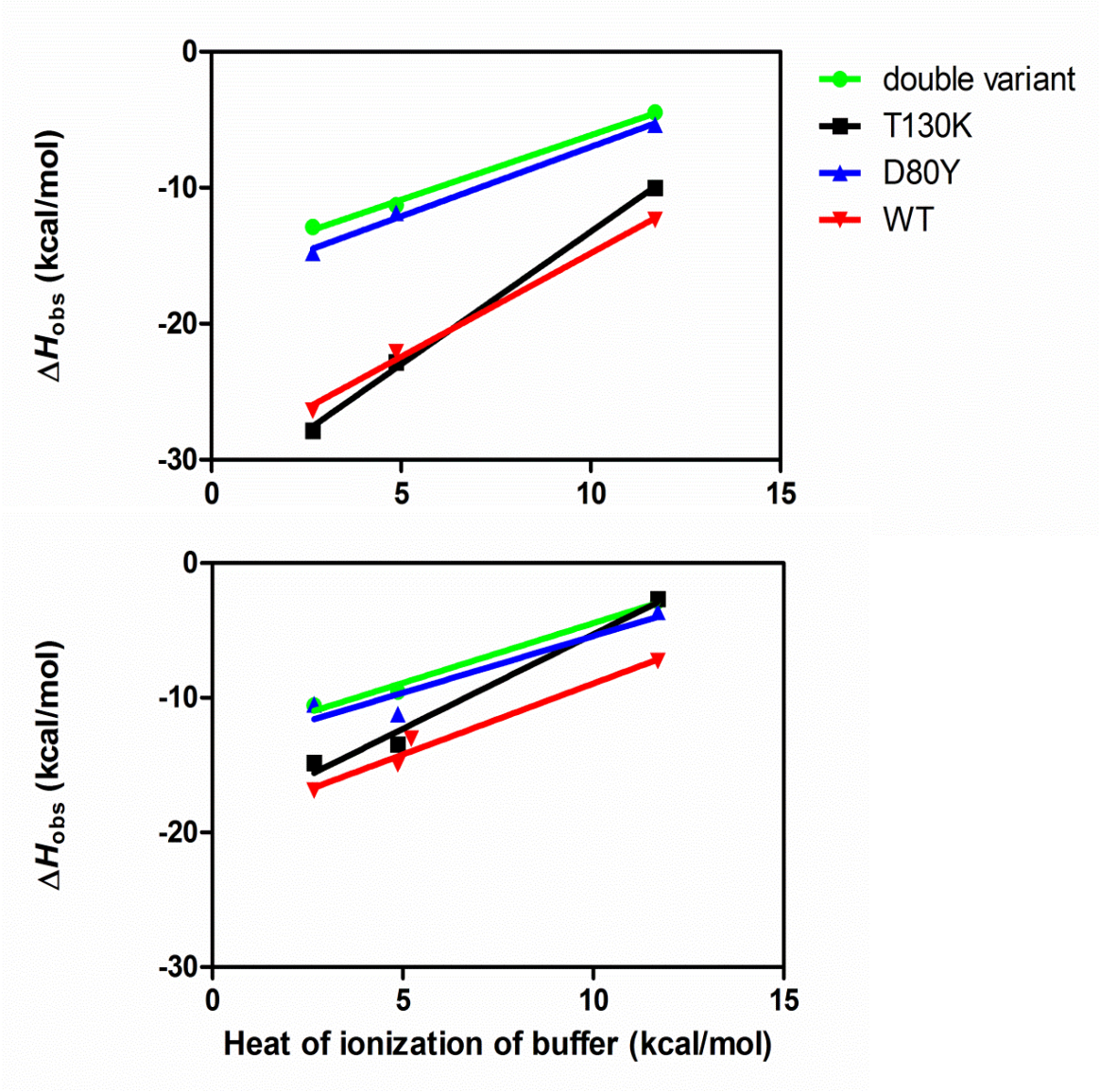

Figure 10. Effect of titratable groups on the observed enthalpy of binding for WT(red), T130K variant (black), D80Y variant (blue) and D80Y/T130K variant (green). Observed enthalpies of neomycin (top panel) tobramycin (bottom panel) as a function of the heat of ionization of the buffer used which are11.70 kcal/mol for Tris, 4.87 kcal/mol for HEPES and 2.67 kcal/mol for PIPES.

Table 3. Thermodynamic parameters of neomycin (Table 3A) and tobramycin (Table 3B) binding to ANT determined by ITC at 25℃. K_d is the dissociation constant, ΔH_{int} is intrinsic enthalpy of binding, ΔG is the Gibbs energy of binding, $T\Delta S$ is entropy of binding, Δn is net transfer of protons by the buffer upon complex formation. In all the cases, the best fit was obtained by using the single-site binding model.

Table 3A Thermodynamic parameters of Neo-enzyme binary complexes*				
	Wild type	T130K	D80Y	T130K D80Y
K_d	39.51±5.56**nM**	24.27±5.51**nM**	0.97±0.45**uM**	0.80±0.34**uM**
TΔ*S* (kcal/mol)	-19.93	-22.36	-8.89	-7.23
Δ*G* (kcal/mol)	-10.11±0.08	-10.40±0.12	-8.32±0.25	-8.41±0.23
ΔH_{in}(kcal/mol)	-30.04±0.77	-32.76±0.58	-17.21±0.58	-15.64±0.38
Δn	1.52±0.10	1.95±0.08	1.02±0.08	0.95±0.05
*Given errors are calculated as the standard error of the mean of three trials. Errors in the intrinsic enthalpy and in net protonation are derived from the deviation from linearity of ΔH_{obs} vs ΔH_{ion} curves. $T\Delta S$ are calculated from ΔH_{in} - ΔG				

Table 3B Thermodynamic parameters of Tob-enzyme binary complexes*				
	Wild type	T130K	D80Y	T130K D80Y
K_d	2.50±0.35**uM**	1.11±0.19**uM**	1.68±0.62**uM**	2.02±0.66**uM**
TΔ*S* (kcal/mol)	-11.84	-11.18	-5.90	-5.52
Δ*G* (kcal/mol)	-7.65±0.09	-8.14±0.10	-7.95±0.20	-7.82±0.18
ΔH_{in}(kcal/mol)	-19.49±0.85	-19.32±1.40	-13.85±2.10	-13.34±0.76
Δn	1.06±0.12	1.40±0.19	0.84±0.28	0.89±0.10
*Given errors are calculated as the standard error of the mean of three trials. Errors in the intrinsic enthalpy and in net protonation are derived from the deviation from linearity of ΔH_{obs} vs ΔH_{ion} curves. $T\Delta S$ are calculated from ΔH_{in} - ΔG				

2.5 Discussion

D80Y and T130K variants adopt different strategies to achieve heat resistance

The 80th residue of the wild type enzyme, aspartic acid is located at the end of the forth strand of beta sheet. In the D80Y variant, Tyr80 is close to the exterior of the protein but the side chain points toward the interior of the protein and does not appear to be directly interacting with solvent molecules. Since the tertiary structures of WT and T130K variant have not been characterized, it is difficult to identify the positions of Asp80 and neighboring residues in the three dimensional structures of enzymes. CD data in near UV region suggest that the aromatic side chains of WT and D80Y variant are in similar environment. (Figure 11)

In spite of the similarity in static structural features, one dynamic property- the monomer-dimer equilibrium is distinct for all enzymes. To obtain information of protein dynamics taking place in a faster time-scale, we examined the local flexibility of enzymes using Molecular Dynamics (MD) simulations in collaboration with Dr. Jerome Baudry (University of Tennessee, Knoxville).

The root mean square fluctuation (RMSF) of each Cα atom from apo-WT, apo-T130K and apo-D80Y during 100ns simulation runs are shown in Figure 12. For all three enzymes, the peak regions of RMSF locate in turns or loops or edges of secondary structures (Figure 13 and 14). Residue 80 is close to one of the peak regions. It is somewhat surprising that T130K, a thermostable variant, resembles WT in local flexibility of most regions of protein, especially the N-terminal domain (amino acid 1-125); however, D80Y presents greater fluctuations compared with WT.

The relation between dynamics and thermostability has been controversial. Most studies in the 1990s suggested that there is an inverse correlation between protein thermostability and flexibility. Thermophilic/thermostable proteins exhibit an increased number of intramolecular interactions that stabilizing protein compared to their mesophilic counterparts(27). As a result, a thermophilic protein would be sturdier with flexibility being less dependent on temperatures than mesophilic proteins. Comparative

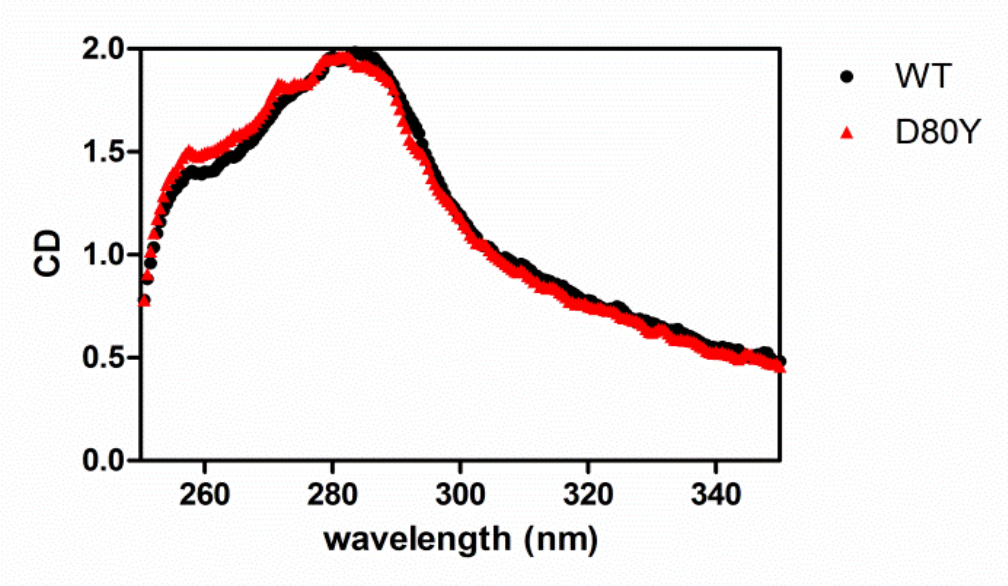

Figure 11. Circular Dichroism characterization of wild type and D80Y ANT in near UV range.

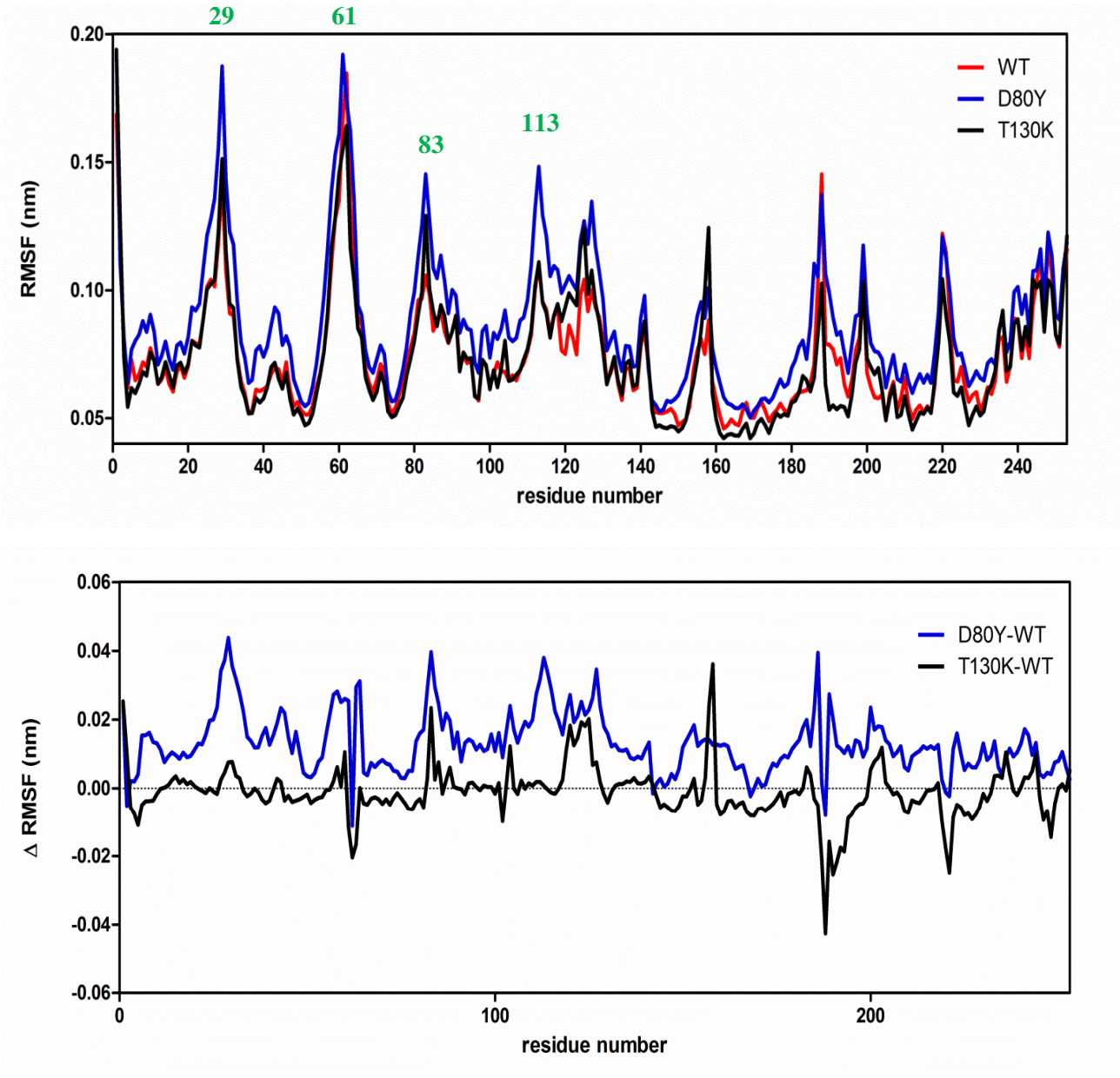

Figure 12. Rms positional fluctuations of each Cα atom of WT, T130K and D80Y from MD simulations. WT (red), T130K (black) and D80Y (blue).The rms positional fluctuations were calculated over each trajectory after rigid body alignment against each subunit of the average structures. Bottom panel- relative Rms positional fluctuation of Cα atom of T130K (black) and D80Y (blue) with respect to WT.

Figure 13. Locations of the residues corresponding to the positions of the peaks in Figure 12.

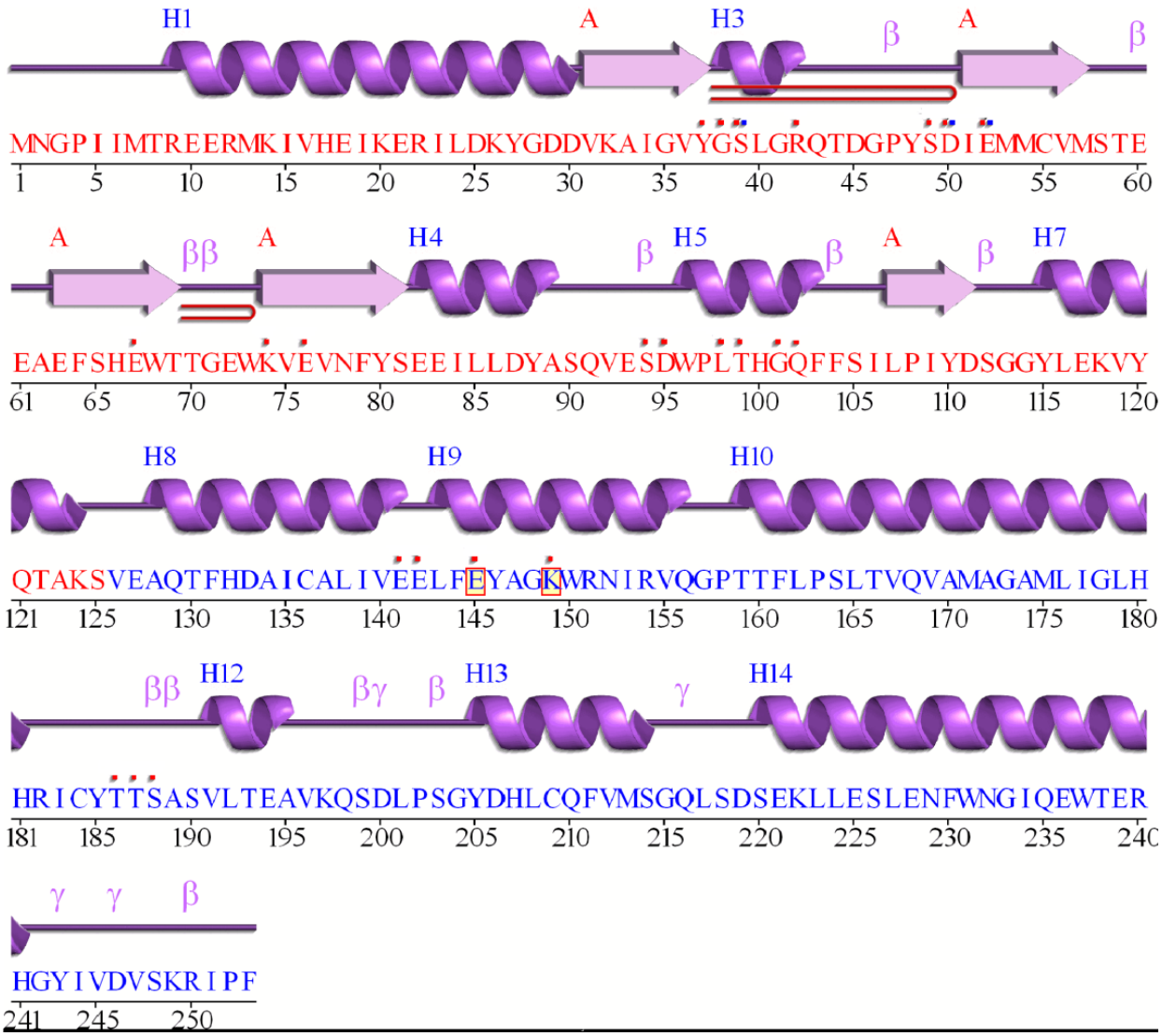

Figure 14. Secondary structure elements of D80Y variant. Helices are labelled as H1, H2… and strands are labelled as their sheets A. Beta turn, gamma turn are labelled as β and γ. Residues contact to ligand and metal are indicated by red and metal squares respectively.

hydrogen-deuterium exchange study on a pair of thermophilic-mesophilic enzymes showed that the thermophilic enzyme is significantly more rigid (less flexible) at room temperature than its mesophilic counterpart(28). However, in recent years, a positive correlation of protein thermostability and flexibility has been proposed and supported by extensive molecular dynamics simulation studies, hydrogen/deuterium exchange studies, nuclear magnetic resonance studies and neutron scattering studies on atomic fluctuations from pairs of thermophilic-mesophilic counterparts. It is found that comparable or larger atomic fluctuations were observed in thermophilic protein than mesophilic ones depending on the time- and length-scale tested. It is suggested that an enzyme with greater flexibility have more sub-conformers at its native state and entropy associated with folding is enhanced(34).

The 130th residue is positioned at the beginning of the fifth major alpha-helical region. Asp133 and Glu127 are within 4.5Å of Thr130 (Figure 15). Substitution of Thr130 with Lys130 is likely to introduce an ionic interaction with one of these residues based on their proximity. This effect, if possible, may result in a linchpin to rigidify the relative orientation of two helices as shown in Figure 15. However, no such specific interactions are possible for Y80 as judged from the crystal structure of D80Y variant.

We hypothesize that thermostability of D80Y and T130K variants are caused by different effects in enhancing enzyme thermostability. T130→K130 improves thermostability by increasing numbers of ionic interactions without significantly changing enzyme fluctuations at native state. It is possible that D80→Y80 replacement stabilizes previously sub-stable conformers in mesophilic enzyme and displays more stable basins that native protein can visit, thus increasing the conformational entropy and the heat resistance capability. D80→Y80 may also benefit a tighter internal hydrophobic packing of enzyme by introducing an aromatic residue replacing a residue with ionizable side chain.

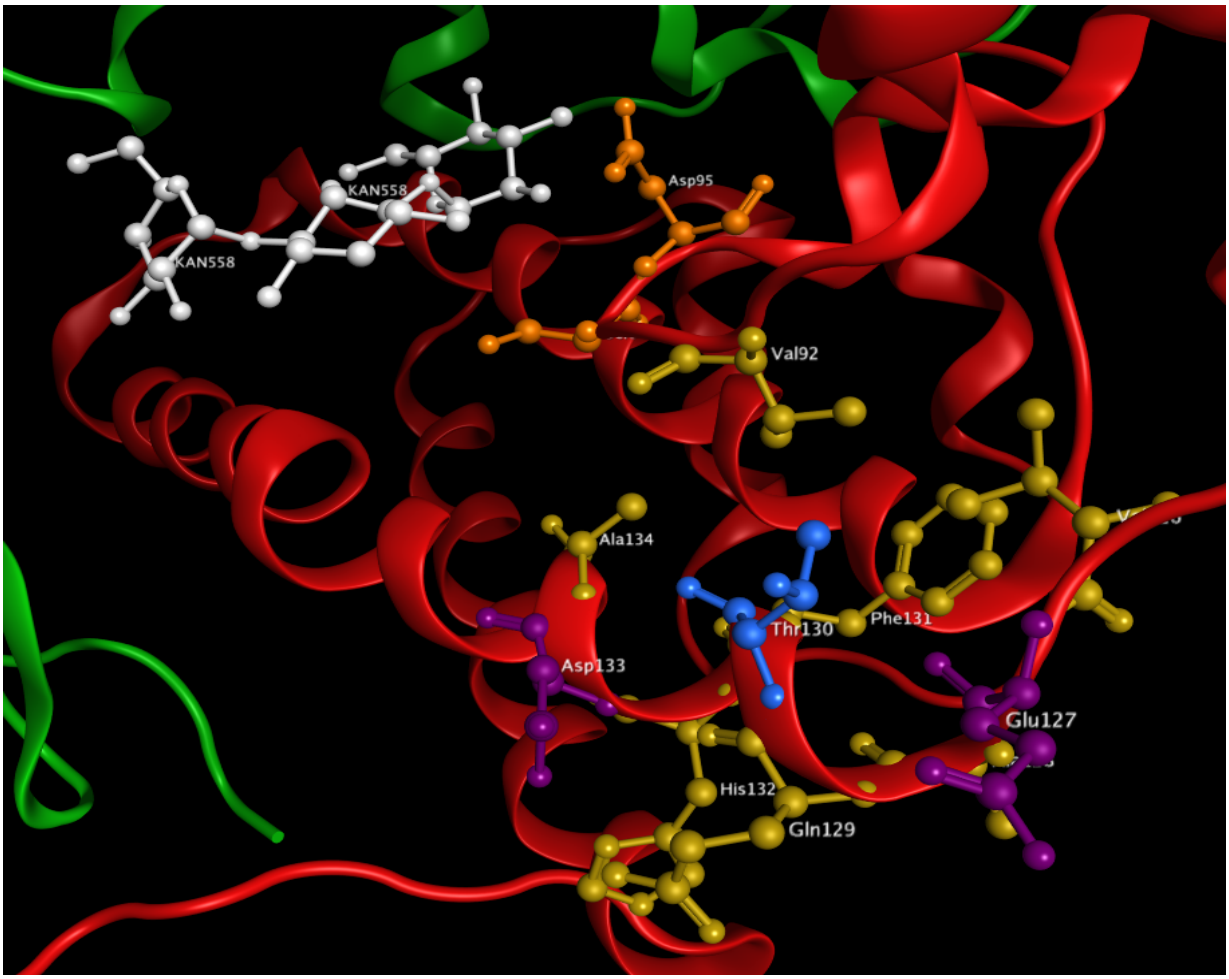

Figure 15. Residue contacts of Thr130 (blue) in structure of D80Y variant. Acidic residues are highlighted in purple and other contacts are shown in yellow. Two subunits are shown in red and green ribbons. Kanamycin A molecule is shown in white. Asp95 (orange) locates at the downstream of Val92 and directly forms an electrostatic interaction with kanamycin A.

A fine line between thermophilic and heat stable mesophilic enzymes

Taken together, two thermostable variants T130K and D80Y differ by only a single residue replacement of the wild type mesophilic enzyme. Both variants display enhanced melting temperatures and execute catalysis at high temperatures at which the mesophilic enzyme is inactive. However, T130K variant still keeps molecular properties of mesophilic enzyme. T130→K130 does not trigger significant change in enzyme local flexibility or ligand binding while D80Y variant has distinct properties in ligand recognition and dynamics as summarized in Table 4. Thus, it appears that T130K is simply a heat stable mesophilic enzyme, instead of being a true thermophilic enzyme.

We note that much effort has been made to improve thermostability of certain enzymes by simply introducing single or multiple mutation sites. It is found that simultaneous introduction of several selected mutations had almost identical effect towards T_m enhancement as the accumulation of each individual replacement(63). Each replacement triggered a slight conformational change occurring predominantly around respective mutations sites but has barely global effects on protein backbone conformation(64). Each local mutation only contributes to enzyme stability by rigidifying local interaction network in an independent manner. Ratcliff et al questioned the nature of engineered thermostable protein to be a thermostable mesophilic enzyme instead of a true thermophilic enzyme(65).

Many heat resistant enzymes, including naturally existing ones as well as engineered enzymes, display higher melting temperature as a result of stabilizing interactions from residue mutagenesis but still keep many features of mesophilic enzymes. Here we attempt to draw a line separating such heat resistance enzymes from true thermophilic enzyme.

Table 4. Summary of our investigations on thermostable variants of ANT4.

	Wild type	**T130K**	**D80Y**
T_m	40.9±0.5℃	49.1±0.6℃	56.2±0.2℃
Optimum temperature(53)	~52℃	~57℃	~60℃
Kd(dimer formation)	28.2 ~ 31.6uM	1.58 ~ 1.78uM	0.78 ~ 0.93uM
Kd(neo)	39.51±5.56nM	24.27±5.51nM	0.97±0.45uM
ΔH_{Tob}(kcal/mol)	19.49±0.85	-19.32±1.40	-13.85±2.10
Local flexibility	Resembles T130K	Resembles WT	Larger RMSF
*** ΔH_{Tob} is the intrinsic enthalpy of tob-enzyme binary complexes**			

Criteria separating thermophilic and heat stable mesophilic enzymes

If thermophilic and heat stable mesophilic enzymes are indeed different, what are the criteria (molecular properties) separating the two types of enzymes? The apparent differences between T130K and D80Y variants are observed ligand binding and internal atomistic fluctuations.

We hypothesize that protein dynamics which also affects thermodynamics of protein-ligand interactions is the key feature separating thermophilic and heat stable mesophilic enzymes. As discussed in the prior sections, molecular reasons for thermophilicity have evolved over years from structural rigidity to the effects of dynamic properties of proteins. We speculate that heat stable mesophilic enzyme exhibit comparable flexibility with mesophilic counterparts at room temperature while true thermophilic enzymes show greater flexibility and sample more accessible states resulting in enhanced entropies and thus higher stability. As a result, more accessible states would also generate more binding-favorable/unfavorable states so that substrate binding of thermophilic enzymes could be different with mesophilic homologs. Thus, thermodynamic properties of ligand binding to enzymes may yield clues on their "thermophilicity".

Another possible criterion separating thermophilic and heat stable mesophilic enzymes would be solvent effects. Both ligand binding and local flexibility are linked with solvent effects. Previous studies suggest that the more significant local fluctuations of thermophilic/thermostable proteins compared to their mesophilic counterparts (which protect proteins against thermal stress by increasing conformational entropy of native state) are likely induced by solvent effects. Comparison of solvent-protein interactions for many thermophilic, mesophilic and psychrophilic enzymes suggests a continuum of adjustment of solvents effects accompany to thermostability adjustment. Aminoglycoside binding sites are largely solvent-exposed as indicated in the crystal structure of D80Y. Previous ligand binding studies on one of the variant T130K suggested that the role of water molecules and their interaction with the ligand and the enzyme are different for different aminoglycosides. Therefore, it is highly likely that different effects of solvent reorganization on ligand recognition by the thermophilic

variants will be observed. Such effects may also account for the different binding behaviors observed for D80Y and T130K enzymes. We thus speculate that solvent effects may be different for the thermophilic (D80Y) and the heat stable mesophilic (T130K) enzymes and serve as (one of) the molecular mechanism(s) attributing to real thermophilicity.

Residue substitutions distal from active sites affect ligand binding

Residues D80 and T130 are distal from the active site. Substitution at each position induced changes ligand binding. It is possible that D80→Y80 replacement stabilizes a previously sub-stable conformation in mesophilic enzyme and creates more stable basins for native enzyme. As a result, solvent molecules associating with protein surface reorganize and affect ligand binding by modifying the entropic contribution of the binding free energy of ligands/substrates to the protein. Another possible yet con-competing mechanism would be that small structural rearrangements of the active site leading to modifications of the network of water molecules affecting the protein: ligand interactions.

In order to pinpoint the potential long-range interaction cascade of residues, we mapped the residues within 4.5Å of Thr130 (Figure 15) and Tyr80 (Figure 16) on D80Y crystal structure. Thr130 and Val92 forms hydrophobic interactions. It is likely that for T130K variant, the positively charged Lys130 would cause a rearrangement of interactions around Val92 thus affecting location of downstream Ser94 and Asp95 which make important contacts with kanamycin A (Figure 15). Similarly, one of the neighboring residues of Tyr80 - Asn78, forms hydrogen bonds with Glu76 and Glu67, which are the key residues interacting with antibiotics by electrostatic bonding (Figure 16). It is possible that WT with Asp80 may result in different local interactions of these residues.

.

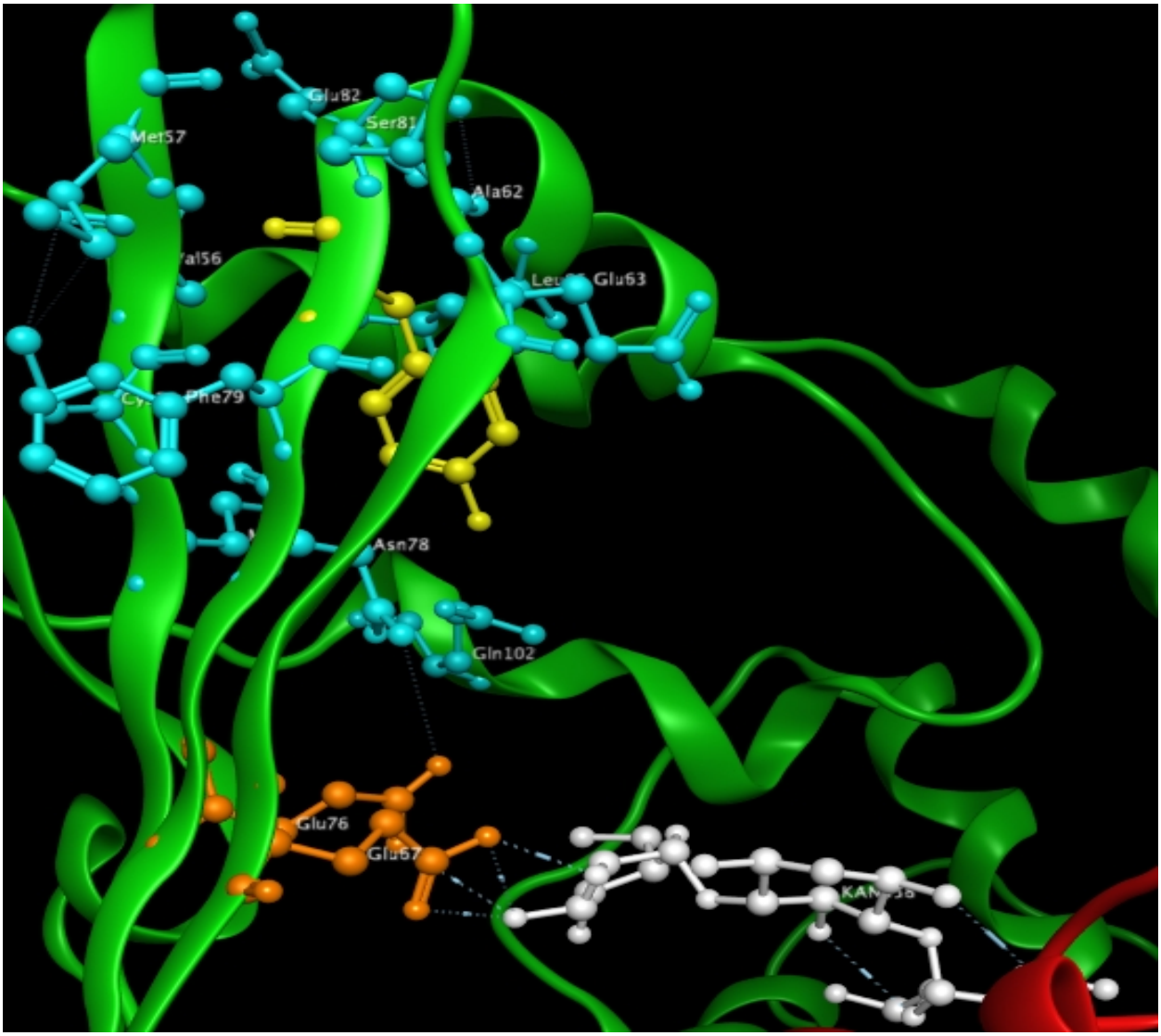

Figure 16. Residue contacts of Tyr80 (yellow) in structure of D80Y variant are shown in blue. Kanamycin A molecule is shown in white. Glu67 and Glu76 are shown in orange.

Oligomerization and thermophilicity

There are records of many thermophilic enzymes adopting different oligomerization states compare to their mesophilic counterpart. For example, methionine amino peptidase exists as a dimer for the thermophilic enzyme from *Pyrococcus furiosus* and as monomers for the mesophilic enzyme from *Escherichia coli*(66). However, these proteins have similar subunit folds but very different primary sequences. To our knowledge, this is the first work showing monomer-dimer equilibria are different for a dimeric mesophilic enzyme and thermophilic counterparts with a single residue difference between the variants.

Implications to thermophilic protein design

Thermophilic proteins adopt various strategies to achieve thermal adaptation. Extended comparisons between thermophilic and mesophilic counterparts have revealed that salt bridges(12-15), side chain-side chain hydrogen bonds and internal hydrophobic packing increase in the majority of the thermophilic proteins. Protein conformational flexibility(34) and water-protein surface(1) have also been suggested to be crutial to thermostability. It is difficult to draw a common conclusion to underlie the mechanisms of all thermophilic proteins. Some studies were also focused on what types of amino acids would stabilize protein by strengthening local contacts. Our work suggests that the global effects instead of specific local interactions caused by residue replacements would be more important to the heat resistance improvement of enzyme. Enhancement on global protein flexibility rather than local interactions is more powerful in improving enzyme thermophilicity.

CHAPTER III

THERMODYNAMIC CHARACTERIZATOIN OF A THERMOSTABLE ANTIBIOTIC RESISTANCE ENZYME, THE AMINOGLYCOSIDE NUCLEOTIDYLTRANSFERASE 4'

A version of this chapter was originally published by Xiaomin Jing, Edward Wright, Amber N. Bible, Cynthia B. Peterson, Gladys Alexandre, Barry Bruce and Engin H. Serpersu in *Biochemistry,* 2012, 51(45): 9147-9155.

3.1 Abstract

The crystal structure of ANT shows that the enzyme is a homodimer and each subunit binds one kanamycin and one Mg-AMPCPP where the transfer of the nucleotidyl group occurs between the substrates bound to different subunits. Sedimentation velocity analysis of ANT by analytical ultracentrifugation showed the enzyme is a mixture of monomer and dimer in solution and that dimer formation is driven by hydrophobic interactions between the subunits. In this chapter, we examine the effects of ligand in monomer-dimer equilibrium using T130K variant. The binding of aminoglycosides shifts the equilibrium towards dimer formation while the binding of the co-substrate, MgATP, has no effect on the monomer-dimer equilibrium. Surprisingly, binding of several divalent cations including Mg^{2+}, Mn^{2+} and Ca^{2+} to the enzyme also shifted the equilibrium in favor of dimer formation. Binding studies, performed by electron paramagnetic resonance spectroscopy, showed that divalent cations bind to the aminoglycoside binding site in the absence of substrates with a stoichiometry of 2:1. The binding of all aminoglycosides to ANT was determined by isothermal titration calorimetry to be enthalpically favored and entropically disfavored with an overall favorable Gibbs energy. Aminoglycosides in the neomycin class each bind to the enzyme with significantly different enthalpic and entropic contributions while those of the kanamycin class bind with similar thermodynamic parameters.

3.2 Introduction

ANT4 catalyze the covalent attachment of nucleotide monophosphate to hydroxyl groups of aminoglycosides via a metal-ATP cofactor. To date, there are only a few studies describing enzymatic and thermodynamic properties of these enzymes (67-72). In this work, we have used a previously described kanamycin-resistance gene (73) from the thermophilic bacterium *Bacillus stearothermophilus* that encodes a thermostable kanamycin nucleotidyltransferase. Prior to use this gene was modified to be codon optimized for expression in *Thermosynechococcus elongatus (74)*. This thermostable variant of the aminoglycoside nucleotidyltransferase (4′) was found to confer resistance to a large number of aminoglycosides (68). A crystal structure is available for an ANT variant, D80Y/T130K, which was determined at 3.0Å resolution in the absence of substrates (51). Additionally, the D80Y variant was solved at 2.5Å resolution with kanamycin and MgAMPCPP (52). Both the apo- and substrate-bound structures are homodimers with high similarity and a 0.75 Å root-mean-square deviation of superimposed alpha carbon positions. Each monomer is shown to bind both, the antibiotic and the metal-nucleotide (Figure 3). The binding sites for both substrates are solvent-exposed and contain charged residues contributed by both subunits, establishing an active site between the two protein monomers. The orientation of substrates facilitates transfer of the nucleotidyl group between the substrates bound to different monomers. In this paper, we describe unique features of subunit-subunit interactions that are differentially affected by substrates, as well as the thermodynamic properties of enzyme–aminoglycoside complexes. Data presented represent the first characterization of the thermodynamic properties of a thermostable variant of aminoglycoside- modifying enzymes.

3.3 Experimental procedures

Reagents

All materials were of the highest purity commercially available and were purchased from Sigma-Aldrich Co. (St. Louis, Mo) unless otherwise noted. Ni^{2+} Sepharose High Performance resin was purchased from GE Healthcare (formerly Amersham, Piscataway, NJ). Marco-Prep High Q Support strong anion exchange column was purchased from Bio-Rad Laboratories (Hercules, CA). Thrombin, prepared from thrombostat by cation exchange chromatography as described previously (54), was graciously provided by Dr. Elias Fernandez (The University of Tennessee).

Protein Expression and Purification.

Bacteria containing plasmid were selected on LB plates with 50 µg/ml ampicillin and 34 µg/ml chloramphenicol. Cells were grown at 37°C, induced by 1 mM IPTG and harvested after four hours of induction. Cells were re-suspended in 50 mM Tris-HCl, pH 7.5, 100 mM NaCl, and 1 mM EDTA and lysed by three freeze-thaw cycles. The lysate was treated with DNase for 1h and centrifuged at 14,000 rpm for 30 min. ANT, carrying a Histag made up of 6 histidines, was isolated by Ni^{2+} affinity chromatography. The 6xHis tag was removed by thrombin cleavage for 1 h at room temperature. Following cleavage, the protease was removed by chromatography over a strong anion exchange resin. Fractions containing ANT were pooled and dialyzed against 50 mM PIPES buffer pH 7.5, concentrated by ultrafiltration, and stored at 4°C. Under these conditions, the enzyme remained active for several weeks. Protein concentrations were determined by absorbance at 280 nm using an extinction coefficient of 50,880 M^{-1} cm^{-1}. Protein concentrations are reported as monomer concentrations unless otherwise indicated.

Analytical Ultracentrifugation (AUC)

Sedimentation velocity experiments were performed in a Beckman XL-I analytical ultracentrifuge using an An-50Ti rotor. Sample volumes of 400 µL were loaded into double-sector cells and allowed to equilibrate for an hour at 25°C prior to the run. Absorbance scans at 280 nm were collected at a rotor speed of 50,000 rpm at 25°C.

Sedimentation data were fit to a continuous (c(s)) distribution model using SEDFIT (version 12.44) (55). Protein partial specific volume, buffer density and buffer viscosity were calculated using SEDNTERP (56).

Prior to all experiments, the enzyme was dialyzed extensively against the buffer of interest. For analysis of salt-dependent and concentration-dependent dimerization of ANT, the buffer contained 50 mM PIPES, pH 7.5, and variable concentrations of NaCl. For analysis of aminoglycoside-dependent, nucleotide-dependent, and divalent cation-dependent dimerization, the buffer contained 50 mM PIPES pH 7.5 and 100 mM NaCl. For pH dependence, a triple buffer system (10 mM MES, 10 mM HEPES and 10 mM BICINE, 50 mM NaCl) was used to minimize any non-pH related effects arising from usage of different buffer components. For temperature dependence, the buffer consisted of 50 mM MOPS pH 7.5 and 50 mM NaCl. To evaluate the effect of metals on the monomer-dimer equilibrium of this enzyme, 2.0 mM Mg^{2+}, Mn^{2+} or Ca^{2+} was added to 10 µM ANT.

For quantitative analysis of the monomer-dimer equilibrium of ANT, a concentration range of 1-40 µM protein was used. Different detection strategies were required to maximize sensitivity and ensure that measurements were within the linear region over this concentration range. At lower concentrations (1.0-3.5 µM) absorbance at 230 nm was used to monitor sedimentation. Absorbance data at 280 nm were acquired for ANT at 5-20 µM and at 40 µM enzyme the interference optical system was used for detection. For data analysis, the weight-average sedimentation coefficients ($s_w(S)$) were determined at each concentration by integrating the peaks from the c(s) distributions using SEDFIT (55). Isotherm analysis of $s_w(S)$ as a function of protein concentration with the monomer-dimer self-association model in SEDPHAT was employed to determine the dissociation constant (57). The values from isotherm analysis were used as the initial guesses in global analysis to determine the kinetics of the interaction (57, 58). For the determination of k_{off}, multiple data sets were analyzed in SEDPHAT using a form of the Lamm equation that explicitly incorporates the reaction kinetics occurring during sedimentation (75). All reported errors from data analyses with SEDPHAT were generated using the F-statistics calculator.

Electron Paramagnetic Resonance.

Continuous wave X-band (9.78 GHz) EPR spectra of free Mn^{2+} were recorded by using a Bruker (Billerica, MA) EMX spectrometer. All EPR experiments were performed at room temperature using a thin wall quartz capillary with a volume of 80 µl. Spectra were collected with 20 mW power, 100 kHz modulation frequency, 4.0 G modulation amplitude and 4 scans. All the samples were prepared in 50 mM Pipes, 100 mM NaCl, pH 7.5. Enzyme concentration was 60 µM for all EPR experiments and the manganese concentration ranged from 10 to 300 µM. To observe the effect of aminoglycoside on metal binding, the concentration of neomycin was adjusted to 100 µM to achieve > 99% enzyme saturation.

Isothermal Titration Calorimetry.

ITC experiments were performed at 25℃ using a VP_ITC mircocalorimeter from Microcal, Inc. (Northampton, MA). The concentrations of aminoglycoside antibiotics were determined by enzymatic assay with aminoglycoside acetyltransferase(3)-IIIb as described previously (59). Both enzyme and ligand solutions were degassed under vacuum for 10 min at 20℃. Titrations consisted of 27 injections of 10 µL and were separated by 240 s and Cell stirring speed of 300 rpm was used. The observed heat change (Δ*H*) evolving from binary complex formation and the binding affinity were directly determined from titration. Free energy (Δ*G*) and entropy (Δ*S*) changes associated with binding were determined from equations (1) and (2). All data were fit to a single-site binding model using Origin 5.0 software from Microcal, Inc.

$$\Delta G = -RTlnK_a \qquad (1)$$

$$\Delta G = \Delta H - T\Delta S \qquad (2)$$

Determination of the intrinsic enthalpy of binding was done as described earlier (60). Briefly, the following equation was used to evaluate and subtract the contribution, if any, by pK_a shifts of titratable sites:

$$\Delta H_{obs} = \Delta H_{int} + \Delta H_{ion}\Delta n \qquad (3)$$

Here, ΔH_{obs} is the observed enthalpy change, ΔH_{ion} is the heat of ionization of the buffer and $\mathbf{\Delta}n$ is the net transfer of protons by the buffer upon complex formation. ΔH_{int} and Δn are determined from the intercept and slope respectively. Under these experimental conditions, a net proton uptake by the enzyme-ligand complex yields a positive Δn.

3.4 Results and Discussion

ANT is in equilibrium between monomeric and dimeric forms.

Initial sedimentation velocity data with ANT T130K variant at 5 µM in the absence of substrates showed a broad peak with a sedimentation coefficient (S) of 3.7 and a frictional coefficient (f/f_0) of 1.17. These values result in a molecular weight of 43.2 kDa which is intermediate of the monomeric (28.9 kDa) and dimeric species of this protein. Subsequent experiments showed a concentration-dependent increase in S (Figure 17). These observations suggested that the apo-enzyme is in equilibrium between monomer and dimer species with fast association/dissociation kinetics relative to the timescale of the sedimentation experiment. Therefore the observed peak positions reflect the weight-average S of monomeric and dimeric species.

The weight average sedimentation coefficients were plotted as a function of protein concentration to determine the distribution of species and the monomer-dimer equilibrium constant. Figure 6 (upper right panel) shows isotherm analysis using the data acquired with a concentration range of 1 to 40 µM enzyme. The data were fitted to the monomer-dimer self-association model in SEDPHAT (57). The curve represents the best fit to the data points which yields a dissociation constant of 1.7 ± 0.4 µM for the dimer and sedimentation coefficients of 2.7 S and 4.4 S for the monomer and dimer respectively. Global analysis of the sedimentation velocity data acquired at 280 nm showed the dissociation rate constant (k_{off}) to be 10^{-2} sec^{-1} for the ANT dimer in the absence of substrates (Figure 6 upper right).

Binding of aminoglycosides promotes dimerization of T130K variant.

The crystal structure shows that the C4□-OH of kanamycin is ~5Å away from the α-phosphorus of the nucleotide bound to the opposite subunit. This is an optimal orientation for a direct nucleophilic attack to facilitate nucleotide transfer. However, the distance between the substrates bound to the same monomer is ~24 Å, indicating that the enzyme must be in its dimeric form to catalyze the reaction (52). Since solution studies showed that the enzyme exists in equilibrium between the monomeric and dimeric forms, we evaluated the effect of various factors on this equilibrium. First, two different substrates, kanamycin and neomycin, representing each of the two major structurally different groups of aminoglycoside antibiotics (Figure 2), were tested. As shown in Figure 18, increasing concentrations of either aminoglycoside cause a clear shift to higher S values. These results demonstrate that aminoglycosides shift the equilibrium heavily in favor of dimer formation. Additionally, both antibiotics slow the dissociation rate of the dimer by more than a hundred-fold ($k_{off} \geq 10^{-4}$ sec^{-1}). Unlike the apo-enzyme, two separate signals for monomer and dimer respectively are clearly visible in binary enzyme–aminoglycoside complexes confirming the slow dissociation rates of the dimer in the presence of both antibiotics. Neomycin is able to achieve this effect at lower concentrations reflecting the tighter binding of neomycin compared to kanamycin A. An additional 2.5-fold increase in the neomycin concentration above the saturation level did not lead to the formation of any higher order complexes. In contrast, the binding of the co-substrate MgATP to the enzyme does not lead to dimerization of the enzyme. These data are consistent with the kinetic studies that showed that substrate binding is ordered where the aminoglycoside binds before the nucleotide (68) . Thus the binding of an aminoglycoside to the enzyme induces the formation of the "active" form of the enzyme.

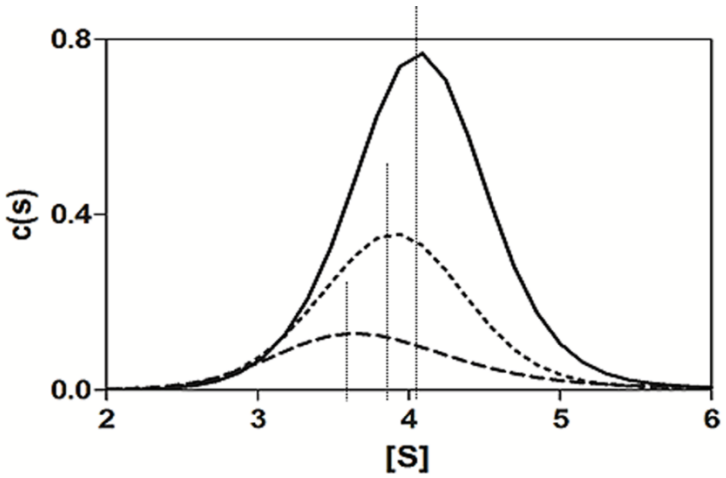

Figure 17. Size distribution of apo-T130K variant at different concentrations. Dashed, dotted and full lines represent 5μM, 10 μM and 20 μM enzyme respectively. All the runs were performed in 50 mM PIPES pH 7.5, 100 mM NaCl.

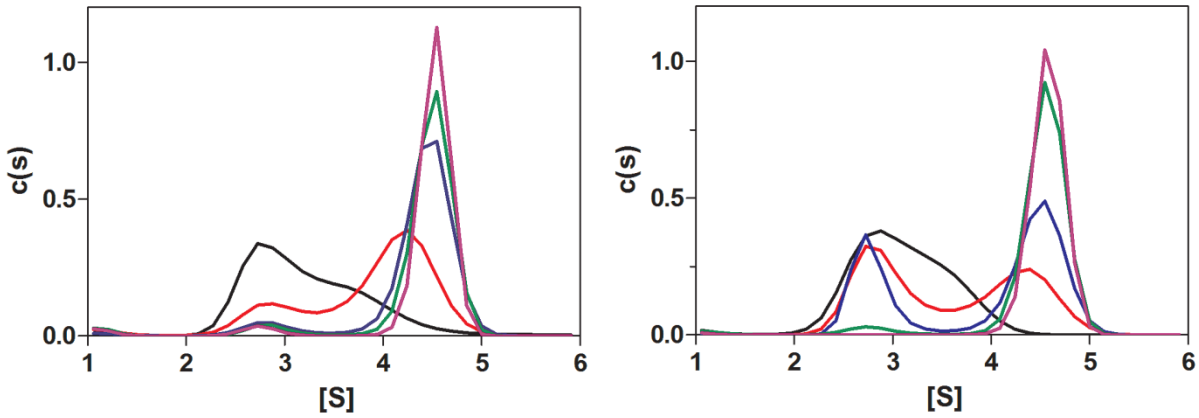

Figure 18. Effect of aminoglycosides on monomer-dimer equilibrium of T130K variant. AUC data for kanamycin (left) and neomycin (right) complexes as a function of increased saturation of enzyme with antibiotics (black, no aminoglycoside, saturation progressively increases with colors orange, blue, green and red where red represents the full saturation). Experiments were performed at 25℃ in 50 mM PIPES, pH 7.5, containing 100 mM NaCl.

Binding of divalent cations to T130K variant induces enzyme dimerization.

In the absence of substrates, the sedimentation velocity results show an increase in sedimentation coefficient consistent with almost complete dimerization for all three of the divalent cations tested (Mg^{+2}, Mn^{+2}, and Ca^{+2}). These observations are consistent with the crystal structure of the apo-protein that showed a dimeric protein with a bound divalent cation to each monomer (51), which was proposed to be Zn^{2+}. However, other transition metals were also consistent with the observed electron density. Our attempts to test the effect of Zn^{2+} were unsuccessful because the presence of millimolar concentrations of zinc caused precipitation of the enzyme under our experimental conditions.

In an attempt to clarify the effects observed with Mg^{2+} versus MgATP, experiments were conducted with ATP in sufficient excess of Mg^{2+} to ensure that all Mg^{2+} was in complex with ATP. In these experiments, no effect on the monomer-dimer equilibrium was observed, indicating that free Mg^{2+} binds to a different site than MgATP. To gain insight on the binding of the divalent cations to the apo-enzyme, we used electron paramagnetic resonance (EPR) spectroscopy. Paramagnetic Mn^{2+} was used as the EPR probe. In aqueous solution free manganese gives a sharp concentration-dependent EPR signal. Upon binding to protein the signal broadens to undetectable levels. Titration of the enzyme with Mn^{2+} showed that Mn^{2+} binds to ANT with a dissociation constant of 100 ± 20 μM and a stoichiometry of 2:1 Mn^{2+}: enzyme. In the crystal structure of apo-ANT, two cations were observed in symmetrical locations between the carboxylate groups of two glutamine residues (Q76 and Q145) from opposite monomers (51). In the substrate bound structure these two residues were shown to make important contacts with the aminoglycoside (52). To test whether aminoglycoside inhibits metal binding, the Mn^{2+} binding experiment was repeated in the presence of Neomycin. The presence of the aminoglycoside prevented binding of Mn^{2+} to the enzyme (Figure 19 and 20) suggesting that the divalent cations exert their effect on the monomer-dimer equilibrium through the antibiotic binding site, which is rich in negatively charged titratable groups.

a.

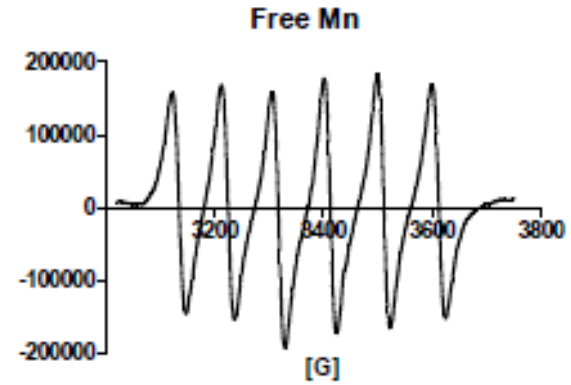

b

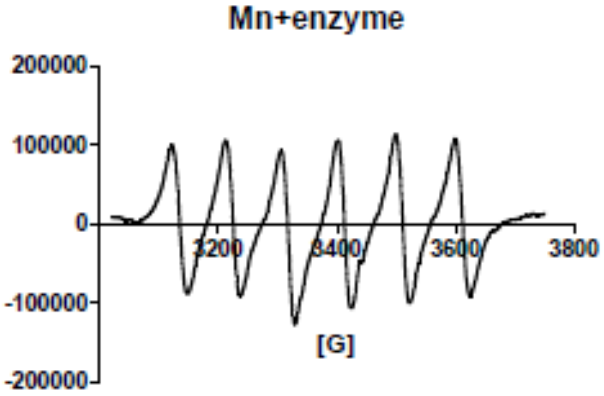

c

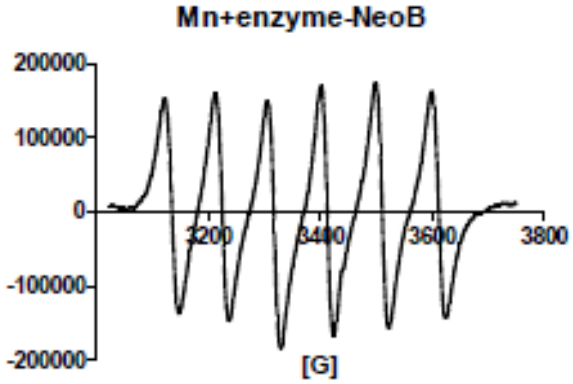

Figure 19. a EPR signal from 50uM Mn in enzyme-free solution. b. EPR signal from 50uM Mn in solution containing 60uM T130K variant. c. EPR signal from 50uM Mn in solution containing 60uM T130K enzyme and 100uM neomycin.

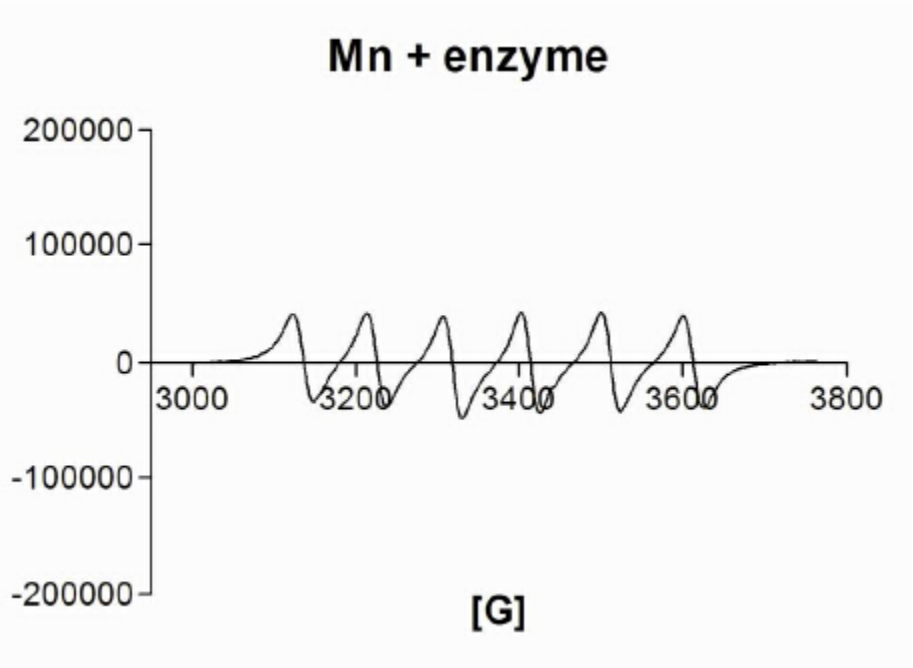

Figure 20. EPR signal from 10uM Mn in the presence of 60uM T130K enzyme.

Effects of salt, pH and temperature on equilibrium.

Other factors were tested in sedimentation velocity experiments to gain insight into the nature of the dimerization process of T130K variant. Increasing salt concentration favored the formation of dimer, suggesting that hydrophobic interactions are the major cause of dimer formation (Figure 21). However, neither pH changes between 6.5 and 8.5 nor the temperature range between 15 ℃ and 35 ℃ showed a significant effect on the monomer-dimer equilibrium.

Thermodynamic properties of aminoglycoside–T130K variant complexes.

Thermodynamic parameters of the binary enzyme–aminoglycoside complexes were determined by isothermal titration calorimetry (ITC) using six different aminoglycosides representing two major groups of aminoglycoside antibiotics, kanamycins and neomycins (Figure 2). Experimental conditions were selected to ensure that the predominant form of the apo-enzyme was a dimer. Therefore, the heat of dimerization, if any, should not contribute significantly to the observed enthalpy. Furthermore, separate experiments showed that no detectable heat was observed as a concentrated enzyme solution was diluted into the ITC cuvette suggesting that the heat of dimerization was very small. A typical ITC data set for the binding of two aminoglycosides with highly different binding affinities to T130K variant is shown in Figure 22.

Binding of all aminoglycosides to T130K variant was enthalpically favored and entropically disfavored (Table 5) following the general trend observed with several different aminoglycoside modifying enzymes (59, 60, 62, 76-79). Enthalpy-entropy compensation plots shown in Figure 23 yield a slope of 1.13 ± 0.1 indicating a slightly more significant role of enthalpy in the formation of the binary enzyme–aminoglycoside complexes. Prior to this work, such data with all other aminoglycoside modifying enzymes yielded slopes in the range 1.00-1.09 (59, 62, 77). Data acquired in this work show that ANT exhibits the most enthalpy-driven ligand binding among the AGMEs tested to date.

The binding enthalpy of kanamycins varied less than 3.5 kcal/mol with similar variations in entropy. This yielded similar Gibbs energies of binding for all three

kanamycins, which are also reflected in the narrow range of dissociation constants for these aminoglycosides (Table 5). In contrast, the neomycin group aminoglycosides showed significant differences in most of the thermodynamic parameters.

One member of the neomycin group, ribostamycin, binds to T130K variant about ~800- and ~80-fold weaker than neomycin and paromomycin respectively. The binding enthalpy for ribostamycin was also significantly less favored compared to the kanamycins. The binding affinity of ribostamycin was also the lowest among all antibiotics tested. These observations are likely due to the structure of ribostamycin, which is identical to neomycin but without the fourth ring (Figure 2). This ring could make a number of contacts with the enzyme leading to the significantly more favorable enthalpy of binding observed with neomycin and paromomycin relative to ribostamycin. Because the crystal structure of the enzyme is available only with bound kanamycin, it is not easy to predict what interactions will occur between the enzyme and the neomycins in order to determine specifically the effect of the fourth ring. However, one may speculate that larger antibiotics such as neomycin and paromomycin would fit into the large active site cavity between the two subunits of the enzyme better than smaller aminoglycosides such as kanamycins and thus would make more favorable contacts with the enzyme. An analogous situation was observed with another aminoglycoside modifying enzyme, the aminoglycoside *N*-acetyltransferase(3)-IIIb, where the larger aminoglycosides with four rings (neomycin, paromomycin) bind to the enzyme with significantly more favorable enthalpies than three ring aminoglycosides. The size of the active site cavity also affected the binding stoichiometry of aminoglycosides to this enzyme such that three-ring aminoglycosides bind to the enzyme with stoichiometries higher than 1 while the complexes of larger aminoglycosides with the enzyme displayed a 1:1 stoichiometry suggesting that bulkier aminoglycosides provide better fits to large active site cavity of this protein as well (59).

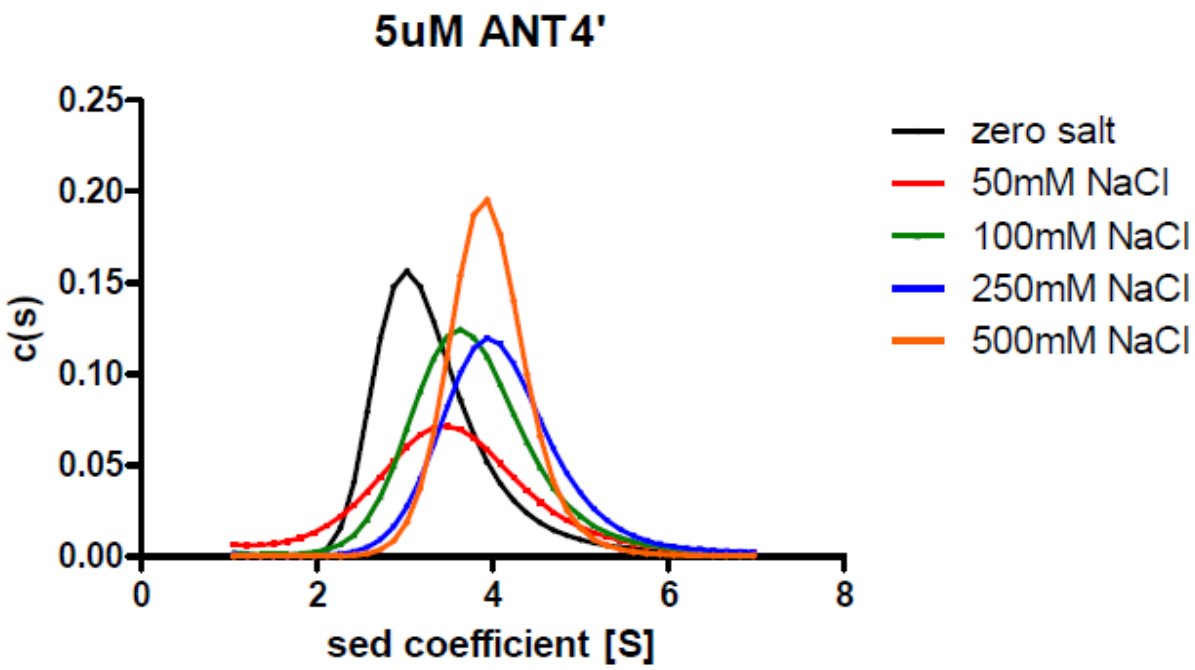

Figure 21. Concentration distribution of 5uM T130K enzyme as a function of salt concentration.

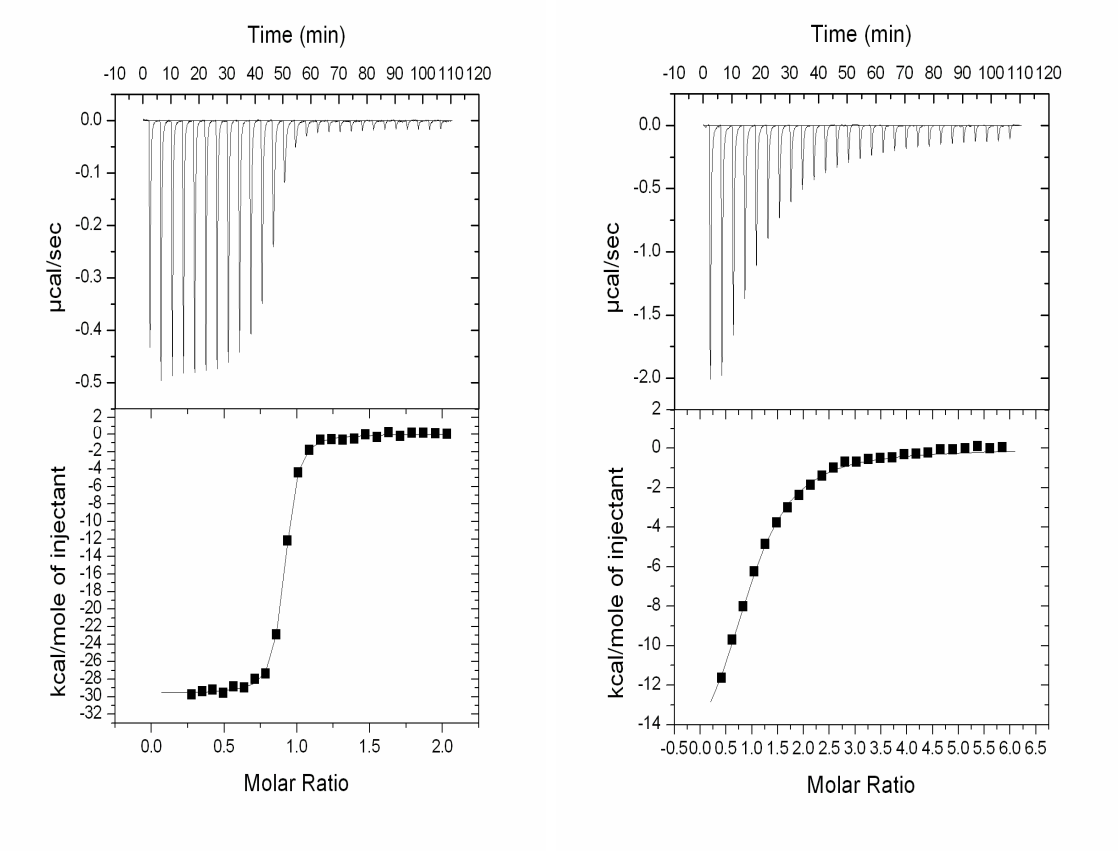

Figure 22. The thermograms (upper panels) and isotherms (lower panels) obtained from the titration of aminoglycosides (left panel; neomycin, right panel; kanamycin A) into a solution containing 20 µM T130K variant in 50 mM PIPES pH 7.5, 100 mM NaCl at 25℃. In both cases, the best fit was obtained from single-site binding model.

Table 5. Thermodynamic parameters of aminoglycoside binding to ANT T130K variant determined by ITC at 25°C. K_d is the dissociation constant, ΔH_{int} is intrinsic enthalpy of binding, ΔG is the Gibbs energy of binding, $T\Delta S$ is entropy of binding, Δn is net transfer of protons by the buffer upon complex formation. In all the cases, the best fit was obtained by using the single-site binding model.

	K_d (μM)	ΔH_{int} (kcal/mol)	$T\Delta S$ (kcal/mol)	ΔG (kcal/mol)	Δn
Kanamycin A	6.6 ± 1.1	-20.7 ± 0.4	-13.6	-7.1 ± 0.1	1.4 ± 0.1
Kanamycin B	4.6 ± 1.6	-22.7 ± 2.8	-15.4	-7.3 ± 0.3	1.3 ± 0.5
Tobramycin	1.1 ± 0.3	-19.3 ± 1.4	-11.2	-8.1 ± 1.0	1.4 ± 0.2
Neomycin B	0.02 ± 0.01	-32. ± 0.6	-22.3	-10.4 ± 0.3	2.0 ± 0.1
Paromomycin	0.2 ± 0.04	-38.0 ± 1.8	-28.9	-9.1 ± 0.1	2.4 ± 0.2
Ribostamycin	15.4 ± 4.2	-12.6 ± 1.2	-6.0	-6.6 ± 0.2	0.7 ± 0.2

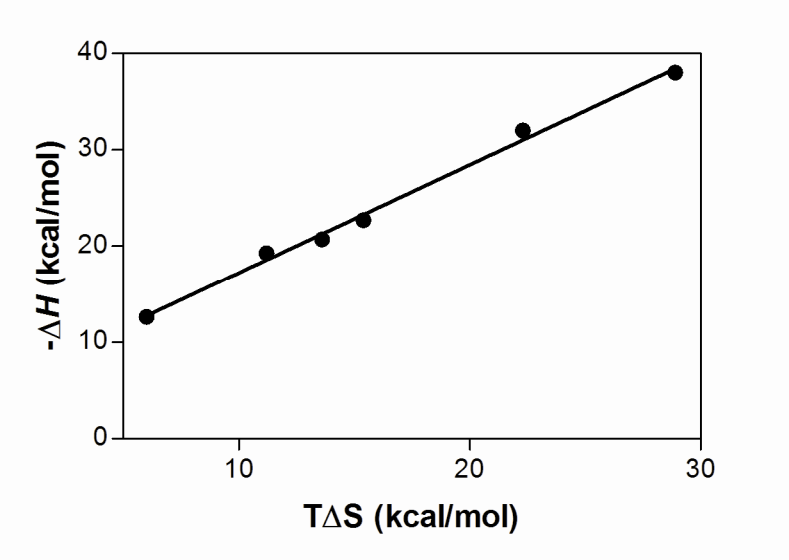

Figure 23. Enthalpy-entropy compensation plot of T130K variant. Data from Table 5 is used to construct the plot.

Binding of aminoglycosides to AGMEs are typically accompanied by changes in the net protonation due to shifts in pK_as of functional groups in both the enzyme and the ligand (59, 60, 62). Therefore, we determined binding enthalpies in three different buffers with different heats of ionization to determine the intrinsic binding enthalpies (ΔH_{int}) and the change in net protonation (Δn) upon binding of aminoglycoside to ANT (Figure 24). Data showed that the net protonation remained the same with all three kanamycin group aminoglycosides, while significant differences were observed between the members of the neomycin group (Table 5). The net protonation was highest with paromomycin with a value of 2.4 ± 0.2 and neomycin with 2.0 ± 0.1. The lowest among all aminoglycosides also belongs to the neomycin group where ribostamycin has a Δn value of 0.7 ± 0.2. This suggests that the two amine functions in the fourth ring of neomycin and paromomycin may have upshifted pK_as in the enzyme–aminoglycoside complexes and their contribution must be significant. Therefore, the lack of the fourth ring in ribostamycin excludes their contribution to the observed Δn. This is also consistent with the differences in binding enthalpies and suggests that multiple strong interactions between the fourth ring in aminoglycosides and the enzyme exist. Other effects such as contributions from the functional groups of the enzyme on the observed Δn, however, cannot be excluded. In fact, attribution of the changes in Δn only to the functional groups of the ligand is incorrect and has already been demonstrated with a different aminoglycoside modifying enzyme (60). Therefore, in the absence of data for the functional groups of the enzyme, any further attributions on the sites that may contribute to Δn will be misleading.

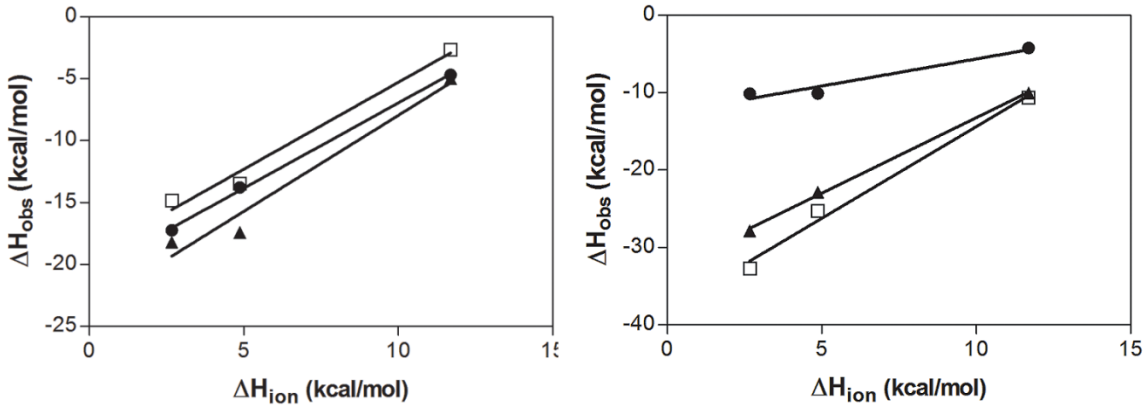

Figure 24. Effect of titratable groups on the observed enthalpy of binding. Observed enthalpies of kanamycins (left) neomycins (right) as a function of the heat of ionization of the buffer used which are11.70 kcal/mol for Tris, 4.87 kcal/mol for HEPES and 2.67 kcal/mol for PIPES.

Aminoglycoside recognition by ANTT130K variant

Single site differences between structurally similar aminoglycosides can lead to dramatic changes in the thermodynamic parameters of enzyme–aminoglycoside complexes(80). If one compares the small differences in thermodynamic parameters of ANT–aminoglycoside complexes it becomes clear that the change of the hydroxyl function (kanamycin A) to amine (kanamycin B) at the C2´ site yields 2 kcal/mol more favorable enthalpy, suggesting that the amine group makes an additional contribution to the enthalpy that may be due to ionic interactions with the enzyme. Two ionizable groups, E67 and E141 are the most likely candidates for the interaction of this site with the enzyme as they are 2.2 and 3.1Å away, respectively (Figure 25a). Although represents a significant difference between the binding enthalpies of kanamycin A and kanamycin B, the observed 2 kcal/mol difference in ΔH_{int} between these two aminoglycosides is smaller when compared to data acquired with other aminoglycoside modifying enzymes (59, 62, 77) suggesting that ANT is the least capable enzyme in differentiating these two aminoglycosides.

Comparison of ΔH_{int} of kanamycin B to tobramycin suggests that the replacement of the hydroxyl group at the C3′ site (kanamycin B) with hydrogen (tobramycin) lowers the binding enthalpy by 3.4 kcal/mol. Since the enthalpy of a hydrogen bond can be between 1 and 5 kcal/mol, these data thus strongly suggest that the –OH group at this site is involved in H-bond interactions. Three residues with a less than 4Å distance from the C3′-OH of kanamycin A are E67, E76 and E145 (Figure 25b) and are good candidates for this interaction. Thus, the observed 3.4 kcal/mol lowering of the binding enthalpy with tobramycin is consistent with the loss of 1 to 2 hydrogen bonds.

Comparison of neomycin and paromomycin reveals the contribution of the group at the C6′ position to the formation of the binary enzyme–aminoglycoside complex. It appears that this site makes the most significant impact on the binding of aminoglycosides to the enzyme among the three similar pairs and suggests that interactions of this site with the enzyme are more susceptible to changes. Substitution of C6′-OH by C6′-NH_2 in neomycin yields a 10-fold increase in binding affinity. The Gibbs energy for the binding of neomycin is more favorable despite the fact that

paromomycin binding to T130K variant is enthalpically favored by 5.3 kcal/mol over neomycin which is slightly overcompensated by a more disfavorable entropy (Table 5).

The kanamycin-bound structure of ANT shows that there are no functional groups in the enzyme within 4 Å distance of the C6′-site. The closest residue is E46, which is 4.9 Å away. Therefore, e insertion of a charged group at this site must lead to an altered binding mode for the aminoglycoside or an altered conformation of the active site which has a significant effect on the thermodynamic parameters of antibiotic association. The result is the significantly different thermodynamic properties observed with these two structurally similar aminoglycosides. Such significant differences between the thermodynamic properties of complexes formed with structurally similar aminoglycosides are not surprising. In fact, far more dramatic differences between the complexes of neomycin and paromomycin has been observed with another aminoglycoside modifying enzyme, the aminoglycoside-*N*-acetyltransferase(3)-IIIb where the change in heat capacity showed opposite signs with these aminoglycosides(80).

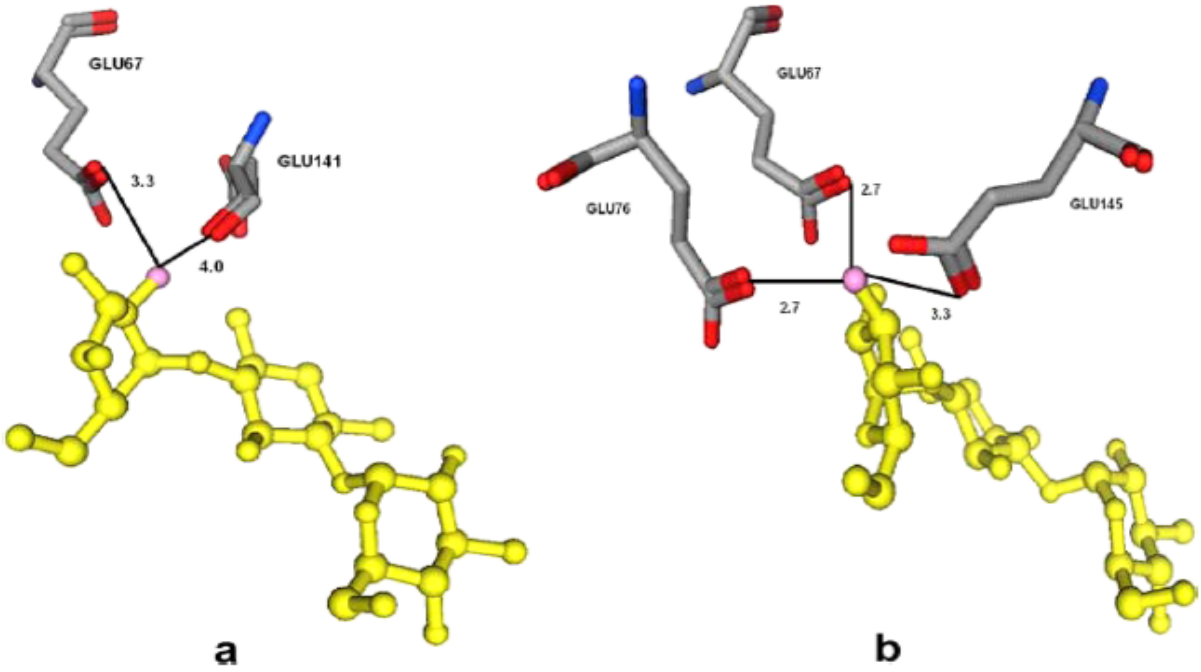

Figure 25. a) Residue contacts of kanamycin 2′-OH within 4.1Å. Residues shown in stick representation are E67, E141. Yellow molecule in ball and stick representation is kanamycin A. 2′-O is highlighted in pink. b. residue contacts of kanamycin A 3′-OH within 4.1Å. Residues shown in stick representation are E67, E76 and E145.Yellow molecule in ball and stick representation is kanamycin A. 3′-C is highlighted in pink.

CHAPTER IV

SOLVENT REORGANIZATION PLAYS A TEMPERATURE DEPENDENT ROLE IN ANTIBIOTIC SELECTION BY A THERMOSTABLE AMINOGLYCOSIDE NUCLEOTIDYLTRANSFERASE 4' T130K

A version of this chapter was originally published by Xiaomin Jing and Engin H. Serpersu in *Biochemistry,* 2014, 53(34):5544-5550.

4.1 Abstract

Effect of solvent reorganization on enzyme-ligand interactions was investigated using one of the thermostable variants- T130K variant. Data showed that the binding of aminoglycosides to T130K variant causes exposure of polar groups to solvent. However solvent reorganization becomes the major contributor to the enthalpy of the formation of enzyme–aminoglycoside complexes only above 20°C. The change in heat capacity (ΔCp) shows an aminoglycoside-dependent pattern such that it correlates with the affinity of the ligand to the enzyme. Differences in ΔCp values determined in H_2O and D_2O also correlated with the ligand affinity. The temperature dependent increase in the offset temperature (T_{off}), the temperature difference required to observe equal enthalpies in both solvents, is also dependent on the binding affinity of the ligand and the steepest increase was observed with the tightest binding aminoglycoside, neomycin. Overall, these data, together with earlier observations with a different enzyme, the aminoglycoside *N3*-acetyltransferase-IIIb (Norris and Serpersu, 2011, Biochemistry, 50;9309) show that solvent reorganization or changes in soft vibrational modes of the protein can have interchangeably the role of major contributor to the complex formation depending on temperature. These data suggest that such effects may be more generally apply to enzyme-ligand interactions and studies at a single temperature may provide only a part of the whole picture of thermodynamics of enzyme-ligand interactions.

4.2 Introduction

Heat capacity is one of the major thermodynamic quantities that are measured in proteins and protein-ligand interactions. The sign of the change in heat capacity (ΔCp) informs on solvation of polar and nonpolar groups. Multiple sources can also affect (ΔCp) of which exposure of hydrophobic surfaces to solvent, changes in soft vibrational modes of proteins and conformational changes may be the more important ones(81). In this work, we investigated the effect of solvent reorganization in recognition of aminoglycosides by T130K variant. Contrary to many observations reported in literature, where the exposure or burial of nonpolar surfaces usually determine effects of solvent on the thermodynamics of protein-ligand interactions, we observed that exposure of polar groups of ANT to solvent dominates thermodynamics of protein-ligand interactions. However, the role of solvent reorganization in enthalpy of ligand binding shows strong temperature dependence and becomes dominant factor only above 20℃.

4.3 Experimental Procedures

Reagents.

All materials were of the highest purity commercially available and were purchased from Sigma-Aldrich Co. (St. Louis, Mo) unless otherwise noted. Deuterium oxide (99.9%) was purchased from Cambridge Isotope Laboratories (Andover, MA). Ultrafiltration membranes were purchased from Millipore (Billerica, MA). IPTG was obtained from Inalco Spa (Milan, Italy) and high-performance Ni-Sepharose resin was purchased from GE healthcare (Pittsburg, PA). Aminoglycosides were purchased as sulfate salts and used only as base after the removal of sulfate ion with ion exchange chromatography.

Protein Expression and Purification.

A thermostable variant of ANT, T130K was purified as described earlier(82). Purified ANT was dialyzed against buffer containing 50 mM MOPS pH 7.5 and 100mM NaCl. For D_2O experiments, enzyme in H_2O was buffer-exchanged with D_2O buffer containing 50mM MOPS pD7.5 (>98%D_2O) and 100mM NaCl using five cycles of ultrafiltration. Purified ANT in H_2O and D_2O were stored at 4°C and the enzyme remained active (>90%) for three weeks. Protein concentrations were determined by absorbance at 280 nm using an extinction coefficient of 50,880 M^{-1} cm^{-1}. Protein concentrations are reported as monomer concentrations unless otherwise indicated.

Isothermal Titration Calorimetry.

ITC experiments were performed at temperature range 5°C to 40°C using a VP-ITC microcalorimeter, from (formerly Microcal) GE healthcare (Pittsburg, PA). Since uncertainty in ligand concentration is a major contributor to the errors in ITC data, in our laboratory, concentrations of aminoglycoside antibiotics were are always determined by enzymatic assays or by NMR (72). In this case we used another aminoglycoside-modifying enzyme, the aminoglycoside acetyltransferase(3)-IIIb, which has high turnover rates (59). Concentration of AGs are determined by 5-6 repetitions and errors ranged between 1% and 3% for different aminoglycosides and included in the data analysis as experimental error.

ITC experiments were performed as described earlier with other aminoglycoside-modifying enzymes (59, 60, 71, 83, 84). Concentration of ANT in the calorimetry cell was 20 μM (monomer). Aminoglycoside concentration in the syringe was in 0.2 to 0.8 mM range. Both enzyme and ligand solutions were degassed under vacuum for 15 min prior to the start of experiments. A buffer system composed of 50 mM MOPS, pH7.5 and 100 mM NaCl was used in all titration experiments. Titrations consisted of 27 injections of 10 μL and were separated by 240 s. Cell stirring speed of 300 rpm was used. The observed heat change (ΔH) evolving from binary complex formation and the binding affinity (K_a) were directly determined from titration. Gibbs energy (ΔG) and

entropy ($T\Delta S$) changes associated with binding were determined from equations (1) and (2).

$$\Delta G = -RTlnK_a \quad (1)$$

$$\Delta G = \Delta H - T\Delta S \quad (2)$$

Origin software package 5.0 was used for nonlinear least-squares fitting of binding data to a single site binding model. Data were also fitted by using global fitting procedure SEDPHAT (57). Errors shown in plots are SEM based on two or more repetitions of the titrations of most of the data points and represent experimental errors rather than curve fitting errors.

4.4 Results

Aminoglycosides show differential effects on the change in heat capacity of ANT T130K variant.

Temperature dependence of the binding enthalpy of four aminoglycosides to T130K variant was measured to determine the change in heat capacity in H_2O and D_2O. Two aminoglycosides from the kanamycin group (kanamycin A and tobramycin) and two from the neomycin group (neomycin and paromomycin) were used (Figure 2). Figure 3 shows data acquired with two of the four aminoglycosides that showed the largest (neomycin) and lowest differences (kanamycin A) in binding enthalpies determined in light and heavy water. The heat capacity change (ΔCp), determined from the slopes of ΔH vs. temperature plots, was negative in all four cases but was dependent on the aminoglycoside (Table 6). With the exception of kanamycin A, all ΔCp values, determined in H_2O, are significantly more negative than those observed in most carbohydrate-protein interactions, which is usually between 0.1 and 0.4 kcal·mol^{-1}·K^{-1}. The determined ΔCp values showed a logarithmic correlation with the binding affinity of the aminoglycoside to the enzyme in both solvents (Figure 26) indicating a direct correlation between Gibbs energy and the heat capacity change.

Table 6. Solvent specific heat capacity changes of T130K variant-AG complexes

	ΔCp (H_2O)	ΔCp (D_2O)	ΔCp_{tr}
Neomycin	-0.81±0.06	-0.47±0.05	0.34±0.06
Paromomycin	-0.67±0.05	-0.41±0.05	0.26±0.05
Tobramycin	-0.55±0.01	-0.39±0.04	0.16±0.04
Kanamycin A	-0.35±0.03	-0.29±0.03	0.06±0.03

Units are in kcal mol^{-1} deg^{-1}. Data shown with fitting errors from ΔH vs. T plots.

$\Delta C_{p\ (tr)} = \Delta C_p(D_2O) - \Delta C_p(H_2O)$.

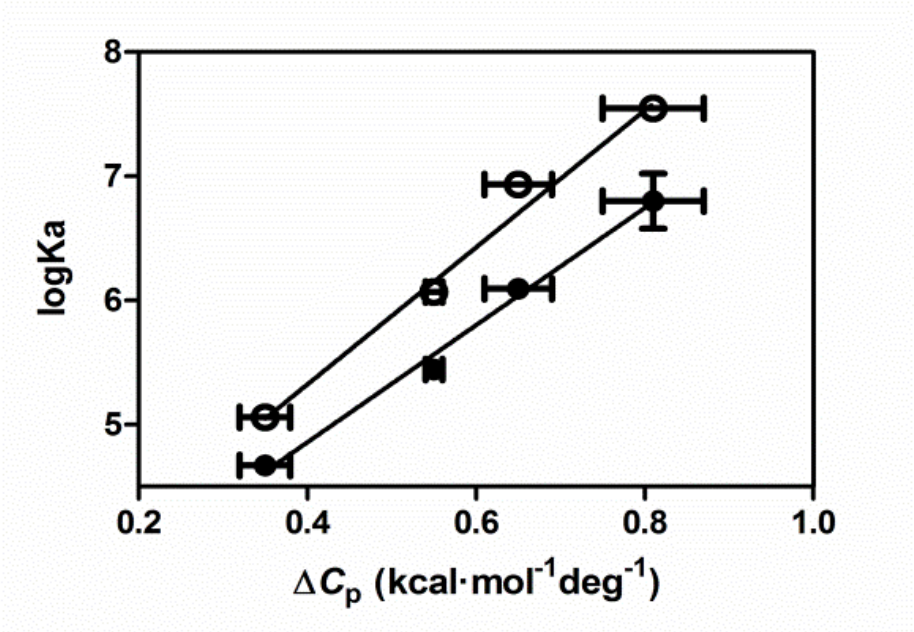

Figure 26. Binding constants (log Ka) aminoglycosides to T130K as a function of the heat capacity change in H2O. Each data point represents a different enzyme–aminoglycoside complex at 25℃ (○) and 40℃ (●). Error bars of log Ka are the standard error of mean from two or three independent trials.

Binding enthalpy in H_2O and D_2O are aminoglycoside dependent.

Binding of all aminoglycosides were enthalpically more favored in H_2O relative to D_2O at temperatures above 10°C. Differences in binding enthalpy of aminoglycosides (ΔH_{H2O} - ΔH_{D2O} = $\Delta\Delta H_{H2O\text{-}D2O}$, henceforth $\Delta\Delta H$), determined from the slopes of ΔH versus temperature plots (Figure 27), are displayed in Figure 28 as a function of temperature. These data show that binding enthalpy becomes more exothermic in D_2O below the range of 5-10°C with the exception of kanamycin A. Excluding neomycin, which is by far the tightest binding antibiotic to ANT, all lines intersect at 17.2 ± 0.2°C. ΔCp was almost identical in H_2O and D_2O for kanamycin A, while it was more negative in H_2O with all others. Differences between the determined ΔCp in H_2O and D_2O (ΔCp_{H2O} - ΔCp_{D2O} = $\Delta\Delta Cp$) were aminoglycoside dependent and the largest $\Delta\Delta Cp$ was observed with neomycin while it was almost zero for the kanamycin A. $\Delta\Delta Cp$ values are also correlated well with the binding affinity of the aminoglycoside to the enzyme such that the largest $\Delta\Delta Cp$ was observed with the tightest binding aminoglycoside neomycin and it was ~0 for the weakest binding kanamycin A (Table 6).

Effect of solvent reorganization on heat capacity is temperature dependent.

The enthalpic difference in H_2O and D_2O ($\Delta\Delta H$) were taken at different temperatures for ANT–aminoglycoside complexes were plotted against ΔCp. A good linear correlation in $\Delta\Delta H$ versus ΔCp plots shows that the solvent reorganization is the main contributor of the binding enthalpy (85). The slope of such plots has the unit of temperature and represents the offset temperature (T_{off}), which is the temperature difference needed to observe identical enthalpies of binding in light and heavy water. When such plots are made for T130K–aminoglycoside complexes, there was a strong dependence on the temperature such that the correlation increased linearly with increasing temperature reaching to a plateau above 20°C. Examples of such plots at three different temperatures are shown in Figure 29A-C. The dependence of correlation coefficient on temperature is shown in Figure 29D.

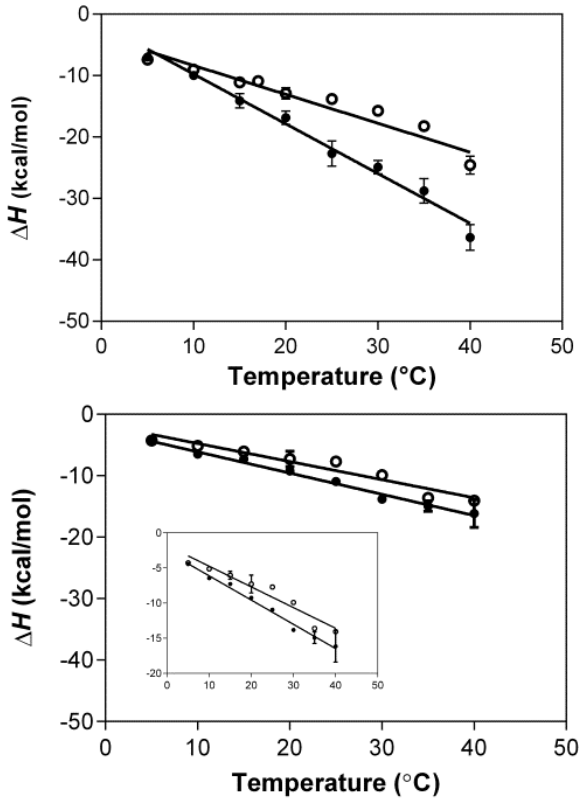

Figure 27. Temperature dependence of binding enthalpy. Binding of neomycin (upper panel) and kanamycin A (lower panel) to ANT in D2O(○) and H2O(●) . Data are shown with linear regression lines. Error bars represent the standard error of mean from two to three independent trials. The inset shows an expanded view of kanamycin A data.

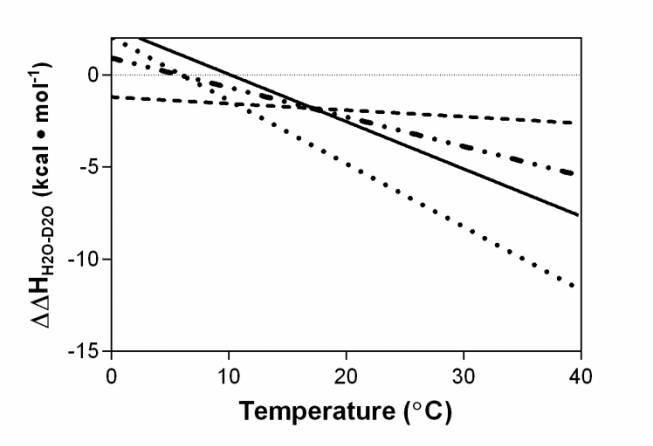

Figure 28. Temperature dependence of ΔΔH of T130K –aminoglycoside complexes. Neomycin (dot), paromomycin (solid), tobramycin (dot-dash) and kanamycin A (dash). ΔΔH values are determined from the slopes of linear regression lines from ΔH vs. T plots (Figure 26).

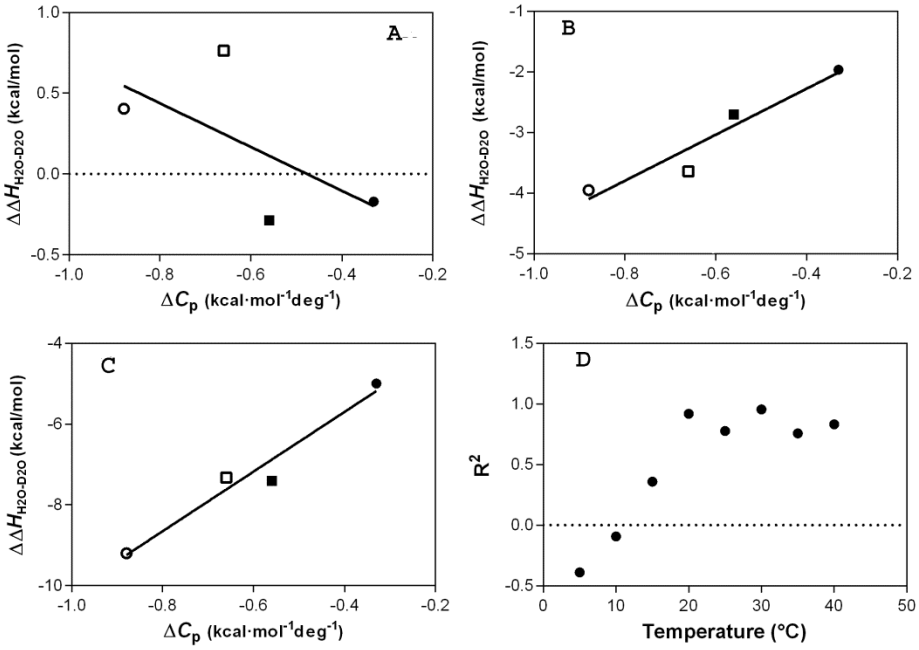

Figure 29. ΔΔH vs. ΔCp plots of T130K-ligand complexes. Panels A, B and C show data at 5℃, 20℃ and 40℃ respectively: neomycin (○), paromomycin (□), tobramycin (■) and kanamycin A (●). Data are shown with regression lines. Panel D shows linear correlation coefficient (R2) of the plots as a function of temperature.

4.5 Discussion

Changes in heat capacity

One of the major factors affecting Δ*Cp* for ligand–protein complexes is the exposure or burial of hydrophobic and polar surfaces (81, 86-88). Hydration of polar and nonpolar groups is negative at low temperatures and changes in opposite directions with increasing temperature such that it becomes more negative with polar groups and less negative with nonpolar groups crossing into positive values in the temperature range of 18-25℃ (89, 90). Data acquired with T130K variant using four different aminoglycosides indicate that the major contribution to the change in heat capacity is the changes in the interaction of polar groups with water (solvent rearrangement). The negative values of ∆*Cp* correlated well with the binding affinity of ligands to T130K yielding the most negative value with the tightest binding neomycin (Table 1). These data are consistent with the protein becoming "stiffer" with the binding of ligands which correlates well with the previous data acquired with analytical centrifugation studies as well as the observed negative Δ*Cp* values (82)

The binding of aminoglycosides to T130K occurs with changes in the net protonation of titratable groups on the ligand and the protein (82). Therefore, we have always used multiple buffers with different heat of ionizations to perform such titration to account for the contribution of the buffer to the observed enthalpy and to determine the intrinsic enthalpy (59, 60, 71, 82, 84, 91). In this case, changes in temperature may cause differential shifts in pKa values of these groups and contribute to the observed ∆*Cp.* However, differences in temperature dependence of buffer pK_a values would complicate the data analysis. Therefore, we used a single buffer (MOPS) with lowest very low temperature dependent p*Ka*. Also, such effects are not likely to be the main cause of differences observed between the determined ∆*Cp* values for different enzyme–aminoglycoside complexes because even 100% protonation of NH_2 to NH_3^+ would decrease ∆*Cp* by only ~9.2 cal mol^{-1} deg^{-1} (89), which is too small to account for the observed differences despite the fact that there are 4-6 amine groups are present in the aminoglycosides used in this work (Figure 2). We should also note that pH versus

pD differences in H_2O and D_2O are usually compensated for proteins in these solvents (92).

Solvent isotope effect

Solvent reorganization and changes in vibrational and conformational modes of protein are usually believed to be the major contributors to ΔCp(81, 93). The relative magnitude of each contribution has long been a source of debate. The $\Delta\Delta H$ versus ΔCp plot has been previously used to test the contribution of solvent reorganization to ΔCp (83, 85). A linear correlation between $\Delta\Delta H$ and ΔCp is an indicative of a major contribution from solvent reorganization and a minor contribution from changes in protein dynamics. To determine the contribution of solvent reorganization to ΔCp, we investigated binding of aminoglycosides to T130K variant in $H_2O$and D_2O as solvents. There are only a few cases where heat capacity changes were determined in both solvents. In these studies it was observed that ΔCp can be different in both solvents or remain the same. T130K-aminoglycoside interactions showed strong temperature dependence and at low temperatures no correlation exists between ΔΔH and ΔCp. Contrary to this, at higher temperatures there is a very strong correlation. These data indicate that changes in heat capacity are mostly reflecting the effects of solvent reorganization above 20℃. At lower temperatures, it is likely that change in soft vibrational modes of the protein may become more dominant contributor to the change in heat capacity (81, 83, 85). Since ΔCp shows a linear correlation with log K_a, the association constant for the enzyme–aminoglycoside complex, these observations suggest that the major contributor to ΔCp may also be the major contributor to ΔG for the complex formation. This is consistent with the solvent reorganization being the major contributor of the complex formation between the enzyme and aminoglycosides above 20℃.

Most studies, described in literature, have been performed at 25℃ only. The first study showing that effect of solvent reorganization on binding enthalpy can be temperature dependent was performed with the aminoglycoside *N3*-acetyltransferase-IIIb (AAC) where the linear correlation between ΔΔH and ΔCp increased with increasing temperature (83). This work represents observation of such effect for the

second time. Although both AAC and ANT are members of a large family that modify aminoglycoside antibiotics, they catalyze different reactions and have no significant sequence or structural homology to each other and yet solvent reorganization contributes to the change in heat capacity in a temperature dependent manner with the formation of enzyme–aminoglycoside complexes with both enzymes. These observations suggest that temperature dependence of solvent reorganization may more general than being specific for a these two enzymes but has not been investigated before. These findings also demonstrate that different factors may become dominant as a function of temperature and such dependence may have other consequences in protein-ligand interactions at different temperature regimes.

It is likely that the role of water molecules and their interaction with the ligand and the enzyme may be different with each aminoglycoside and it may alter the correlation between the change in heat capacity and $\Delta\Delta H$ at different temperatures. Variations in $\Delta\Delta H$ for each aminoglycoside can either be due to different exposure of polar groups or spatial distribution water in the active site (94). The lack of crystal structure with different aminoglycosides precludes us making this distinction; however, it is likely that both factors contribute to the observed differences between different aminoglycosides. Interactions with solvent may have a significant impact in carbohydrate conformation (95) and if conformational fluctuations of aminoglycosides favor different conformations with temperature variations, interactions with solvent may be different and alter energetics of desolvation and binding at different temperatures. To this end, earlier work showed that aminoglycosides can bind the aminoglycoside-modifying enzymes in multiple conformations (96-99). Since strong temperature dependence of water reorientation in hydrophobic hydration shells have been shown before(100), our data suggest that reorientation of water on polar surfaces may also have a dependence on temperature .

Enthalpy of transfer from H_2O to D_2O ($\Delta H_{tr} = \Delta H_{D2O} - \Delta H_{H2O}$) has been reported to be slightly negative or close to zero (101, 102) or positive (94, 103) for polar groups at 25°C. Our results show that ΔH_{tr} becomes more positive with increasing temperature. Data shown in Figure 30 are determined from the slopes of $\Delta\Delta H$ vs. ΔCp plots (Figure

29) and demonstrate the progressive increase in T_{off} with increasing temperature. This indicates that at higher temperatures the temperature difference to obtain equal binding enthalpy in water and heavy water becomes larger. The offset temperature observed in other systems at 25°C yielded values such that they are reminiscent of other offsets between H_2O and D_2O attributed to different hydrogen bonding strengths (85). These include boiling points (1.4K), critical points (3.8K), melting points (4K), triple points (4K) and temperatures of maximum density (8K). Our results with another AGME, the aminoglycoside *N3*-acetyltransferase-IIIb also fall in the same range (83). However, results of this work support the notion that this need not be the case. With ANT, differences are in this range only at low temperature regime and as temperature increases from 25°C to 40°C, T_{off} is found to systematically increase and exceed the T_{off} range that was observed by previous studies. In our case, the T_{off} is around 10K for 25°C and goes up to 20K at 40°C. These data suggest that T_{off} is not a simple representation of differences between physical properties of light and heavy water but may include contributions from other properties of the enzyme and/or the ligand.

Differences in binding enthalpy of a ligand in H_2O and D_2O is thought to represent enthalpy of transfer of part of the ligand and enzyme active site that is desolvated during binding (104). This difference in enthalpy is also interpreted as the measure of enthalpy available through desolvation of the ligand and the protein (94). It is interesting to note that the difference grows larger at higher temperatures for this thermostable variant of ANT and directly correlated to the affinity of the ligand to the protein such that it is largest with the tightest binding neomycin. We should also note that among these four aminoglycosides, the two tightest binding ligands are also the two largest, neomycin and paromomycin. Since T_{off} increases faster with increasing temperature for these two aminoglycosides, it is reasonable to assume that the largest surface area may need to be desolvated on the enzyme and the ligand. Contrary to this, the sign of $\Delta\Delta H$ and its variation with temperature were different even with structurally almost identical aminoglycosides with AAC (83).

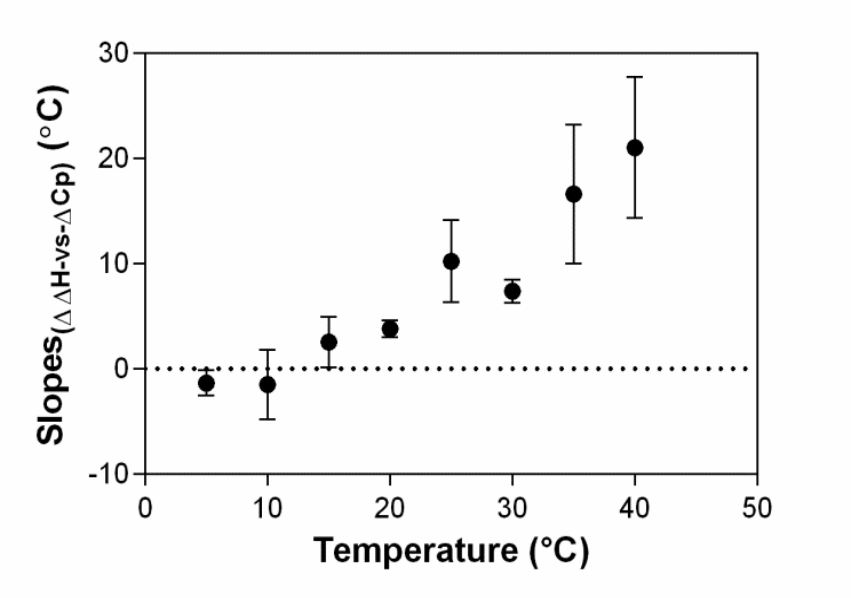

Figure 30. Slopes of ΔΔH vs. ΔCp plots. Data are shown as a function of temperature.

Crystal structure of ANT with bound kanamycin A shows that the antibiotic is completely surrounded by polar side chains. A close up view of the active site is shown in Figure 31 where the carboxylic side chains are in yellow and other polar side chains are in orange. ΔCp for the transfer of NH_2/NH_3^+ groups from H_2O to D_2O at temperatures above 25°C occurs with (86). The thermodynamic data shown in Table 6 are also consistent with this structure.

Finally, plots of ΔH vs. $T\Delta S$ showed variable slopes as a function of temperature (Figures 32 and 33). Although slopes of ΔH vs. ΔS plots were significantly different from the temperature of the experiment, the data are acquired with only four ligands and quite noisy. Therefore no firm interpretations can be made, however it is tempting to suggest that the balance of enthalpic and entropic contributions to the complex formation may also be dependent on temperature.

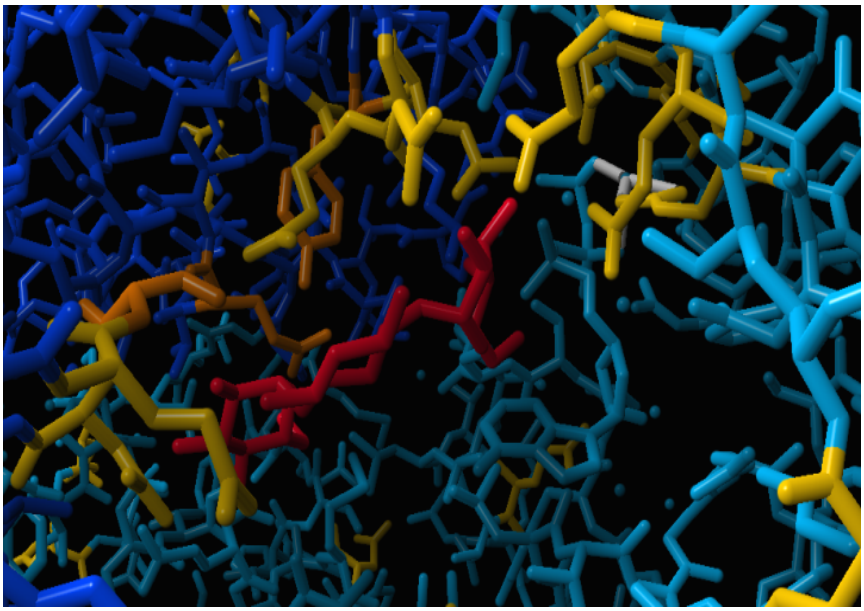

Figure 31. A close up view of the ANT active site(52). Kanamycin A (red) is completely surrounded by polar side chains. Carboxylic side chains are in yellow and other polar side chains are in orange.

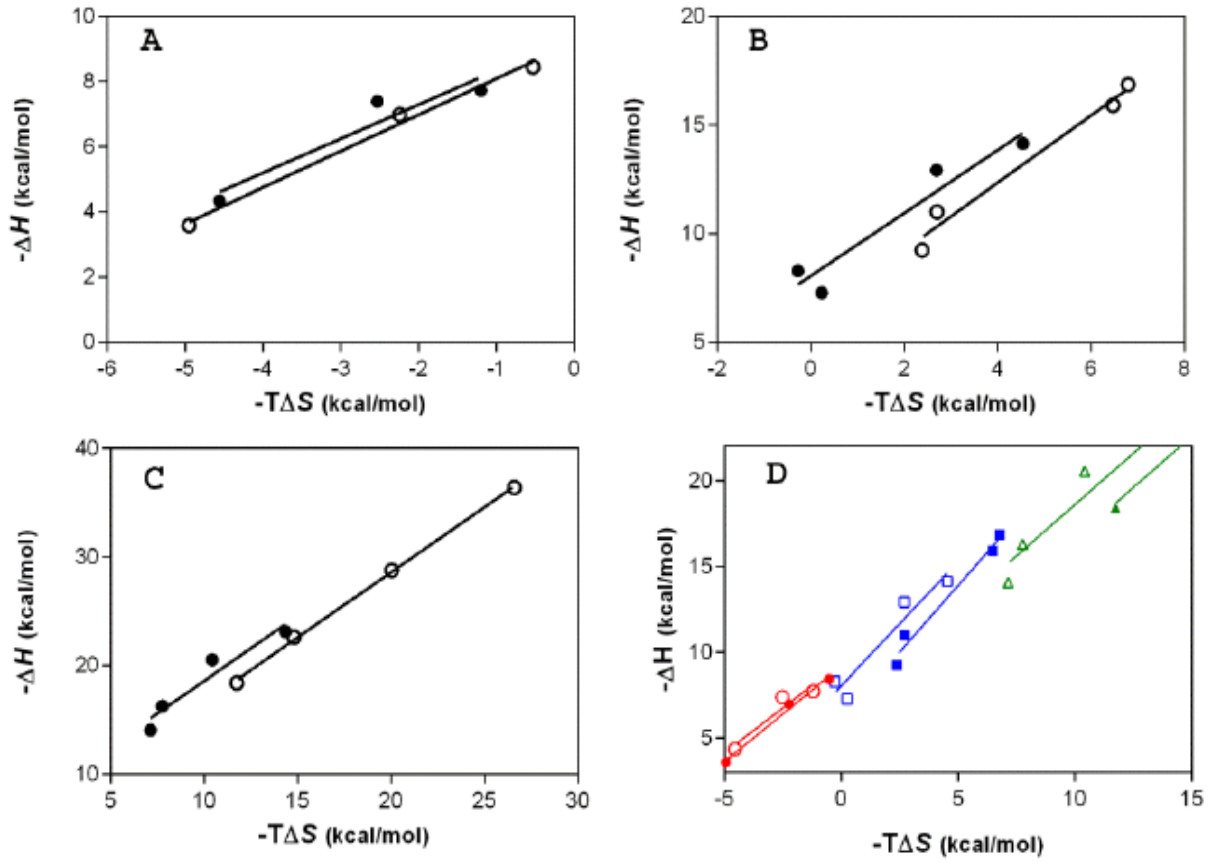

Figure 32. Panels A, B and C represent data acquired at 5℃, 20℃ and 40℃ respectively. Data from panel A, B and C shown in an expanded manner on the same scale in panel D for visual comparison. Data are shown with regression lines.

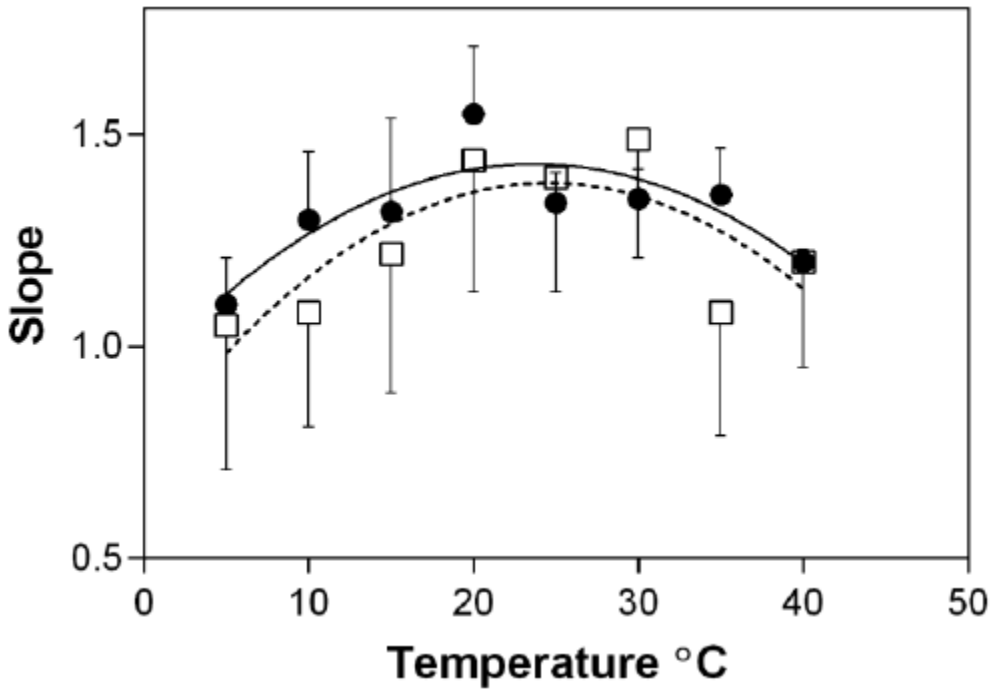

Figure 33. Slopes of regression lines from Δ*H* vs *T*Δ*S* plots. Data are shown as a function of temperature. Lines show Gaussian fits (R2=0.732-0.734). Fits for straight lines not good (R2=0.004).

CHAPTER V

CONCLUSIONS AND FUTURE DIRECTIONS

5.1 Conclusions

Thermostable variants of ANT- T130K, D80Y and D80Y/T130K , as a result of direct evolution, have systematically increasing melting temperatures in the order of wild type (40.9±0.5℃), T130K variant (49.1±0.6℃), D80Y variant (56.2±0.2℃) and double variant (62.6±0.1℃). All three thermostable variants adopt similar three dimensional folds than the mesophilic enzyme. This set of ANT enzyme exists as mixtures of monomers and dimers in solution, however, the dissociation constant of dimers steadily increased in the order of D80Y/T130K variant → D80Y variant → T130K variant → WT (mesophilic). Hydrophobic interactions are suggested to be the driving force for dimerization. Furthermore, T130K variant resembles WT in binding parameters to both tested aminoglycosides – neomycin and tobramycin; while D80Y variant displays distinct thermodynamic properties of ligand binding. Additionally, the similar local fluctuations for WT and T130K variant are observed in most regions; however, D80Y displays greater atomistic fluctuations especially in the N-terminal domain, compared to WT and T130K variant. These observations indicated the different structural strategies of improving thermostability for T130K variant and D80Y variant. T130K variant- a mesophilic enzyme with enhanced thermostability due to more specific stabilizing interactions from residue replacement; D80Y variant may stabilize previously sub-stable conformers in mesophilic enzyme and display more stable basins that native protein can visit, thus increasing the entropic change associated with enzyme denaturation and the heat resistance capability. We hypothesize that T130K and D80Y variants represent two different categories of heat resistance enzymes: heat stable mesophilic versus true thermophilic enzymes respectively. We further speculate that solvent effects, internal fluctuations and ligand binding may be the criteria that separate these two types of enzymes.

Monomer-dimer equilibrium of T130K variant was further characterized in detail. Although the binding pockets for both the aminoglycoside and nucleotide are composed of amino acids contributed by both subunits of the dimer, only the aminoglycoside affects the monomer-dimer equilibrium of the enzyme by favoring dimer formation. A

large excess of aminoglycosides does not cause any further aggregation, indicating that the dimer formation is specific and relevant to catalytic activity of the enzyme. This is also consistent with kinetic data that showed that the aminoglycoside substrate binds first to the enzyme. Surprisingly, divalent cations also shifted the equilibrium towards the dimer formation through the aminoglycoside binding site, in contrast to no effect by MgATP. Such ligand-dependent monomer-dimer equilibrium has not been observed with any other AGME.

Thermodynamic parameters of aminoglycosides binding to T130K were further investigated in depth. It is found that binding of aminoglycosides occurs with a favorable enthalpy and unfavorable entropy yielding an overall favorable Gibbs energy. This is similar to the observations with other AGMEs. The size of aminoglycosides has a significant effect on the binding enthalpy, and the presence of the fourth ring on aminoglycosides renders the binding significantly more favorable. These studies also showed that ANT is the least capable AGME characterized to date to discriminate the substitution at the C-2′ site of aminoglycosides (kanamycin A versus kanamycin B). The most significant effects are observed with the changes in the substitution at the C-6′ site (neomycin versus paromomycin), which is the most distant position from the nucleotidylation site. Data also suggested that the binding of aminoglycosides to ANT causes exposure of polar groups to solvent. However solvent reorganization becomes the major contributor to the enthalpy of the formation of enzyme–aminoglycoside complexes only above 20 °C. The change in heat capacity (ΔCp) shows an aminoglycoside-dependent pattern such that it correlates with the affinity of the ligand to the enzyme. Differences in ΔCp values determined in H_2O and D_2O also correlated with the ligand affinity. The temperature dependent increase in the offset temperature (T_{off}), the temperature difference required to observe equal enthalpies in both solvents, is also dependent on the binding affinity of the ligand and the steepest increase was observed with the tightest binding aminoglycoside, neomycin. Overall, these data, together with earlier observations with a different enzyme, the aminoglycoside *N3*-acetyltransferase-IIIb show that solvent reorganization or changes in soft vibrational modes of the protein can have interchangeably the role of major contributor to the complex formation depending on temperature. These data suggest that such effects may be more

generally apply to enzyme-ligand interactions and studies at a single temperature may provide only a part of the whole picture of thermodynamics of enzyme-ligand interactions.

5.2 Future directions

Characterize the role of solvent reorganization in the ligand binding of D80Y variant and WT enzyme

Our data suggest that D80→Y80 replacement triggers greater atomistic fluctuations in most regions of protein. As a result, solvent molecules within protein hydration layer would possibly reorganize and further affect ligand binding by modifying the entropic contributions of the binding free energies of ligands to the protein. In order to test our hypothesis that solvent effects are distinct to the thermophilic (D80Y) and hyper-stable mesophilic (T130K) enzymes thus serving as (one of) the molecular mechanism(s) attributing to real thermophilicity, contribution of solvent reorganization towards heat capacities of protein-ligand complexes should be investigated. Our ligand binding studies on one of the variant T130K suggests that the role of water molecules and their interaction with the ligand and the enzyme are different for different aminoglycosides. It is very possible that different solvent reorganization, if any, accounts for the different binding behaviors observed for D80Y and T130K enzymes. This study would examine whether or not solvent reorganization is the indicator for thermophilicity such that it shows distinguishable properties for wild type and D80Y variant (the true thermophilic variant, if our hypothesis is correct) while the wild type and T130K (heat stable mesophilic enzyme) are indistinguishable from each other.

Characterize residue specific ^{15}N relaxation pattern

Our simulation data suggest that atomistic fluctuations in nanosecond time scale differ for D80Y and T130K variants and those motions are likely to be a molecular

feature separating hyper-stable mesophilic enzyme and thermophilic enzyme. We ask that whether or not motions at other time scale are also distinguishable for T130K (heat stable mesophilic enzyme) and D80Y (thermophilic enzyme) variants.

Protein dynamics exhibit a hierarchy network of protein motions at timescale spanning from femtosecond to second(105). In recent years, extensive hydrogen/deuterium exchange studies suggested that thermophilic enzymes exhibit similar or less dynamic properties with mesophilic counterparts in millisecond time scale while nuclear magnetic resonance, neutron scattering and MD simulation studies have observed that thermophilic enzymes exhibit similar or greater dynamic properties from pico- to micro- second timescale.

To test our hypothesis (that local atomic fluctuations are distinguishable for thermostable mesophilic enzyme and true thermophilic ones) and to expand our study on protein flexibility-thermostability relation, fast motion dynamics (pico- to nanosecond time scale) as well as motion in intermediate time scale (micro- to millisecond range) of wild type, T130K and D80Y variants would be tested by using ^{15}N relaxation NMR. Relaxation times (T1 and T2), heteronuclear NOE data, generalized order parameter S^2 (indicator of motions on pico- to nanosecond time-scale) and microenvironment change on micro- to millisecond time scale Δ_{ex} will be obtained on a per residue basis. By comparison of obtained parameters of each residue in wild type, T130K and D80Y variants, information regarding the most affected motions by D80→Y80 replacement will be revealed including time scale and location. This experiment will also reveal the different solvent effects, if any, in D80Y and T130K variants and test our hypothesis stated in prior section. If solvent-protein interactions are indeed different for T130K and D80Y variants, but indistinguishable for wild type and T130K variant, the most affected residues are expected to locate on the protein surface and to directly interact with the solvent.

Characterize and quantify the role of protein dynamics in the thermal stability of ANT variants

Our results point to a potentially important role of the protein dynamics in their stability at high temperatures, beyond and in addition to a purely “structural” view that heat resistance proteins exhibit more stabilizing internal interactions. We will be collaborating with Dr. Jerome Baudry (University of Tennessee, Knoxville) to quantify the contribution of protein dynamics towards the thermophilicity of ANT4 variants. Wild type, D80Y and T130 variants will be calculated in 100-ns MD simulations at a range of temperature points above melting points of the various species. The dependency of the dynamics on the temperature will be calculated as root mean square fluctuations at each temperature simulation. Previous study identified a regularly alternating pattern of flexible and rigid segments in thermophilic enzymes and suggested its possible function in preventing progressive unfolding at high temperature(34). These suggested correlated motions will also be calculated. This study will examine our hypothesis that protein atomistic fluctuations differ for thermophilic and hyper-stable mesophilic enzymes. This will also provide a novel view on the relationship between structure, dynamics and thermophilicity for several mutations of the same protein.

Predict mutated protein species that are expected to exhibit thermophilic properties

The temperature dependency of protein dynamics stated in prior future direction will provide metrics to identify and characterize the thermophilicity of a given ANT4 mutant sequence. Several single mutants of ANT can be easily modeled from the D80Y structure. Molecular dynamics simulations of these proteins will be performed to identify predicted changes in the metrics of the thermophilicity. The sequences predicted to exhibit thermophilic properties will be experimentally generated and tested in thermal denaturation and ligand binding. This will provide, for the first time to the best of our knowledge, a platform to predict the thermal properties of protein species.

REFERENCES

1. Sterpone F, Bertonati C, Briganti G, Melchionna S. Key role of proximal water in regulating thermostable proteins. The Journal of Physical Chemistry B. 2008;113(1):131-7.
2. Vieille C, Zeikus GJ. Hyperthermophilic enzymes: sources, uses, and molecular mechanisms for thermostability. Microbiology and Molecular Biology Reviews. 2001;65(1):1-43.
3. Davies GJ, Gamblin SJ, Littlechild JA, Watson HC. The structure of a thermally stable 3-phosphoglycerate kinase and a comparison with its mesophilic equivalent. Proteins: Structure, Function, and Bioinformatics. 1993;15(3):283-9.
4. Vieille C, Hess JM, Kelly RM, Zeikus JG. xylA cloning and sequencing and biochemical characterization of xylose isomerase from Thermotoga neapolitana. Applied and environmental microbiology. 1995;61(5):1867-75.
5. Auerbach G, Ostendorp R, Prade L, Korndörfer I, Dams T, Huber R, Jaenicke R. Lactate dehydrogenase from the hyperthermophilic bacterium Thermotoga maritima: the crystal structure at 2.1 Å resolution reveals strategies for intrinsic protein stabilization. Structure. 1998;6(6):769-81.
6. Hopfner K-P, Eichinger A, Engh RA, Laue F, Ankenbauer W, Huber R, Angerer B. Crystal structure of a thermostable type B DNA polymerase from Thermococcus gorgonarius. Proceedings of the National Academy of Sciences. 1999;96(7):3600-5.
7. Isupov MN, Fleming TM, Dalby AR, Crowhurst GS, Bourne PC, Littlechild JA. Crystal structure of the glyceraldehyde-3-phosphate dehydrogenase from the hyperthermophilic archaeon Sulfolobus solfataricus. Journal of molecular biology. 1999;291(3):651-60.
8. Maes D, Zeelen JP, Thanki N, Beaucamp N, Alvarez M, Thi MHD, Backmann J, Martial JA, Wyns L, Jaenicke R. The crystal structure of triosephosphate isomerase (TIM) from Thermotoga maritima: a comparative thermostability structural analysis of ten different TIM structures. Proteins: Structure, Function, and Bioinformatics. 1999;37(3):441-53.
9. Russell RJ, Ferguson JM, Hough DW, Danson MJ, Taylor GL. The crystal structure of citrate synthase from the hyperthermophilic archaeon Pyrococcus furiosus at 1.9 Å resolution. Biochemistry. 1997;36(33):9983-94.

10. Zwickl P, Fabry S, Bogedain C, Haas A, Hensel R. Glyceraldehyde-3-phosphate dehydrogenase from the hyperthermophilic archaebacterium Pyrococcus woesei: characterization of the enzyme, cloning and sequencing of the gene, and expression in Escherichia coli. Journal of bacteriology. 1990;172(8):4329-38.
11. Bauer MW, Kelly RM. The family 1 β-glucosidases from Pyrococcus furiosus and Agrobacterium faecalis share a common catalytic mechanism. Biochemistry. 1998;37(49):17170-8.
12. Elcock AH. The stability of salt bridges at high temperatures: implications for hyperthermophilic proteins. Journal of molecular biology. 1998;284(2):489-502.
13. Xiao L, Honig B. Electrostatic contributions to the stability of hyperthermophilic proteins. Journal of molecular biology. 1999;289(5):1435-44.
14. Dominy BN, Minoux H, Brooks CL. An electrostatic basis for the stability of thermophilic proteins. Proteins: Structure, Function, and Bioinformatics. 2004;57(1):128-41.
15. Missimer JH, Steinmetz MO, Baron R, Winkler FK, Kammerer RA, Daura X, Van Gunsteren WF. Configurational entropy elucidates the role of salt-bridge networks in protein thermostability. Protein science. 2007;16(7):1349-59.
16. Macedo-Ribeiro S, Darimont B, Sterner R, Huber R. Small structural changes account for the high thermostability of 1 [4Fe–4S] ferredoxin from the hyperthermophilic bacterium Thermotoga maritima. Structure. 1996;4(11):1291-301.
17. Wallon G, Kryger G, Lovett ST, Oshima T, Ringe D, Petsko GA. Crystal structures of Escherichia coli and Salmonella typhimurium 3-isopropylmalate dehydrogenase and comparison with their thermophilic counterpart from Thermus thermophilus. Journal of molecular biology. 1997;266(5):1016-31.
18. Gromiha MM, Oobatake M, Sarai A. Important amino acid properties for enhanced thermostability from mesophilic to thermophilic proteins. Biophysical chemistry. 1999;82(1):51-67.
19. Chakravarty S, Varadarajan R. Elucidation of determinants of protein stability through genome sequence analysis. Febs Letters. 2000;470(1):65-9.
20. Kumar S, Nussinov R. How do thermophilic proteins deal with heat? Cellular and Molecular Life Sciences CMLS. 2001;58(9):1216-33.

21. Cambillau C, Claverie J-M. Structural and genomic correlates of hyperthermostability. Journal of Biological Chemistry. 2000;275(42):32383-6.
22. Tanner JJ, Hecht RM, Krause KL. Determinants of enzyme thermostability observed in the molecular structure of Thermus aquaticus D-glyceraldehyde-3-phosphate dehydrogenase at 2.5 Å resolution. Biochemistry. 1996;35(8):2597-609.
23. Kawamura S, Tanaka I, Yamasaki N, Kimura M. Contribution of a salt bridge to the thermostability of DNA binding protein HU from Bacillus stearothermophilus determined by site-directed mutagenesis. Journal of biochemistry. 1997;121(3):448-55.
24. Yip KS, Britton KL, Stillman TJ, Lebbink J, de Vos WM, Robb FT, Vetriani C, Maeder D, Rice DW. Insights into the molecular basis of thermal stability from the analysis of ion-pair networks in the glutamate dehydrogenase family. European Journal of Biochemistry. 1998;255(2):336-46.
25. Kumar S, Tsai C-J, Nussinov R. Factors enhancing protein thermostability. Protein Engineering. 2000;13(3):179-91.
26. Lebbink JH, Knapp S, van der Oost J, Rice D, Ladenstein R, de Vos WM. Engineering activity and stability of Thermotoga maritima glutamate dehydrogenase. II: construction of a 16-residue ion-pair network at the subunit interface. Journal of molecular biology. 1999;289(2):357-69.
27. Szilágyi A, Závodszky P. Structural differences between mesophilic, moderately thermophilic and extremely thermophilic protein subunits: results of a comprehensive survey. Structure. 2000;8(5):493-504.
28. ZAvodszky P, Kardos J, Svingor Á, Petsko GA. Adjustment of conformational flexibility is a key event in the thermal adaptation of proteins. Proceedings of the National Academy of Sciences. 1998;95(13):7406-11.
29. Wrba A, Schweiger A, Schultes V, Jaenicke R, Zavodszky P. Extremely thermostable D-glyceraldehyde-3-phosphate dehydrogenase from the eubacterium Thermotoga maritima. Biochemistry. 1990;29(33):7584-92.
30. Tang KE, Dill KA. Native protein fluctuations: the conformational-motion temperature and the inverse correlation of protein flexibility with protein stability. Journal of Biomolecular Structure and Dynamics. 1998;16(2):397-411.

31. Fitter J, Heberle J. Structural equilibrium fluctuations in mesophilic and thermophilic α-amylase. Biophysical journal. 2000;79(3):1629-36.
32. Tehei M, Madern D, Franzetti B, Zaccai G. Neutron scattering reveals the dynamic basis of protein adaptation to extreme temperature. Journal of Biological Chemistry. 2005;280(49):40974-9.
33. Meinhold L, Clement D, Tehei M, Daniel R, Finney JL, Smith JC. Protein dynamics and stability: the distribution of atomic fluctuations in thermophilic and mesophilic dihydrofolate reductase derived using elastic incoherent neutron scattering. Biophysical journal. 2008;94(12):4812-8.
34. Kalimeri M, Rahaman O, Melchionna S, Sterpone F. How Conformational Flexibility Stabilizes the Hyperthermophilic Elongation Factor G-Domain. The Journal of Physical Chemistry B. 2013;117(44):13775-85.
35. Nemethy G, Peer W, Scheraga H. Effect of protein-solvent interactions on protein conformation. Annual review of biophysics and bioengineering. 1981;10(1):459-97.
36. Hernández G, Jenney FE, Adams MW, LeMaster DM. Millisecond time scale conformational flexibility in a hyperthermophile protein at ambient temperature. Proceedings of the National Academy of Sciences. 2000;97(7):3166-70.
37. Sterpone F, Bertonati C, Briganti G, Melchionna S. Water around thermophilic proteins: the role of charged and apolar atoms. Journal of Physics: Condensed Matter. 2010;22(28):284113.
38. Feller G. Psychrophilic enzymes: from folding to function and biotechnology. Scientifica. 2013;2013.
39. Hakim A, Nguyen JB, Basu K, Zhu DF, Thakral D, Davies PL, Isaacs FJ, Modis Y, Meng W. Crystal structure of an insect antifreeze protein and its implications for ice binding. Journal of Biological Chemistry. 2013;288(17):12295-304.
40. Garnham CP, Campbell RL, Davies PL. Anchored clathrate waters bind antifreeze proteins to ice. Proceedings of the National Academy of Sciences. 2011;108(18):7363-7.
41. Nutt DR, Smith JC. Dual function of the hydration layer around an antifreeze protein revealed by atomistic molecular dynamics simulations. Journal of the American Chemical Society. 2008;130(39):13066-73.

42. Van den Burg B, Vriend G, Veltman OR, Venema G, Eijsink VG. Engineering an enzyme to resist boiling. Proceedings of the National Academy of Sciences. 1998;95(5):2056-60.
43. Liang Z-X, Lee T, Resing KA, Ahn NG, Klinman JP. Thermal-activated protein mobility and its correlation with catalysis in thermophilic alcohol dehydrogenase. Proceedings of the National Academy of Sciences of the United States of America. 2004;101(26):9556-61.
44. Brock TD, Freeze H. Thermus aquaticus gen. n. and sp. n., a nonsporulating extreme thermophile. Journal of Bacteriology. 1969;98(1):289-97.
45. de Miguel Bouzas T, Barros-Velázquez J, Gonzalez Villa T. Industrial applications of hyperthermophilic enzymes: a review. Protein and peptide letters. 2006;13(7):645-51.
46. Jana S, Deb J. Molecular understanding of aminoglycoside action and resistance. Applied microbiology and biotechnology. 2006;70(2):140-50.
47. Lacey R, Chopra I. Genetic studies of a multi-resistant strain of Staphylococcus aureus. Journal of medical microbiology. 1974;7(2):285-97.
48. Matsumura M, Aiba S. Screening for thermostable mutant of kanamycin nucleotidyltransferase by the use of a transformation system for a thermophile, Bacillus stearothermophilus. Journal of Biological Chemistry. 1985;260(28):15298-303.
49. Liao H, McKenzie T, Hageman R. Isolation of a thermostable enzyme variant by cloning and selection in a thermophile. Proceedings of the National Academy of Sciences. 1986;83(3):576-80.
50. Liao HH. Thermostable mutants of kanamycin nucleotidyltransferase are also more stable to proteinase K, urea, detergents, and water-miscible organic solvents. Enzyme and microbial technology. 1993;15(4):286-92.
51. Sakon J, Liao HH, Kanikula AM, Benning MM, Rayment I, Holden HM. Molecular-Structure of Kanamycin Nucleotidyltransferase Determined to 3.0-Angstrom Resolution. Biochemistry. 1993;32(45):11977-84. PubMed PMID: ISI:A1993MG89300006.

52. Pedersen LC, Benning MM, Holden HM. Structural Investigation of the Antibiotic and ATP-Binding Sites in Kanamycin Nucleotidyltransferase. Biochemistry. 1995;34(41):13305-11. PubMed PMID: ISI:A1995TB58400005.
53. Matsumura M, Yasumura S, Aiba S. Cumulative effect of intragenic amino-acid replacements on the thermostability of a protein1986.
54. Lundblad RL, Kingdon HS, Mann KG. Thrombin. Meth Enzymol. 1976;45:156-76.
55. Schuck P. Size-distribution analysis of macromolecules by sedimentation velocity ultracentrifugation and Lamm equation modeling. Biophys J. 2000;78(3):1606-19. PubMed PMID: ISI:000085697800047.
56. Laue TM, Shah BD, Ridgeway TM, Pelletier SL. Analytical Ultracentrifugation in Biochemistry and Polymer Science. In: Harding SE, Rowe, A. J., and Horton, J. C., editor. Cambridge, UK: Royal Society of Chemistry; 1992. p. 90-125.
57. Schuck P. On the analysis of protein self-association by sedimentation velocity analytical ultracentrifugation. Anal Biochem. 2003;320(1):104-24. doi: Doi 10.1016/S0003-2697(03)00289-6. PubMed PMID: ISI:000184794200011.
58. Brautigam CA. Using Lamm-Equation modeling of sedimentation velocity data to determine the kinetic and thermodynamic properties of macromolecular interactions. Methods. 2011;54:4-15.
59. Norris AL, Ozen C, Serpersu EH. Thermodynamics and Kinetics of Association of Antibiotics with the Aminoglycoside Acetyltransferase (3)-IIIb, a Resistance-Causing Enzyme. Biochemistry. 2010;49(19):4027-35. doi: Doi 10.1021/Bi100155j. PubMed PMID: ISI:000277398100004.
60. Ozen C, Malek JM, Serpersu EH. Dissection of aminoglycoside-enzyme interactions: A calorimetric and NMR study of neomycin B binding to the aminoglycoside phosphotransferase(3 ')-IIIa. J Am Chem Soc. 2006;128(47):15248-54. PubMed PMID: ISI:000242216100054.
61. Greenfield NJ. Using circular dichroism collected as a function of temperature to determine the thermodynamics of protein unfolding and binding interactions. Nature protocols. 2006;1(6):2527-35.

62. Wright E, Serpersu EH. Molecular determinants of affinity for aminoglycoside binding to the aminoglycoside nucleotidyltransferase (2")-Ia. Biochemistry. 2006;45(34):10243-50.
63. Kimura S, Nakamura H, Hashimoto T, Oobatake M, Kanaya S. Stabilization of Escherichia coli ribonuclease HI by strategic replacement of amino acid residues with those from the thermophilic counterpart. Journal of Biological Chemistry. 1992;267(30):21535-42.
64. Haruki M, Tanaka M, Motegi T, Tadokoro T, Koga Y, Takano K, Kanaya S. Structural and thermodynamic analyses of Escherichia coli RNase HI variant with quintuple thermostabilizing mutations. FEBS journal. 2007;274(22):5815-25.
65. Ratcliff K, Corn J, Marqusee S. Structure, stability, and folding of ribonuclease H1 from the moderately thermophilic Chlorobium tepidum: comparison with thermophilic and mesophilic homologues. Biochemistry. 2009;48(25):5890-8.
66. Huber R, Huber H, Stetter K. Towards the ecology of hyperthermophiles: biotopes, new isolation strategies and novel metabolic properties. FEMS Microbiology Reviews. 2000;24(5):615-23.
67. Gates CA, Northrop DB. Substrate Specificities and Structure Activity Relationships for the Nucleotidylation of Antibiotics Catalyzed by Aminoglycoside Nucleotidyltransferase-2"-I. Biochemistry. 1988;27(10):3820-5. PubMed PMID: ISI:A1988N530700045.
68. Chen-Goodspeed M, Vanhooke JL, Holden HM, Raushel FM. Kinetic mechanism of kanamycin nucleotidyltransferase from Staphylococcus aureus. Bioorg Chem. 1999;27(5):395-408. PubMed PMID: ISI:000083388200006.
69. Revuelta J, Corzana F, Bastida A, Asensio J. The Unusual Nucleotide Recognition Properties of the Resistance Enzyme ANT(4′): Inorganic Tri/Polyphosphate as a Substrate for Aminoglycoside Inactivation. Chem Eur J. 2010;16(29):8635-40. doi: 10.1002/chem.201000641.
70. Revuelta J, Vacas T, Torrado M, Corzana F, Gonzalez C, Jimenez-Barbero J, Menendez M, Bastida A, Asensio JL. NMR-based analysis of aminoglycoside recognition by the resistance enzyme ANT(4'): The pattern of OH/NH3+ substitution

determines the preferred antibiotic binding mode and is critical for drug inactivation. J Am Chem Soc. 2008;130(15):5086-103. PubMed PMID: ISI:000254933000033.
71. Wright E, Serpersu EH. Molecular determinants of affinity for aminoglycoside binding to the aminoglycoside nucleotidyltransferase(2 '')-Ia. Biochemistry. 2006;45(34):10243-50. doi: Doi 10.1021/Bi060935d. PubMed PMID: ISI:000239922200009.
72. Wright E, Serpersu EH. Enzyme-substrate interactions with an antibiotic resistance enzyme: Aminoglycoside nucleotidyltransferase(2 '')-Ia characterized by kinetic and thermodynamic methods. Biochemistry. 2005;44(34):11581-91. doi: Doi 10.1021/Bi050797c. PubMed PMID: ISI:000231587900029.
73. Matsumura M, Katakura Y, Imanaka T, Aiba S. Enzymatic and nucleotide sequence studies of a kanamycin-inactivating enzyme encoded by a plasmid from thermophilic bacilli in comparison with that encoded by plasmid pUB110. J Bacteriol. 1984;160:413-20.
74. Onai K, Morishita M, Kaneko T, Tabata S, Ishiura M. Natural transformation of the thermophilic cyanobacterium Thermosynechococcus elongatus BP-1: a simple and efficient method for gene transfer. Mol Gen Genom. 2004;271(1):50-9. doi: DOI 10.1007/s00438-003-0953-9. PubMed PMID: ISI:000189000800006.
75. Dam J, Velikovsky CA, Mariuzza RA, Urbanke C, Schuck P. Sedimentation velocity analysis of heterogeneous protein-protein interactions: Lamm equation modeling and sedimentation coefficient distributions c(s). Biophys J. 2005;89(1):619-34. doi: DOI 10.1529/biophysj.105.059568. PubMed PMID: ISI:000230114500062.
76. Norris AL, Serpersu EH. Interactions of Coenzyme A with the Aminoglycoside Acetyltransferase (3)-IIIb and Thermodynamics of a Ternary System. Biochemistry. 2010;49(19):4036-42. doi: Doi 10.1021/Bi1001568. PubMed PMID: ISI:000277398100005.
77. Özen C, Serpersu EH. Thermodynamics of aminoglycoside binding to aminoglycoside-3'-phosphotransferase IIIa studied by isothermal titration calorimetry. Biochemistry. 2004;43(46):14667-75.
78. Boehr DD, Farley AR, LaRonde FJ, Murdock TR, Wright GD, Cox JR. Establishing the principles of recognition in the adenine-binding region of an

aminoglycoside antibiotic kinase APH(3 ')-IIIa. Biochemistry. 2005;44(37):12445-53. PubMed PMID: ISI:000231942200020.
79. Hedge SS, Dam, T. K., Brewer, C. F., Blachard, J. S. Thermodynamics of aminoglycoside and acyl-coenzyme A binding to the salmonella enterica AAC(6')-Iy aminoglycoside N-acetyltransferase. Biochemistry. 2002;41:7519-27.
80. Serpersu EH, Norris AL. Effect of Protein Dynamics and Solvent in Ligand Recognition by Promiscuous Aminoglycoside-Modifying Enzymes. In: Derek H, editor. Advances in Carbohydrate Chemistry and Biochemistry: Academic Press; 2012. p. 221-48.
81. Sturtevant JM. Heat-Capacity and Entropy Changes in Processes Involving Proteins. Proc Natl Acad Sci. 1977;74(6):2236-40. PubMed PMID: ISI:A1977DL65800011.
82. Jing X, Wright E, Bible AN, Peterson CB, Alexandre G, Bruce BD, Serpersu EH. Thermodynamic Characterization of a Thermostable Antibiotic Resistance Enzyme, the Aminoglycoside Nucleotidyltransferase (4′). Biochemistry. 2012;51(45):9147-55.
83. Norris AL, Serpersu EH. Antibiotic Selection by the Promiscuous Aminoglycoside Acetyltransferase-(3)-IIIb Is Thermodynamically Achieved through the Control of Solvent Rearrangement. Biochemistry. 2011;50(43):9309-17. doi: Doi 10.1021/Bi2011916. PubMed PMID: ISI:000296217000014.
84. Norris AL, Serpersu EH. Ligand promiscuity through the eyes of the aminoglycoside N3 acetyltransferase IIa. Prot Sci. 2013; "accepted":DOI: 10.1002/pro.2273.
85. Chervenak MC, Toone EJ. A Direct Measure of the Contribution of Solvent Reorganization to the Enthalpy of Ligand-Binding. Decreased dH in D2O represents differential interactions with solute and solvent. J Am Chem Soc. 1994;116(23):10533-9. PubMed PMID: ISI:A1994PT13000021.
86. Makhatadze GI, Privalov PL. Heat-Capacity of Proteins .1. Partial Molar Heat-Capacity of Individual Amino-Acid-Residues in Aqueous-Solution - Hydration Effect. J Mol Biol. 1990;213(2):375-84. doi: Doi 10.1016/S0022-2836(05)80197-4. PubMed PMID: ISI:A1990DE23600021.

87. Prabhu NV, Sharp KA. HEAT CAPACITY IN PROTEINS. Ann Rev Phys Chem. 2005;56(1):521-48. doi: doi:10.1146/annurev.physchem.56.092503.141202. PubMed PMID: 15796710.
88. Kresheck GC, Schneide.H, Scheraga HA. Effect of D20 on Thermal Stability of Proteins . Thermodynamic Parameters for Transfer of Model Compounds from H2o to D2o. J Phys Chem-Us. 1965;69(9):3132-&. PubMed PMID: ISI:A19656825200054.
89. Makhatadze GI, Privalov PL. Contribution of Hydration to Protein-Folding Thermodynamics .1. The Enthalpy of Hydration. J Mol Biol. 1993;232(2):639-59. doi: DOI 10.1006/jmbi.1993.1416. PubMed PMID: ISI:A1993LQ98500025.
90. Baldwin RL. Desolvation Penalty for Burying Hydrogen-Bonded Peptide Groups in Protein Folding. J Phys Chem B. 2010;114(49):16223-7. doi: Doi 10.1021/Jp107111f. PubMed PMID: ISI:000284990700023.
91. Ozen C, Serpersu EH. Thermodynamics of aminoglycoside binding to aminoglycoside-3 '-phosphotransferase IIIa studied by isothermal titration calorimetry. Biochemistry. 2004;43(46):14667-75. PubMed PMID: ISI:000225172800017.
92. Bundi A, Wuthrich K. H-1-NMR PARAMETERS OF THE COMMON AMINO-ACID RESIDUES MEASURED IN AQUEOUS-SOLUTIONS OF THE LINEAR TETRAPEPTIDES H-GLY-GLY-X-L-ALA-OH. Biopolymers. 1979;18(2):285-97. doi: 10.1002/bip.1979.360180206. PubMed PMID: WOS:A1979GF86200005.
93. Cooper A. Heat capacity effects in protein folding and ligand binding: a re-evaluation of the role of water in biomolecular thermodynamics. Biophysical chemistry. 2005;115(2):89-97.
94. Isbister BD, StHilaire PM, Toone EJ. Spatial organization versus total surface area as a predictor of protein hydrophobicity. The hydrophobicity of the concanavalin a binding site. J Am Chem Soc. 1995;117(51):12877-8. doi: Doi 10.1021/Ja00156a033. PubMed PMID: ISI:A1995TM48300033.
95. Kirschner KN, Woods RJ. Solvent interactions determine carbohydrate conformation. Proc Natl Acad Sci. 2001;98(19):10541-5. doi: DOI 10.1073/pnas.191362798. PubMed PMID: ISI:000170966800010.
96. Cox JR, Serpersu EH. Biologically important conformations of aminoglycoside antibiotics bound to an aminoglycoside 3'-phosphotransferase as determined by

transferred nuclear Overhauser effect spectroscopy. Biochemistry. 1997;36(9):2353-9. PubMed PMID: ISI:A1997WL64300003.
97. DiGiammarino EL, Draker K, Wright GD, Serpersu EH. Solution studies of isepamicin and conformational comparisons between isepamicin and butirosin A when bound to an aminoglycoside 6 '-N-acetyltransferase determined by NMR spectroscopy. Biochemistry. 1998;37(11):3638-44. PubMed PMID: ISI:000072759300008.
98. Ekman DR, DiGiammarino EL, Wright E, Witter ED, Serpersu EH. Cloning, overexpression, and purification of aminoglycoside antibiotic nucleotidyltransferase (2 '')-Ia: Conformational studies with bound substrates. Biochemistry. 2001;40(24):7017-24. PubMed PMID: ISI:000169366000004.
99. Owston MA, Serpersu EH. Cloning, overexpression, and purification of aminoglycoside antibiotic 3-acetyltransferase-IIIb: Conformational studies with bound substrates. Biochemistry. 2002;41(35):10764-70. doi: Doi 10.1021/Bi0261241. PubMed PMID: ISI:000177746300004.
100. Petersen C, Tielrooij KJ, Bakker HJ. Strong temperature dependence of water reorientation in hydrophobic hydration shells. J Chem Phys. 2009;130(21). doi: Artn 214511Doi 10.1063/1.3142861. PubMed PMID: ISI:000266674400032.

101. Makhatadze GI, Clore GM, Gronenborn AM. Solvent Isotope Effect and Protein Stability. Nat Struct Biol. 1995;2(10):852-5. PubMed PMID: ISI:A1995TD29300012.
102. Dahlberg DB. Aqueous-Solution Structure as Determined from Thermodynamic Parameters of Transfer from Water to Heavy-Water. J Phys Chem-Us. 1972;76(14):2045-&. doi: Doi 10.1021/J100658a024. PubMed PMID: ISI:A1972M917600024.
103. Rekharsky MV, Inoue Y. Solvent and guest isotope effects on complexation thermodynamics of alpha-, beta-, and 6-amino-6-deoxy-beta-cyclodextrins. J Am Chem Soc. 2002;124(41):12361-71. doi: Doi 10.1021/Ja027031. PubMed PMID: ISI:000178514700059.
104. Connelly PR, Thomson JA, Fitzgibbon MJ, Bruzzese FJ. Probing Hydration Contributions to the Thermodynamics of Ligand-Binding by Proteins - Enthalpy and Heat-Capacity Changes of Tacrolimus and Rapamycin Binding to Fk506 Binding-

Protein in D2o and H2o. Biochemistry. 1993;32(21):5583-90. doi: Doi 10.1021/Bi00072a013. PubMed PMID: ISI:A1993LF06300013.

105. Henzler-Wildman K, Kern D. Dynamic personalities of proteins. Nature. 2007;450(7172):964-72.

VITA

Xiaomin Jing was born in Zibo, Shandong, China on May 13, 1987. After finishing high school education at Shandong Zibo Experimental School in 2005, Xiaomin started her bachelor study in biotechnology at Shandong Normal University in Jinan, Shandong, China. Between 2007 and 2009, Xiaomin took a part in a research program led by Prof. Hui Zhang to study the molecular mechanism of salinity stress of halophytes in College of Life Sciences, Shandong Normal University. She received her B.S. in Biotechnology from Shandong Normal University in June 2009. In August 2009, Xiaomin joined the doctoral program in department of Biochemistry, Cellular and Molecular Biology in University of Tennessee, Knoxville. After first year laboratory rotations, Xiaomin joined the laboratory of Prof. Engin Serpersu to study protein biochemistry and biophysics in June 2010. In the future, Xiaomin wishes to continue the study in protein biochemistry and to translate fundamental research insights into protein engineering and novel protein therapeutics.